241

0-315-12552-7

National Library
of Canada

Bibliothèque nationale
du Canada

Canadian Theses Division

Division des thèses canadiennes

Ottawa, Canada
K1A 0N4

60463

PERMISSION TO MICROFILM — AUTORISATION DE MICROFILMER

- Please print or type — Écrire en lettres moulées ou dactylographier

Full Name of Author — Nom complet de l'auteur

Artur Senftleben

Date of Birth — Date de naissance

May, 12, 1982

Country of Birth — Lieu de naissance

Germany

Permanent Address — Résidence fixe

Am Hornbusch 23
4132 Kamp-Lintfort
Federal Republic of Germany

Title of Thesis — Titre de la thèse

Geometric Nonlinear Analysis of Circular Cylindrical Shells

University of Alberta, Edmonton, Alberta

University — Université

Master of Science

Degree for which thesis was presented — Grade pour lequel cette thèse fut présentée

1982

Year this degree conferred — Année d'obtention de ce grade

Dr. Terry Hrudey

Name of Supervisor — Nom du directeur de thèse

Permission is hereby granted to the NATIONAL LIBRARY OF CANADA to microfilm this thesis and to lend or sell copies of the film.

The author reserves other publication rights, and neither the thesis nor extensive extracts from it may be printed or otherwise reproduced without the author's written permission.

L'autorisation est, par la présente, accordée à la BIBLIOTHÈQUE NATIONALE DU CANADA de microfilmer cette thèse et de prêter ou de vendre des exemplaires du film.

L'auteur se réserve les autres droits de publication; ni la thèse ni de longs extraits de celle-ci ne doivent être imprimés ou autrement reproduits sans l'autorisation écrite de l'auteur.

Date

June, 10, 1982

Signature

NL-91 (4/77)

CANADIAN THESES ON MICROFICHE

I.S.B.N.

THESES CANADIENNES SUR MICROFICHE

National Library of Canada
Collections Development Branch

Canadian Theses on
Microfiche Service

Ottawa, Canada
K1A 0N4

Bibliothèque nationale du Canada
Direction du développement des collections

Service des thèses canadiennes
sur microfiche

NOTICE

The quality of this microfiche is heavily dependent upon the quality of the original thesis submitted for microfilming. Every effort has been made to ensure the highest quality of reproduction possible.

If pages are missing, contact the university which granted the degree.

Some pages may have indistinct print especially if the original pages were typed with a poor typewriter ribbon or if the university sent us a poor photocopy.

Previously copyrighted materials (journal articles, published tests, etc.) are not filmed.

Reproduction in full or in part of this film is governed by the Canadian Copyright Act, R.S.C. 1970, c. C-30. Please read the authorization forms which accompany this thesis.

THIS DISSERTATION
HAS BEEN MICROFILMED
EXACTLY AS RECEIVED

AVIS

La qualité de cette microfiche dépend grandement de la qualité de la thèse soumise au microfilmage. Nous avons tout fait pour assurer une qualité supérieure de reproduction.

S'il manque des pages, veuillez communiquer avec l'université qui a conféré le grade.

La qualité d'impression de certaines pages peut laisser à désirer, surtout si les pages originales ont été dactylographiées à l'aide d'un ruban usé ou si l'université nous a fait parvenir une photocopie de mauvaise qualité.

Les documents qui font déjà l'objet d'un droit d'auteur (articles de revue, examens publiés, etc.) ne sont pas microfilmés.

La reproduction, même partielle, de ce microfilm est soumise à la Loi canadienne sur le droit d'auteur, SRC 1970, c. C-30. Veuillez prendre connaissance des formules d'autorisation qui accompagnent cette thèse.

LA THÈSE A ÉTÉ
MICROFILMÉE TELLE QUE
NOUS L'AVONS REÇUE

NL-339 (r. 82/08)

Canada

THE UNIVERSITY OF ALBERTA

GEOMETRIC NONLINEAR ANALYSIS OF CIRCULAR CYLINDRICAL SHELLS

by

Ⓒ ARTUR SENFTLEBEN

A THESIS
SUBMITTED TO THE FACULTY OF GRADUATE STUDIES AND RESEARCH
IN PARTIAL FULFILMENT OF THE REQUIREMENTS FOR THE DEGREE
OF MASTER OF SCIENCE
IN
CIVIL ENGINEERING

DEPARTMENT OF CIVIL ENGINEERING

EDMONTON, ALBERTA
FALL, 1982

THE UNIVERSITY OF ALBERTA

RELEASE FORM

NAME OF AUTHOR

ARTUR SENFTLEBEN

TITLE OF THESIS

GEOMETRIC NONLINEAR ANALYSIS OF CIRCULAR CYLINDRICAL SHELLS

DEGREE FOR WHICH THESIS WAS PRESENTED MASTER OF SCIENCE

YEAR THIS DEGREE GRANTED 1982

Permission is hereby granted to THE UNIVERSITY OF ALBERTA LIBRARY to reproduce single copies of this thesis and to lend or sell such copies for private, scholarly or scientific research purposes only.

The author reserves other publication rights, and neither the thesis nor extensive extracts from it may be printed or otherwise reproduced without the author's written permission.

(SIGNED) ....

PERMANENT ADDRESS:

Am Hornbusch 23
4132 Kamp-Lintfort
Federal Republic of Germany

DATED 9th of June, 1982

THE UNIVERSITY OF ALBERTA
FACULTY OF GRADUATE STUDIES AND RESEARCH

The undersigned certify that they have read, and recommend to the Faculty of Graduate Studies and Research, for acceptance, a thesis entitled GEOMETRIC NONLINEAR ANALYSIS OF CIRCULAR CYLINDRICAL SHELLS submitted by ARTUR SENFTLEBEN in partial fulfilment of the requirements for the degree of MASTER OF SCIENCE in CIVIL ENGINEERING.

T. Hrudey
....
Supervisor

Gary Faulkner
....

S. H. Simmonds
....

Date. 4th June, 1982

Abstract

A modification to a previously developed finite element for circular cylindrical shells is presented and its linear and nonlinear stiffness matrices are defined. The element is tested on various linear and nonlinear problems and shows good agreement for cases which have already been investigated with finite elements. The linear bending of circular cylinders is extensively discussed and the element displacement field is checked for its approximations towards the linear bending theory. The induced stresses for rigid body motions are studied for the element and it is successfully tested on the nonlinear problems of a pinched barrel vault and a circular arch. This work concludes with the geometric nonlinear bending analysis of circular cylinders. Recommendations for further studies are given.

Acknowledgement

The author wishes to thank Dr. Terry Hrudey for his interest and support for this project and acknowledges the financial support by the National Science and Engineering Research Council.

The author also extends his thanks to Thomas Casey and various staff members of the Department of Computing Services for their invaluable help with textformatting and programming problems.

Table of Contents

Chapter Page

1. Introduction 1

2. Literature Review 4

2.1 Analytical Approaches 4

2.2 Finite Elements for Cylindrical Shells 7

2.3 Finite Elements Based on Strain Functions 13

3. Formulation of a New Strain Element 19

3.1 Displacement Function 19

3.2 Formulation of the Strain Energy Expression 22

3.3 Derivation of the Stiffness Matrices 25

3.4 Newton-Raphson Method Solution Procedure 27

4. Linear Solutions 32

4.1 Pinched Cylinder Problem 32

4.2 Cylinder under Bending 36

4.2.1 Boundary Conditions and Theoretical Results .36

4.2.2 Element Approximation of Cylinder under Bending 40

4.2.3 Results of Linear Tests 43

5. Nonlinear Problems 59

5.1 Introduction 59

5.2 The Circular Arch 60

5.3 The Barrel Vault Problem 66

5.4 Nonlinear Strains and Rigid Body Motions 70

5.4.1 Rotation around the $\bar{x}$-Axis 70

5.4.2 Rotation around the $\bar{y}$-Axis 71

5.4.3 Rotation around the $\bar{z}$-Axis 74

5.4.4 Summary of the Rigid Body Rotations 77

5.5 Cylinder under Bending 80

5.5.1 Review of Earlier Investigations 80

5.5.2 Boundary Conditions and Their Representation 81

5.5.3 Prescribed Displacements at the Cylinder Ends 82

5.5.3.1 Shortening of Cylinder due to Bending 83

5.5.3.2 Nonlinear Boundary Conditions for End Rotation 85

5.5.4 Discussion of Test Results 88

5.5.4.1 Rigid and Semi-Rigid Cylinder Ends ..88

5.5.4.2 The Short Cylinder 91

5.5.4.3 The Long Cylinder 96

6. Summary and Conclusions 104

References 107

Appendix A.1: Inverse of the Matrix [T] 113

Appendix A.2: Linear Strain Fields in Terms of Nodal Displacements 115

Appendix B.1: Listing of the Finite Element Program 117

Appendix B.2: Input Description 157

List of Tables

Table	Description	Page
4.1	Deflection of Thick Pinched Cylinder under Load.	34
4.2	Deflection of Thin Pinched Cylinder under Load.	35
4.3	Approximations of the Element Displacement Field.	41
4.4	Cylinder Data for Linear Bending Tests.	43
4.5	Ratio of Bottom Fibre Centre Deflections to Beam Theory for Long Cylinder with Rigid Ends.	45
4.6	Ratio of End Moment to Beam Theory for Long Cylinder with Rigid Ends.	45
4.7	Ratio of Computed Δv to Donnell Solution for Long Cylinder with Rigid Ends.	46
4.8	Ratio of End Moment to Beam Theory for Long Cylinder with Semi-Rigid Ends.	49
4.9	Ratio of Computed Δv to Donnell Solution for Long Cylinder with Semi-Rigid Ends.	49
4.10	Ratio of Bottom Fibre Deflection to Beam Theory for Short Cylinder with Rigid Ends.	50
4.11	Ratio of Computed Δv to Donnell Solution for Short Cylinder with Rigid Ends.	51
4.12	Ratio of End Moment to Beam Theory for Short Cylinder with Rigid Ends.	51
4.13	Ratio of Computed Δv to Donnell Solution for Short Cylinder with Semi-Rigid Ends.	55
4.14	Ratio of Cylinder Moment to Beam Moment for Short Cylinder with Semi-Rigid Ends.	55
5.1	Loads (lbs) for Prescribed Deflections of Two Cylindrical Arches.	65
5.2	Loads for Prescribed Deflections of a Hinged Barrel Vault under Single Load.	69
5.3	Circumferential Strain Induced by Rotation around the $\bar{y}$-Axis.	74

5.4 Circumferential Strain Induced by Rotation around the $\bar{z}$-Axis. 77

5.5 Maximum of Induced Strains from Rigid Body Motions. 77

5.6 Ratio of max $\bar{\delta}/\delta$cr for Three Cylinders. 84

5.7 Effects of Axially Fixed Ends and Prescribed Circumferential Strain on the Long Cylinder by Stephens *et al.*[38] with 4×2 Elements and $\beta=\beta$cr. ..89

5.8 Nonlinear Results of Short Cylinder under Bending. 91

5.9 Nonlinear Results of Long Cylinder under Bending.97

5.10 Ovalization of Long Cylinder under Bending. 98

List of Figures

Figure Description Page

2.1 Local Coordinate System for a Thin Cylindrical Shell. 8

2.2 Shell Element with Local and Global Axes. 16

3.1 Element with Centre Coordinate System and Corner Nodes. 21

3.2 The Newton-Raphson Method for a One-Degree-of-Freedom System. 30

4.1 Pinched Cylinder under Load with Element Mesh for One Octant. 32

4.2 Left Half of Cylinder under Bending with Linearized Boundary Conditions. 36

4.3 Slope Variation of Long Cylinder with Rigid Ends.47

4.4 Variation of Parameter Δv for Long Cylinder with Rigid Ends. 48

4.5 Deflection of Short Cylinder with Rigid Ends. ...52

4.6 Variation of Δv of Short Cylinder with Rigid Ends. 54

5.1 Circular Arch under Concentrated Load. 60

5.2 Load Deflection Curve for Cylindrical Arch (R=250 in.) under Concentrated Load. 63

5.3 Load Deflection Curve for Cylindrical Arch (R=150 in.) under Concentrated Load. 64

5.4 Hinged Barrel Vault under Single Load. 66

5.5 Load Deflection Curve of a Hinged Barrel Vault under Single Load. 68

5.6 Stresses for Short Cylinder at Mid-Section for $\beta = 0.4\ \beta cr$. 94

5.7 Incremental Deflections of Long Cylinder under Bending. 100

5.8 Stresses of Long Cylinder at $\beta = 0.3\ \beta cr$. 102

List of Symbols

Special Symbols

$\langle\ \rangle, \{\ \}^T$	denotes row vectors
$\{\ \}, \langle\ \rangle^T$	denotes column vectors
$[\ ]$	denotes a matrix
$[\ ]^{-1}$	denotes a matrix inverse
$[\ ]^T$	denotes a transposed matrix
$\|\ \|$	denotes a determinant of a matrix or a vector norm
,	denotes differentiation of preceding expression with respect to the following variables
$\_$	underlined term includes nonlinear parts
$\sim$	underlined strain term includes in-plane and out-of-plane strain contributions

Roman Symbols

A	area described by middle surface of shell element
$\langle Bx \rangle$, $\langle Bø \rangle$, $\langle Bu \rangle$, $\langle Bv \rangle$	displacement derivatives defined in Eq. 3.16
c	cos(p)
C	in-plane plate stiffness $Et/(1-\nu^2)$
D	plate bending stiffness $Et^3/12(1-\nu^2)$,
E	Young's modulus
[E]	elasticity matrix
I	moment of inertia
$[I]$	identity matrix
$[K^T]$	tangent stiffness matrix
K^2ij, K^3ijk, K^4ijkl	stiffness coefficient of second, third and fourth order, respectively
kx	curvature in x-direction
$kø$	curvature in ø-direction
$kxø$	twisting curvature
l	half length of element
L	length of cylinder
Le	distance from left end of cylinder
$\bar{L}$	cylinder length after bending with fixed ends
m	number of buckles in longitudinal direction
M	cylinder end moment

M_B	critical cylinder moment by Brazier (Eq. 2.4)
M_{cr}	cylinder moment causing δ_{cr}
N	axial force in cylinder
N_{cr}	axial force in cylinder causing δ_{cr}
NP	number of elements in the circumferential direction
NX	number of elements in the longitudinal direction
$2p$	angle prescribed by cylindrical shell element
P	magnitude of a single concentrated load
$\{q\}$	nodal displacement vector
$\{q^i\}$	nodal displacement vector after i-th equilibrium iteration
$\{Q\}$	nodal force vector
$\{Q^i\}$	nodal force vector after i-th equilibrium iteration
R	radius of cylinder or cylindrical element
$\bar{R}$	radius of curvature of cylinder under bending
s	sin(p)
t	shell thickness
$[T]$	coefficient matrix relating generalized degrees of freedom α_i to nodal displacements
U	strain energy

u, v, w	displacements in x-y-z coordinate directions, respectively
W	potential of external forces
x, y, z	local element coordinates
$\bar{x}, \bar{y}, \bar{z}$	global element coordinates
$[O]$	zero-matrix

Greek Symbols

α_i	i-th parameter of displacement function (Eq. 3.1)
$\{\alpha\}$	vector of displacement parameters α_i
$\langle\alpha x\rangle$, $\langle\alpha\phi\rangle$, $\langle\alpha x\phi\rangle$	bending strain field defined by Eq. 3.16
β	end rotation of cylinder
βcr	end rotation causing δcr
βx_1, βx_2, βx_3, $\beta\phi_1$, $\beta\phi_2$, $\beta\phi_3$	displacement derivatives defined by Eq. 3.13
βx, $\beta\phi$	rotation of the tangent to the mid-surface about the local x and ϕ axes, respectively
$\gamma x\phi$	linear shear strain
$\underline{\gamma} x\phi$	nonlinear shear strain
Δ	as a prefix denotes an increment, alone denotes a rigid body rotation
ΔL	elongation of cylinder due to bending with fixed ends
Δv	vertical deflection of cylinder side due to circumferential stretching
Δw	ovalization of cross-section of cylinder under bending
$\{\underset{\sim}{\epsilon}\}$	vector of strain components
ϵx	linear strain in x-direction
$\underline{\epsilon} x$	nonlinear strain in x-direction

ϵ_ϕ	linear strain in ϕ-direction
$\underline{\epsilon}_\phi$	nonlinear strain in ϕ-direction
ϵ_ϕ^{*}	circumferential strain induced by rigid body motions
$\langle\theta_x\rangle$, $\langle\theta_\phi\rangle$, $\langle\theta_{x\phi}\rangle$	in-plane strain fields defined by Eq. 3.16
ν	Poisson's ratio
Π	potential energy
$\{\sigma\}$	stress vector
σ_B	Brazier's critical stress
σ_{cr}	classical elastic buckling stress for axially loaded cylinder
σ_x	longitudinal stress
σ_ϕ	circumferential stress
$\bar{\sigma}$	longitudinal stress of cylinder with axially fixed ends under bending
$\tau_{x\phi}$	shear stress
ϕ	circumferential element coordinate = y/R
$\bar{\phi}$	cylinder angle, measured from the top fibre
ϕ°	cylinder angle, measured from the side edge downwards

1. Introduction

Since the development of shell theories around 1900, an increasing interest has been shown in the behaviour of circular cylinders under various loads.

Flügge[25] solved the linear elastic buckling problem of circular cylinders under compression and bending by using a simplified shell theory. The discrepancy between his theoretical results and the loads from structural tests activated researchers to study the effect of initial imperfections and residual stresses, which may significantly reduce the load. Another problem of comparing analytical loads with test results is the definition of appropriate boundary conditions at the cylinder ends, which are often selected to facilitate the analysis. In structural tests similar difficulties are encountered with boundary conditions. The appropriate assessment of flexible or rigid boundaries is a necessity to avoid unexpected collapse loads.

As opposed to the failure of a thin-walled cylinder under compression, the buckling of a cylinder under bending occurs after large elastic deformations take place.
The deflections, even for moderate dimensions, can be in the order of 20 times the wall thickness. Analysis of this problem requires a large displacement formulation. Short thin-walled cylinders under bending show a buckling mode with longitudinal wrinkles, whereas cylinders with a high length-to-radius ratio fail due to ovalization of the cross-

section. With increasing moment the bending stiffness and the section modulus are reduced. Cylinders with moderate dimensions may exhibit a combination of these two modes (Stephens *et al.*[38], Flügge[26]) which complicates the analysis. With the assumption of particular displacement functions or buckling modes the limit load is easily overestimated which explains the somewhat scattered data from analytical studies.

In the last few decades, thin-walled cylinders have been used extensively in off-shore drilling platforms and aerospace vehicles. With the use of cylinders in space structures there was a need to reduce the weight as much as possible. This led to very thin-walled structures. As a consequence the elastic buckling problem has been emphasized since the inelastic buckling prevails in thicker-walled structures. One of the latest achievements in the analysis and design of thin cylinders are to be seen in the Skylab and Space Shuttle programs of the National Aeronautics and Space Administration.

The motivation for this study lies in the design of circular steel cylinders for the use as long-span beams. Such cylinders are often used for surface pipelines which are subject to large bending moments. Another application are galleries which support conveyor systems for the transport of loose materials. These long-span cylinders are primarily stressed by bending moments so that the present study deals mainly with cylinders under pure bending and excludes torsional moments, shear forces, and axial loads.

Following this introduction a review of analytical studies in circular cylinders and finite elements for cylindrical shells is given. Then a modification to a previous finite element is presented whose displacement functions are based on an assumed strain field. The stiffness matrices are defined and the solution procedure is described. After the linear test problem of a pinched cylinder the linear bending of circular cylinders is discussed and the approximations of the element displacement field are investigated. Next the element is applied to the geometric nonlinear problems of a pinched barrel vault and a circular arch under single load. Then the strains induced by rigid body motions of a cylinder under bending are discussed. The strains caused by axially fixed ends of a cylinder under bending are computed and the nonlinear boundary conditions for rigid cylinder ends are given. After a discussion of the circumferential stretching associated with the linear Donnell solution for cylinders under bending, various boundary conditions are tested. Finally the results for the geometrically nonlinear bending of two cylinders are presented and compared with results from previous studies.

2. Literature Review

2.1 Analytical Approaches

The buckling moment for a cylindrical shell under bending was, in early studies, correlated to the buckling stress of a cylinder under compression. The classical solution for the latter case was derived by Flügge[25]. The displacement function he used was a combination of trigonometric functions in the longitudinal and circumferential direction. With the assumption that the stresses do not change during initial deformations, his analysis can be described as a linear elastic buckling problem. He assumed that the displacements are infinitesimally small and derived a stability criterion using the principle of minimum potential energy. Neglecting certain strain terms, he obtained the critical stress σcr for an axially compressed cylinder:

$$\sigma cr = Et/R \cdot [3(1-\nu^2)]^{-0.5} \qquad (2.1)$$

$$= 0.605\ Et/R \qquad \text{for } \nu = 0.3, \qquad (2.2)$$

where E denotes Young's modulus of elasticity, ν is Poisson's ratio, and R and t are the radius of the cylinder and its wall thickness, respectively. The corresponding critical moment for $\nu = 0.3$ is:

$$Mcr = 0.605\ \pi E t^2 R. \qquad (2.3)$$

Brazier[10] studied the flattening of long cylinders under bending and derived an expression for the potential energy of an infinite cylinder under bending. By minimizing the strain energy he found the critical moment to occur when the flattening of the cross-section reached 2/9 R. The critical moment is:

$$M_B = 2\times 2^{0.5}/9\ E\pi t^2 R(1-\nu^2)^{-0.5}. \qquad (2.4)$$

Assuming an undeformed cross-section and ν equal to 0.3 this corresponds to a buckling stress of

$$\sigma_B = 0.329\ Et/R. \qquad (2.5)$$

Flügge[25] investigated the buckling behaviour of cylinders with a Poisson's ratio of 1/6 and a radius to thickness ratio R/t of 289. He assumed a failure mode with a longitudinal wave-length ratio

$$m = L/R\pi,$$

with m being the number of longitudinal waves and L the length of the cylinder. The analysis thus considered longitudinal waves only with a wave-length equal to half the circumference. The buckling stress found was 30 % higher than the solution for axial compression (Eq. 2.2). Supported by various results of moment tests, which indicated somewhat higher stresses than for the equivalent compression problem, and overlooking the restrictions due to the assumed buckling mode, a performance factor of 1.3 was accepted and has been used subsequently to estimate the elastic buckling load of cylinders under bending.

Seide and Weingarten[36] investigated the buckling of circular cylinders using a modified form of the Donnell equations and the Galerkin method. Using four different R/t ratios they demonstrated that for most practical length to radius ratios the critical bending stress is insignificantly higher than the stress for pure compression.

Stephens *et al.*[38] used the computer code STAGS, a two-dimensional, energy formulation, finite difference program, and analyzed cylinders under bending with an R/t ratio of 100 and various length to radius ratios. By introducing imperfections in the order of t/1000, they were able to follow the nonlinear loading path and determine a limit point that for practical purposes can be assumed to be a bifurcation point. Their results indicate that the critical buckling stress of cylinders coincides with the classical stress σ_{cr} for very short cylinders and decreases with increasing L/R. For an L/R ratio of 20 the buckling moment was approximately that predicted by Brazier and occurred at a cross-section flattening of 0.22 times the radius.

Fabian[25] studied the behaviour of infinite cylinders using the finite difference technique. By prescribing the possible deformation modes he separated the ovalization effect from longitudinal wrinkling. For a cylinder with

$R/t=60$ and $\nu=1/3$ he found the moment to be about 53 % of M_{cr}, which is slightly below Brazier's solution.

2.2 Finite Elements for Cylindrical Shells

Thin shell theories, as opposed to three-dimensional theory, are based on the Love-Kirchhoff hypothesis that straight lines normal to the middle surface remain straight and unchanged in length during deformation. This implies that the deformation of the shell can be described by the deformation of its middle surface and that there are no transverse strains. With decreasing shell thickness t the transverse stresses become negligibly small compared to all other stresses and allow the assumption of plane stress.

The first complete set of kinematic relations for cylindrical shells was developed by Flügge[25]. Because of the awkward nonlinearities involved, various approximations and simplifications were suggested. Further approximations based on the negligibility of certain strain terms led to a variety of shell theories, of which the three major ones are reviewed below.

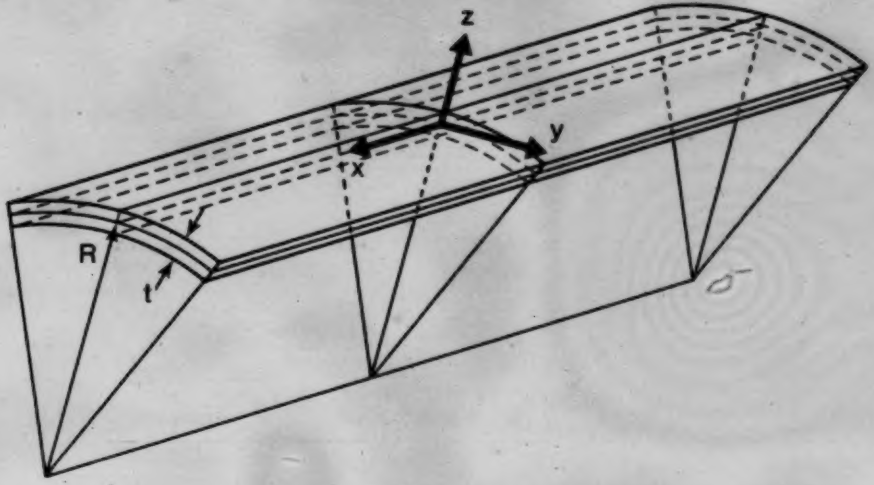

Fig. 2.1: Local Coordinate System for a Thin Cylindrical Shell.

Donnell obtained the following strain displacement expressions.

$$\epsilon x = u,x, \tag{2.6a}$$

$$\epsilon \phi = (v,\phi + w)/R, \tag{2.6b}$$

$$\gamma x\phi = u,\phi/R + v,x, \tag{2.6c}$$

$$kx = - w,xx, \tag{2.6d}$$

$$k\phi = - (w,\phi\phi)/R^2, \tag{2.6e}$$

$$kx\phi = - (w,x\phi)/R. \tag{2.6f}$$

The comma denotes the differentiation with respect to the following coordinates, and u, v, and w are displacements along the x-y-z coordinate axes, shown in Fig. 2.1.

In comparison with the classical plate theory, the y-coordinate is replaced by $R \cdot \phi$ and the normal displacement w contributes to the circumferential strain $\epsilon\phi$.

Timoshenko and Woinoisky-Kreiger's[40] formulation differs for the circumferential and twisting curvature by considering the influence of circumferential displacements. The resulting curvature expressions are

$$k\phi = (v,\phi - w,\phi\phi)/R^2, \tag{2.7a}$$

$$kx\phi = (v,x - w,x\phi)/R. \tag{2.7b}$$

A third set of strain expressions are the equations by Koiter and Sanders. These are regarded by some as the 'best' linear shell theory, because they satisfy strainless rigid body motions.

$$\epsilon x = u,x, \tag{2.8a}$$

$$\epsilon\phi = (v,\phi + w)/R, \tag{2.8b}$$

$$\gamma x\phi = u,\phi/R + v,x, \tag{2.8c}$$

$$kx = - w,xx, \tag{2.8d}$$

$$k\phi = (v,\phi - w,\phi\phi)/R^2, \tag{2.8e}$$

$$kx\phi = (3v,x - 4w,x\phi - u,\phi/R)\ /4R. \tag{2.8f}$$

The only difference from Timoshenko and Woinoisky-Kreiger's equations is in the expression for the twisting curvature. A detailed discussion of the approximations in these shell theories is given by Dym[33].

During the continuing development of the finite element method many attempts have been made to model shells with finite elements. Besides the curved finite strip (Cheung[16], Dawe[21]) and various hybrid formulations (e.g. Horrigmoe[28]), most elements can be categorized as either flat, three-dimensional (degenerated), or 'true' curved shell elements.

The modelling of shells as an assembly of flat elements was the first and probably is still the easiest approach. It is however a crude approach. The elements are derived by superposition of the independent in-plane (stretching) and out-of-plane behaviour (bending) of plates. With increasing mesh refinement they can represent a curved surface.
The coupling of the bending and stretching effects occurs during the assembly of the elements and with the transformation of the nodal degrees of freedom from the local element coordinates to a global coordinate system. One of the latest developments with flat finite elements is that of Argyris and Dunne[2] who employed a triangular plate element for postbuckling studies of cylindrical panels.

The three-dimensional brick element was originally developed for structures with thick walls and was later used for shells with a low R/t ratio. For thin shells the element showed an overemphasized shear stiffness, and caused numerical accuracy problems. Zienkiewicz and Hinton[45] eliminated this problem by using a reduced order of integration for the shear strain.

Kanok-Nukulchai[30] and Ramm[32] developed procedures for degenerating three-dimensional isoparametric elements to thin shells and obtained promising results in general shell analysis.

One of the first elements derived directly from a shell theory was a nonconforming rectangular element formulated by Connor and Brebbia[17]. They used a linear polynomial for the in-plane displacement function with a quadratic polynomial for the shear strain and an incomplete quartic polynomial function for the out-of-plane displacements. This element used the geometrical degrees of freedom

$$u,\ v,\ w,\ w_{,x} \text{ and } (w_{,\phi}-v)/R$$

at each of the four corner nodes.

Gallagher[27] added the twisting curvature $w_{,x\phi}$ as an internal degree of freedom to obtain a conforming element. Later Bogner *et al.*[9] increased the degree of the polynomial expressions with Hermitian polynomials. This resulted in 12 degrees of freedom per node, of which 7 represented derivatives proportional to various strains and changes of curvature. To avoid an overstiffening of the structure due to enforcing continuity of internal degrees of freedom, these non-geometric degrees of freedom were assembled at a single artificial node or were eliminated by static condensation.

Curved shell elements based on polynomial displacement functions can represent strainless rigid body motions only approximately. Except for the rotation and translation around the axis of revolution, trigonometric terms are needed to represent rigid motions exactly (compare Eq. 2.11). If the element does not have these functions, rigid body motions induce strains which are normally a higher order in the rigid body displacements. A general criterion, ensuring that a diplacement function is capable of representing rigid body motions is not available. This depends on the structure considered, the displacement function chosen, and the strain formulation used.

Dawe[20] showed that high order polynomials can approximate rigid body motions quite well. He employed quintic polynomials for all three displacement fields and constrained the functions at the edges of the element to be cubic, thereby enforcing compatibility between elements. His element has 54 degrees of freedom (18 per node) and shows considerable success for various arch and shell problems. The only disadvantage is the larger bandwidth due to its triangular shape.

Cantin[13] included strainless rigid body motions for polynomial displacement functions using certain matrix operations. A further discussion of this technique is found in Reference 3.

In order to avoid the difficulties in only approximating rigid body motions by polynomials, several researchers have explicitly included the rigid body displacements in their displacement fields. One of the first attempts was made by Cantin and Clough[14], who modified Gallagher's element. This gave rise to trigonometric terms in the displacement field and also to a coupling of u, v, and w.

Sabir and Lock[33] simplified Cantin and Clough's displacement functions by omitting the highest order terms and eliminating the internal degree of freedom $w,x\phi$. Despite giving a smaller stiffness matrix and violating the compatibility requirements, the element showed no apparent loss of accuracy when compared to the original element.

It should be mentioned here, that the displacements defining the rigid body motions discussed above are based on the strain displacement equations from the linear theory and may cause significant strains in nonlinear shell formulations.

2.3 Finite Elements Based on Strain Functions

By studying finite element solutions for cylindrical rings and arches Ashwell, Sabir and Roberts[3-6] found that a particular arch element, whose strain functions are simple expressions in the element coordinates, showed very good convergence when compared to all other preceding elements.

Sabir and Ashwell[4] concluded that the success of the arch element is due to the smoothness of the strain field:

> *" ... strain energy is calculated from squares and products of the strains, and imposing local variations on an initially smooth distribution without altering the local mean values, increases the value of the squares when they are integrated over the element."*[4]

With the results of this arch element in mind Sabir and Ashwell[4] developed an assumed strain element for cylindrical shells.

Using the strain displacement expressions of Timoshenko and Woinoisky-Kreiger, (Eq. 2.6 and 2.7) the following compatibility equations are obtained:

$$\epsilon_{\phi,xx} + k_x/R + (\epsilon_{x,\phi\phi})/R^2 - (\gamma_{x\phi,\phi x})/R = 0, \qquad (2.9a)$$

$$k_{x\phi,x} - (k_{x,\phi})/R + (\epsilon_{x,\phi})/R^2 - (\gamma_{x\phi,x})/R = 0, \qquad (2.9b)$$

$$k_{\phi,x} - (k_{x\phi,\phi})/R = 0. \qquad (2.9c)$$

With the assumption that $(\epsilon_{x,\phi})/R$ equals $\gamma_{x\phi,x}$ the following more restrictive equations are used.

$$(\epsilon_{x,\phi})/R = \gamma_{x\phi,x}, \qquad (2.10a)$$

$$\epsilon_{\phi,xx} = - k_x/R, \qquad (2.10b)$$

$$(k_{x,\phi})/R = k_{x\phi,x}, \qquad (2.10c)$$

$$k_{\phi,x} = (k_{x\phi,\phi})/R. \qquad (2.10d)$$

In the first step for the derivation of the displacement function, the strain expressions (Eq. 2.6 a-d, 2.7) are integrated to give the strainless rigid body motions. †

$$u = (\alpha_2\cos\phi + \alpha_4\sin\phi)R + \alpha_5, \tag{2.11a}$$

$$v = (\alpha_1 + \alpha_2 x)\sin\phi - (\alpha_3 + \alpha_4 x)\cos\phi + \alpha_6, \tag{2.11b}$$

$$w = -(\alpha_1 + \alpha_2 x)\cos\phi - (\alpha_3 + \alpha_4 x)\sin\phi. \tag{2.11c}$$

The parameters α_i may be identified with the following rigid modes of the element in Fig. 2.2.

α_1 : translation in the $\bar{z}$ direction,
α_2 : rotation around the $\bar{y}$-axis,
α_3 : translation in the $\bar{y}$ direction,
α_4 : rotation around the $\bar{z}$-axis,
α_5 : translation in the $\bar{x}$ direction,
α_6 : rotation around the $\bar{x}$-axis.

---

† The displacements due to rotations are derived from the assumption that the rotations are 'small'. A further discussion of the 'exact' displacements is given in section 5.4.

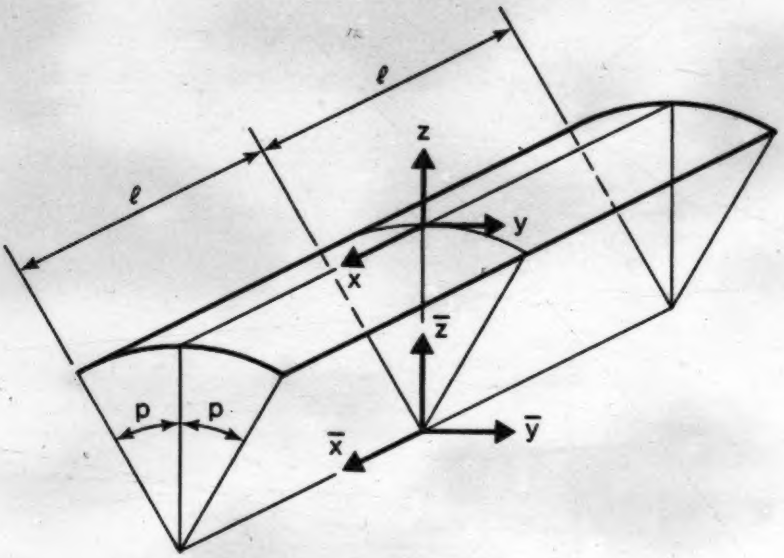

Fig. 2.2: Shell Element with Local and Global Axes.

With 20 nodal degrees of freedom wanted, 14 parameters are left for the strain functions and are distributed as follows:

$$\epsilon x = \alpha_7+\alpha_8 \phi, \qquad (2.12a)$$

$$\epsilon \phi = \alpha_9+\alpha_{10}x-(\alpha_{12}x^2/2R+\alpha_{13}x^3/6R+\alpha_{14}x^2\phi/2R+\alpha_{15}x^3\phi/6R), \qquad (2.12b)$$

$$\gamma x\phi = \alpha_{11}+(\alpha_8 x/R), \qquad (2.12c)$$

$$kx = \alpha_{12}+\alpha_{13}x+\alpha_{14}\phi+\alpha_{15}x\phi, \qquad (2.12d)$$

$$k\phi = \alpha_{16}+\alpha_{17}x+\alpha_{18}\phi+\alpha_{19}x\phi, \qquad (2.12e)$$

$$kx\phi = \alpha_{20}+(\alpha_{14}x/R+\alpha_{15}x^2/2R+R\alpha_{17}\phi+R\alpha_{19}\phi^2/2). \qquad (2.12f)$$

After the unbracketed terms are written, the terms in parentheses are added to satisfy the compatibility equations (Eq. 2.10).

The displacement functions are obtained by integration of the above equations. The integration constants depend on the choice of location of the origin of the local coordinate system. For simplicity this is chosen to be at the middle of the element as shown (Fig. 2.1).

$$U = \alpha_7 x+\alpha_8 x\phi +R\alpha_{11}\phi -0.5R^3\alpha_{17}\phi^2+R^3(\phi-\phi^3/6)\alpha_{19} -R^2\alpha_{20}\phi, \tag{2.13a}$$

$$V = R^2\alpha_{16}\phi +R^2\alpha_{17}x\phi+0.5R^2\alpha_{18}\phi^2+(x\phi\phi/2-1)R^2\alpha_{19} +R\alpha_{20}x, \tag{2.13b}$$

$$W = (R\alpha_9+R\alpha_{10})x-\alpha_{12}x^2/2 -\alpha_{13}x^3/6-\alpha_{14}x^2\phi/2-\alpha_{15}x^3\phi/6 -R^2\alpha_{16} -R^2\alpha_{17}x-R^2\alpha_{18}\phi -R^2\alpha_{19}x\phi. \tag{2.13c}$$

The complete displacement field consists of the equations above plus the rigid body motions (Eq. 2.11).

Ashwell and Sabir obtained very good convergence for their element for the problem of a barrel vault under gravitational load. In section 4.1 its performance is compared to that of the element used in this study for the problem of a pinched cylinder.

Ashwell made the argument that a finite element should be capable of representing the known solutions of certain test problems and therefore altered the strain functions (Eq. 2.12) so as to better represent the stresses in a cylinder under bending. These stresses are functions of the circumferential coordinate only. This requires a $\sin\phi$ term in the expressions for the strains ϵx and kx, and also requires $\gamma x\phi$ to be independent from all the other strains.

$$\epsilon x = \alpha_7+\alpha_8\sin\phi, \tag{2.14a}$$

$$\epsilon\phi = \alpha_9+\alpha_{10}x-(\alpha_{12}x^2/2R+\alpha_{13}x^3/6R+\alpha_{14}x^2\phi/2R+\alpha_{15}x^3\phi/6R), \tag{2.14b}$$

$$\gamma x\phi = \alpha_{11}, \tag{2.14c}$$

$$kx = \alpha_8\sin\phi/R+\alpha_{12}+\alpha_{13}x+\alpha_{14}\phi+\alpha_{15}x\phi, \tag{2.14d}$$

$$k\phi = \alpha_{16}+\alpha_{17}x+\alpha_{18}\phi+\alpha_{19}x\phi, \tag{2.14e}$$

$$kx\phi = \alpha_{20}+(\alpha_{14}x/R+\alpha_{15}x^2/2R+R\alpha_{17}\phi+R\alpha_{19}\phi^2/2). \tag{2.14f}$$

In the displacement function for u, '$\alpha_8 x\phi$' becomes '$\alpha_8 x\sin\phi$' and v and w are supplemented by the terms '$-\alpha_8 x^2\cos\phi/2R^2$' and '$-\alpha_8 x^2\sin\phi/2R$', respectively. With the altered displacement field appreciable improvement is obtained for the barrel vault problem if compared to the element of Ashwell and Sabir[4]. Both strain elements converge to solutions of the 'deep shell' theory.

3. Formulation of a New Strain Element

3.1 Displacement Function

The element in this study is derived from the Koiter-Sander's strain expressions (Eq. 2.8). With the constants α_i defined as for the Sabir-Ashwell element (Eq. 2.11), the displacement functions are developed using the procedure described in section 2.3 and are given in the equations below.

$$u = (\alpha_2\cos\phi+\alpha_4\sin\phi)R+\alpha_5+\alpha_7x+\alpha_8x\sin\phi +0.75R\alpha_{11}\phi -0.5R^3\alpha_{17}\phi^2+R^3(\phi-\phi^3/6)\alpha_{19} -R^2\alpha_{20}\phi, \tag{3.1a}$$

$$v = (\alpha_1+\alpha_2x)\sin\phi-(\alpha_3+\alpha_4x)\cos\phi +\alpha_6-\alpha_8x^2\cos\phi/2R+x\alpha_{11}/4 +R^2\alpha_{16}\phi +R^2\alpha_{17}x\phi+0.5R^2\alpha_{18}\phi^2 +R^2(\phi^2/2-1)\alpha_{19}x +R^2\alpha_{20}x, \tag{3.1b}$$

$$w = -(\alpha_1+\alpha_2x)\cos\phi-(\alpha_3+\alpha_4x)\sin\phi -\alpha_8x^2\sin\phi/2R+R\alpha_9+R\alpha_{10}x -\alpha_{12}x^2/2 -\alpha_{13}x^3/6-\alpha_{14}x^2\phi/2-\alpha_{15}x^3\phi/6 -R^2\alpha_{16}-R^2\alpha_{17}x -R^2\alpha_{18}\phi -R^2\alpha_{19}x\phi. \tag{3.1c}$$

The only differences from the improved element of Ashwell[3] are the change from '$R\alpha_{11}\phi$' to '$0.75\ R\alpha_{11}\phi$' in the expression for u, and the addition of '$x\alpha_{11}/4$' to the expression for v. The resulting assumed strains are:

$$\epsilon x = \alpha_7+\alpha_8\sin\phi, \tag{3.2a}$$

$$\epsilon\phi = \alpha_9+\alpha_{10}x-(\alpha_{12}x^2/2R+\alpha_{13}x^3/6R +\alpha_{14}x^2\phi/2R+\alpha_{15}x^3\phi/6R),$$

$$(3.2b)$$

$$\gamma x\phi = \alpha_{11}, \qquad (3.2c)$$

$$kx = \alpha_8 \sin\phi/R+\alpha_{12}+\alpha_{13}x+\alpha_{14}\phi+\alpha_{15}x\phi, \qquad (3.2d)$$

$$k\phi = \alpha_{16}+\alpha_{17}x+\alpha_{18}\phi+\alpha_{19}x\phi, \qquad (3.2e)$$

$$kx\phi = (\alpha_{14}x/R+\alpha_{15}x^2/2R+R\alpha_{17}\phi+R\alpha_{19}\phi^2/2)+\alpha_{20}. \qquad (3.2f)$$

The vector of the displacement parameters $\{\alpha\}$ is related to the nodal displacement vector $\{q\}$ by the matrix $[T]$, the inverse of which is given in Appendix A.1.

$$\{q\} = [T]\ \{\alpha\}, \qquad (3.3a)$$

$$= < u_1\ v_1\ w_1\ \beta x_1\ \beta\phi_1\ \ u_2\ v_2\ w_2\ \beta x_2\ \beta\phi_2$$

$$u_3\ v_3\ w_3\ \beta x_3\ \beta\phi_3\ \ u_4\ v_4\ w_4\ \beta x_4\ \beta\phi_4 >^T. \qquad (3.3b)$$

The indices denote the node number. With the explicit form of the inverse of $[T]$ it is possible to write the element shape functions explicitly for each of the 20 degrees of freedom. This is not done here due to the lengthiness of the resulting expressions.

The Eqs. 3.2 and 3.3a define the strain functions in terms of nodal displacements. Instead of using the explicit shape functions, the strain functions are used directly for the formulation of the stiffness matrices.

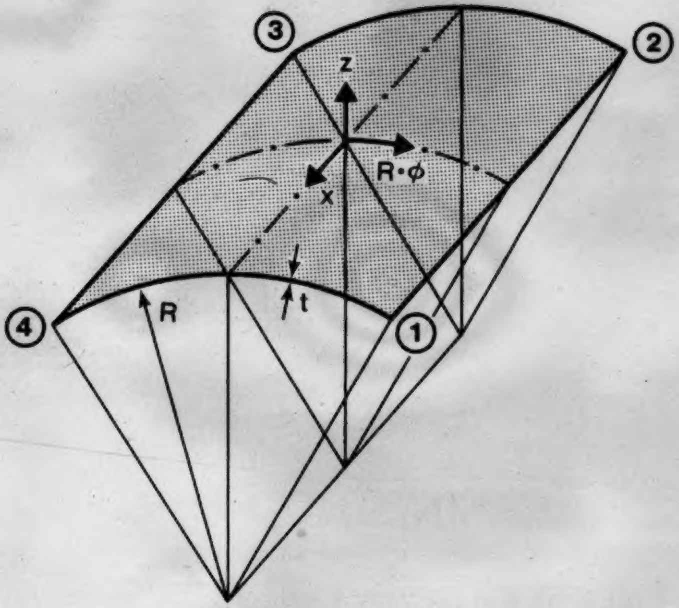

Fig. 3.1: Element with Centre Coordinate System and Corner Nodes.

5

The degrees of freedom u, v, and w are the displacements along the local x, y, and z coordinate directions, respectively, and βx and $\beta\phi$ are the rotations of the normal about the local x and ϕ axes, respectively. In terms of the displacements, these rotations are given by

$$\beta x = w_{,x}, \tag{3.4a}$$

$$\beta\phi = (w_{,\phi} - v)/R. \tag{3.4b}$$

3.2 Formulation of the Strain Energy Expression

The element used in this study is based on a displacement field (Eqs. 3.1) derived from an assumed strain field. Following the usual steps in the classical displacement method, the stiffness matrices for the element are derived using the Principle of the Stationary Potential Energy. The potential energy Π is the difference of the strain energy U and the potential W of the external loads Q_i with respect to the corresponding displacements q_i.

$$\Pi = U - W. \tag{3.5}$$

The strain energy is defined as

$$U = 1/2 \int_V \{\sigma\}^T \{\underset{\sim}{\epsilon}\} \, dV , \tag{3.6}$$

with V being the volume of the structure considered. The strain and stress vectors $\{\sigma\}$ and $\{\underset{\sim}{\epsilon}\}$ for the assumed plane stress state in thin shells take the form

$$\{\sigma\} = < \sigma x \ \sigma \phi \ \tau x \phi >^T, \tag{3.7a}$$

$$\{\underset{\sim}{\epsilon}\} = < \underset{\sim}{\epsilon} x \ \underset{\sim}{\epsilon} \phi \ \underset{\sim}{\gamma} x \phi >^T. \tag{3.7b}$$

For a linear elastic structure, the stress vector is expressed by the product of the elasticity matrix [E] and the strain vector.

$$\{\sigma\} = [E]\cdot\{\underset{\sim}{\epsilon}\}, \tag{3.8}$$

$$\text{with}\quad [E] = E/(1-\nu^2)\begin{bmatrix} 1 & \nu & 0 \\ \nu & 1 & 0 \\ 0 & 0 & (1-\nu)/2 \end{bmatrix}, \tag{3.9}$$

and the Poisson's ratio ν.

Using Eq. 3.6 the strain energy becomes:

$$U = 1/2\ E/(1-\nu^2) \int_V [\underset{\sim}{\epsilon}_x{}^2+\underset{\sim}{\epsilon}_\phi{}^2+2\nu\underset{\sim}{\epsilon}_x\underset{\sim}{\epsilon}_\phi +(1-\nu)/2\ \underset{\sim}{\gamma}_{x\phi}{}^2]\ dV. \tag{3.10}$$

For later convenience the strains are separated into an in-plane and an out-of-plane part.

$$\begin{bmatrix} \underset{\sim}{\epsilon}_x \\ \underset{\sim}{\epsilon}_\phi \\ \underset{\sim}{\gamma}_{x\phi} \end{bmatrix} = \begin{bmatrix} \underline{\epsilon}_x \\ \underline{\epsilon}_\phi \\ \underline{\gamma}_{x\phi} \end{bmatrix} + z\cdot\begin{bmatrix} k_x \\ k_\phi \\ 2k_{x\phi} \end{bmatrix}. \tag{3.11}$$

Substituting Eq. 3.11 into Eq. 3.10 and performing the integration over the shell thickness t the strain energy is:

$$U = C/2 \int_A [\underline{\epsilon}_x{}^2+\underline{\epsilon}_\phi{}^2+2\nu\underline{\epsilon}_x\underline{\epsilon}_\phi+(1-\nu)/2\ \underline{\gamma}_{x\phi}{}^2)]\ dA$$

$$+\ D/2 \int_A [k_x{}^2+k_\phi{}^2+2\nu k_x k_\phi+2(1-\nu)k_{x\phi}{}^2]\ dA, \tag{3.12}$$

with $C = Et/(1-\nu^2)$,

$D = Et^3/12(1-\nu^2)$,

and A is the middle surface area of the element.

Before the strain equations by Koiter-Sanders are substituted into Eq. 3.12, the strain expressions are divided into linear and nonlinear parts.

$$\begin{aligned}
\underline{\epsilon} x &= \epsilon x + 1/2(\beta x_1{}^2 + \beta x_2{}^2 + \beta x_3{}^2), \\
\underline{\epsilon} \phi &= \epsilon \phi + 1/2(\beta \phi_1{}^2 + \beta \phi_2{}^2 + \beta \phi_3{}^2), \\
\underline{\gamma} x\phi &= \gamma x\phi + \beta x_1 \beta \phi_1 + \beta x_2 \beta \phi_2 + \beta x_3 \beta \phi_3,
\end{aligned}$$

$$\begin{aligned}
kx &= -\beta x{,}x, \\
k\phi &= -\beta\phi{,}\phi/R, \\
kx\phi &= -\beta\phi{,}x - \gamma x\phi/4R, & \gamma x\phi &= \beta x_2 + \beta\phi_1, \\
\beta x_1 &= \epsilon x = u{,}x, & \beta\phi_1 &= u{,}\phi/R, \\
\beta x_2 &= v{,}x, & \beta\phi_2 &= \epsilon\phi = (v{,}\phi + w)/R, \\
\beta x_3 &= \beta x = w{,}x, & \beta\phi_3 &= \beta\phi = (w{,}\phi - v)/R. \quad (3.13)
\end{aligned}$$

Since the strain energy consists of products of the above strains, it is separated into a quadratic, a cubic, and a quartic part.

$$U = U_2 + U_3 + U_4. \qquad (3.14a)$$

$$U_2 = C/2 \int_A [\epsilon x(\epsilon x + \nu\epsilon\phi) + \epsilon\phi(\epsilon\phi + \nu\epsilon x) + (1-\nu)/2\ \gamma x\phi^2]\ dA$$

$$+ D/2 \int_A [kx(kx + \nu k\phi) + k\phi(k\phi + \nu kx) + 2(1-\nu)\ kx\phi^2]\ dA, \qquad (3.14b)$$

$$
\begin{aligned}
U_3 = C/2 \int_A [\; & \epsilon x(\beta x_1^2+\beta x_2^2+\beta x_3^2+\nu\{\beta\phi_1^2+\beta\phi_2^2+\beta\phi_3^2\}) \\
& + \epsilon\phi(\beta\phi_1^2+\beta\phi_2^2+\beta\phi_3^2+\nu\{\beta x_1^2+\beta x_2^2+\beta x_3^2\}) \\
& + (1-\nu)\gamma x\phi(\beta x_1\beta\phi_1+\beta x_2\beta\phi_2+\beta x_3\beta\phi_3)\;]\, dA,
\end{aligned}
\qquad (3.14c)
$$

$$
\begin{aligned}
U_4 = C/8 \int_A [\; & (\beta x_1^2+\beta x_2^2+\beta x_3^2)^2+(\beta\phi_1^2+\beta\phi_2^2+\beta\phi_3^2)^2 \\
& + 2\nu(\beta x_1^2+\beta x_2^2+\beta x_3^2)(\beta\phi_1^2+\beta\phi_2^2+\beta\phi_3^2) \\
& + 2\nu(\beta x_1\beta\phi_1+\beta x_2\beta\phi_2+\beta x_3\beta\phi_3)^2\;]\, dA.
\end{aligned}
\qquad (3.14d)
$$

3.3 Derivation of the Stiffness Matrices

In order to formulate the stiffness matrices the stiffness coefficients have to be defined by the components of the strain energy and the nodal displacements.

$$U = U_2 + U_3 + U_4,$$

$$
\begin{aligned}
U_2 &= 1/2\, K^2ij\; qi\; qj, \\
U_3 &= 1/6\, K^3ijk\; qi\; qj\; qk, \\
U_4 &= 1/12\, K^4ijkl\; qi\; qj\; qk\; ql, \qquad (i,j,k,l = 1 \ldots 20).
\end{aligned}
\qquad (3.15)
$$

In the above, qi is the i-th term of the nodal displacement vector $\{q\}$. With Eqs. 3.2 and 3.13 the strain fields are expressed in the form:

$$\begin{bmatrix} \epsilon x \\ \epsilon \phi \\ \gamma x \phi \\ k x \\ k \phi \\ k x \phi \\ \beta x_3 \\ \beta \phi_3 \\ \beta x_2 \\ \beta \phi_1 \end{bmatrix} = \begin{bmatrix} \langle \theta x \rangle \\ \langle \theta \phi \rangle \\ \langle \theta x \phi \rangle \\ \langle \alpha x \rangle \\ \langle \alpha \phi \rangle \\ \langle \alpha x \phi \rangle \\ \langle B x \rangle \\ \langle B \phi \rangle \\ \langle B u \rangle \\ \langle B v \rangle \end{bmatrix} \{q\}. \tag{3.16}$$

The linear strain functions ($\langle\theta\rangle$ and $\langle\alpha\rangle$) are given in Appendix A.2. Introducing Eq. 3.16 into Eq. 3.14 the stiffness matrices can be computed. The linear stiffness matrix is:

$$\begin{aligned} [K^2] = {} & CR \int_{-p}^{p} \int_{-1}^{1} \Big[\{\theta x\}\langle \theta x + \nu \theta \phi \rangle + \{\theta \phi\}\langle \theta \phi + \nu \theta x \rangle \\ & \quad + (1-\nu)/2 \; \{\theta x \phi\}\langle \theta x \phi \rangle \Big] \, d\phi \, dx \\ & + DR \int_{-p}^{p} \int_{-1}^{1} \Big[\{\alpha x\}\langle \alpha x + \nu \alpha \phi \rangle + \{\alpha \phi\}\langle \alpha \phi + \nu \alpha x \rangle \\ & \quad + 2(1-\nu) \; \{\alpha x \phi\}\langle \alpha x \phi \rangle \Big] \, d\phi \, dx, \end{aligned} \tag{3.17}$$

In the above equations, R is the radius of the cylinder, p is half of the angle subtended by the element and 1 is half of its longitudinal dimension.

The nonlinear stiffness terms of third and fourth order as defined in Eqs. 3.15, are computed in a similar manner.

3.4 Newton-Raphson Method Solution Procedure

An elastic structure follows the principle of stationary potential energy:

> *Of all kinematically admissible displacement fields, the actual equilibrium displacements make the potential energy have a stationary value.*

The term kinematically admissible means that the displacements are continuous within the structure and that they satisfy the kinematic boundary conditions.

A stationary value for the potential energy requires that the first partial derivatives of the potential energy with respect to the nodal displacements are zero. Taking the first derivative of Eq. 3.5 the equilibrium conditions can be written:

$$\Pi_{,qi} = 0 = K^2_{ij}\, q_j + 1/2\, K^3_{ijk}\, q_j\, q_k + 1/3\, K^4_{ijkl}\, q_j\, q_k\, q_l - Q_i. \qquad (3.18)$$

It may be further stated that the equilibrium state that makes Π stationary (first variation equal to zero) is stable if the second variation of Π is positive.

This means that the determinant of the Jacobian matrix of Π

has to be positive. Using Eq. 3.5 this can be expressed as:

$$| \Pi,qi\ qj | > 0 \quad ,\text{or}$$

$$| K^{2}ij + K^{3}ijk\ qk + K^{4}ijkl\ qk\ ql | = | [K^{T}] | > 0, \tag{3.19}$$

where | | denotes the determinant.

The matrix $[K^{T}]$ is referred to as the tangent stiffness matrix and is positive definite for a stable equilibrium configuration. For an unstable equilibrium configuration the determinant of $[K^{T}]$ becomes negative. At a bifurcation point or a limit point (a horizontal tangent in the load-deflection curve), the determinant of $[K^{T}]$ is zero.

To first order in the incremental displacement Δqi, the incremental form of the equilibrium equation 3.18 is

$$K^{T}ij\ \Delta qj = \Delta Qi.$$

In order to be able to prescribe both displacement and force type boundary conditions, the above equation must be modified. In the new equations below a Δ denotes increments in forces or displacements and a star (*) indicates prescribed values. For easier representation the equations have been reordered so that the prescribed incremental forces are grouped together as are the precribed incremental displacements.

$$\begin{bmatrix} [K^{T}_{11}] & [K^{T}_{12}] \\ [K^{T}_{21}] & [K^{T}_{22}] \end{bmatrix} \begin{bmatrix} \{\Delta q_1\} \\ \{\Delta q_2 *\} \end{bmatrix} = \begin{bmatrix} \{\Delta Q_1 *\} \\ \{\Delta Q_2\} \end{bmatrix} . \qquad (3.20)$$

The first equation resulting from this partitioning is then re-arranged so that the unknown displacements may be solved for.

$$[K^{T}_{11}]\ \{\Delta q_1\} = \{\Delta Q_1 *\} - [K^{T}_{12}]\ \{\Delta q_2 *\}.$$

After $\{\Delta qi\}$ is known, the unknown forces $\{\Delta Q_2\}$ can be calculated from the stiffness matrix and the displacements. In the finite element program used, the nodal forces are not needed, and the stiffness matrix and the right hand side are changed for easier application of the equation solver and to obtain a full incremental displacement vector.

$$\begin{bmatrix} [K^{T}_{11}] & [O] \\ [O] & [I] \end{bmatrix} \begin{bmatrix} \{\Delta q_1\} \\ \{\Delta q_2 *\} \end{bmatrix} = \begin{bmatrix} \{\Delta Q_1 *\} - [K^{T}_{12}]\ \{\Delta q_2 *\} \\ \{\Delta q_2 *\} \end{bmatrix} . \qquad (3.21)$$

In the above, $[I]$ denotes the identity and $[O]$ the zero-matrix.

After the new displacements of the structure are found, the equilibrium of the deformed structure can be checked with Eq. 3.18. If the equilibrium equation is not satisfied, the displacements have to be changed until they satisfy Eq. 3.18. One well established procedure for this problem is the Newton-Raphson method which is described in the algorithm given below.

Figure 3.2 shows the Newton-Raphson method for a load step from $\{Q^0\}$ to $\{Q\}$. The corresponding deformations are the vectors $\{q^0\}$ and $\{q\}$.

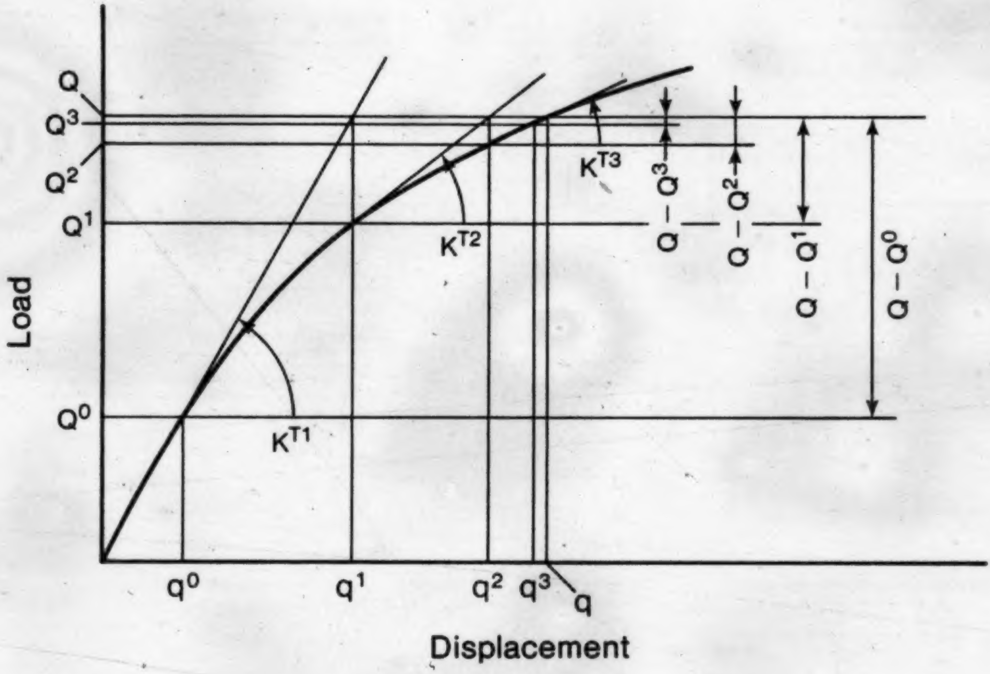
Q
Q³
Q²
Q¹
Q⁰
Load
K^T1
K^T2
K^T3
Q − Q³
Q − Q²
Q − Q¹
Q − Q⁰
q⁰
q¹
q²
q³
q
Displacement

Fig. 3.2: The Newton-Raphson Method for a One-Degree-of-Freedom System.

Algorithm for the Newton-Raphson Method:

1) Start of new load step,
   set i as superscript of $\{q^i\}$, $\{Q^i\}$, and $[K^{T\,i}]$ to one.
2) Form the tangent stiffness matrix,

$K^{Ti}ij = K^2ij + K^3ijk\ q^ik + K^4ijkl\ q^ik\ q^il.$

3) If superscript i is greater than one, go to step 5.
4) Modify the tangent stiffness matrix and the incremental load vector as shown in Eq. 3.21 by including the prescribed incremental loads and displacements for this load step.
5) Calculate the incremental displacements from Eq. 3.21, and update the displacement vector,

   $\{q^i\} = \{q^{i-1}\} + [K^{Ti}]^{-1}\ \{Q-Q^{i-1}\}.$
6) Check if the displacements have converged,

   (if $|q^i-q^{i-1}|$ < tolerance), go to step 10.
7) Compute the internal nodal forces from the equilibrium equation,

   $Q^ii = K^2ij\ q^ij + 1/2\ K^3ijk\ q^ij\ q^ik$

   $\quad + 1/3\ K^4ijkl\ q^ij\ q^ik\ q^il.$
8) Compute the vector $\{Q-Q^i\}$ as a new right hand side of Eq. 3.21.
9) Increase superscript i of $\{q^i\}$, $\{Q^i\}$, and $[K^{Ti}]$ by one, return to step 2.
10) End of load step.

4. Linear Solutions

4.1 Pinched Cylinder Problem

In order to study the convergence behaviour of cylindrical shell finite elements, various sample problems have been utilized. The most often used problem for cylindrical shells is a pinched cylinder as shown in Fig. 4.1.

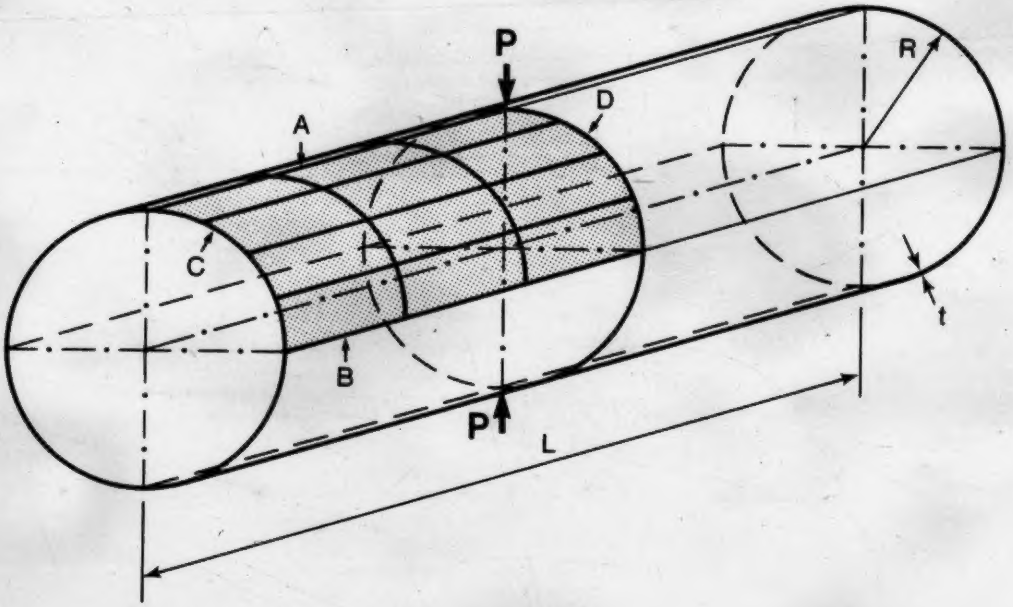

Fig. 4.1: Pinched Cylinder under Load with Element Mesh for One Octant.

The data for this cylinder are:

R = 4.953 in.,

L = 10.35 in.,

t = 0.094 in. for the thick and 0.01548 in. for the thin cylinder,

$E = 1.05\times10^{6}$ lbs/in.^{2},

$\nu = 0.3125$.

The load P is 100 lbs for the thick cylinder and 0.1 lbs for the thin one.

Because of symmetry, only one octant needs to be analyzed, with the appropriate boundary conditions applied as described in the following. The nodal degrees of freedom v and $\beta\phi$ along the top fibre A and the side edge B are set to zero. No displacements are prescribed at end C. Symmetry about the vertical plane and the mid-section D requires u and βx to be zero.

Ashwell and Sabir calculated the deflection under the load for the thick cylinder. Their solution in Reference 4 converges to a value of 0.1137 inches. For the mesh sizes chosen by Ashwell and Sabir no difference could be found between their results and the present results. It would be interesting to compare their solution with more significant figures to determine if there are any differences.
For comparison the results of Cantin[13] are also shown. The latter is believed by Ashwell and Sabir to be the most accurate solution. It converges to a deflection of 0.1139 inches.

Table 4.1: Deflection of Thick Pinched Cylinder under Load.

Mesh size NX × NP	present study, Ashwell and Sabir	Cantin
1×1	0.1041	-
2×2	0.1103	0.0931
4×4	0.1129	0.1126
6×6	0.1135	0.1137
8×8	0.1137	0.1139
10×10	0.1137	0.1139

Despite having 20 % fewer degrees of freedom than the Cantin element, the elements of Ashwell and Sabir and the present study show a similar convergence. The two strain formulation elements give better results for mesh sizes up to 4×4 and converge to a deflection of 99.8 % of Cantin's solution.

For the thin pinched cylinder problem better or worse behaviour can be obtained, depending on the simplifications and assumptions of the shell theory used. In the appendix of Reference 4 Ashwell and Sabir estimate the exact solution to be 0.02439 in., which they believe to be correct to four significant figures.

Table 4.2: Deflections of Thin Pinched Cylinder under Load.

Mesh size NX × NP	Ashwell and Sabir	present study
1×1	0.02301	0.02327
2×1	0.02300	0.02336
3×1	0.02302	0.02337
1×4	0.02403	0.02432
2×4	0.02409	0.02448
3×4	0.02414	0.02452
1×8	0.02406	0.02436
2×8	0.02414	0.02443
3×8	0.02418	0.02448

Despite giving the same results as Ashwell and Sabir for the thick cylinder (R/t=53), the thin cylinder problem (R/t=320) shows a significant difference. For all mesh sizes chosen, the present study gives deflections, that are 1.0 to 1.5 % larger and which are closer to the 'exact' solution of 0.02439 in. than the Ashwell and Sabir solution. Except for the 2×1 mesh, the Sabir Ashwell model softens with increasing number of elements in the circumferential and longitudinal direction and seems to converge to a solution below the 'exact' solution. The present element converges nonmonotonically with respect to grid refinement in the ø-direction to a value above the 'exact' solution.

4.2 Cylinder under Bending

4.2.1 Boundary Conditions and Theoretical Results

With the symmetry of a cylinder under bending only one quarter needs to be analyzed. The symmetry about the central vertical longitudinal plane requires that v and $\beta\phi$ at the top and bottom fibre be zero. Symmetry about the cross-section plane at the mid-cylinder requires that u and βx be zero at that plane.

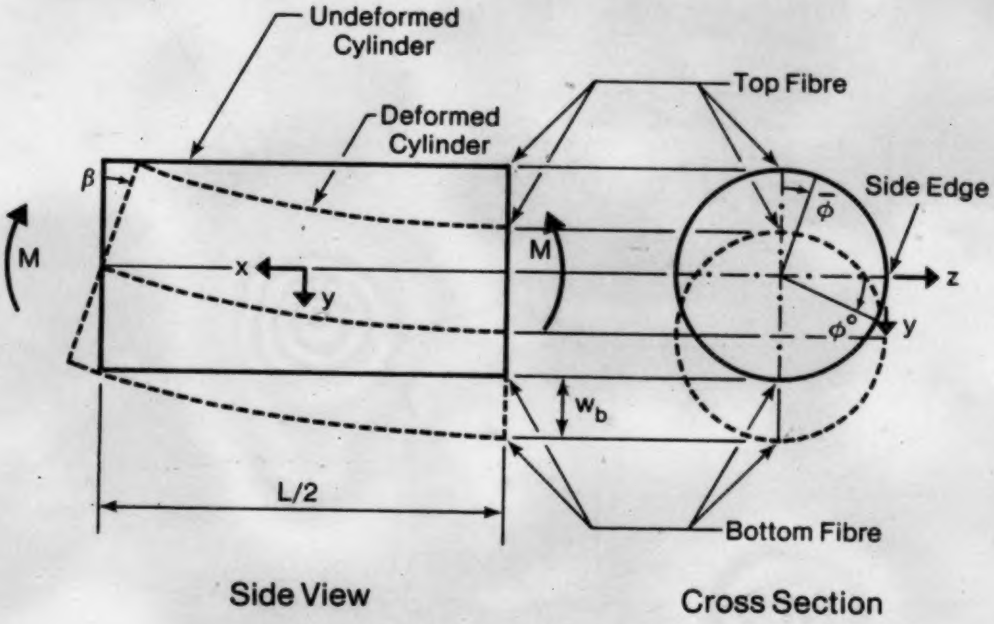
Undeformed Cylinder
Deformed Cylinder
Top Fibre
Side Edge
β
M
x
y
M
$\bar{\phi}$
z
ϕ°
y
w_b
L/2
Bottom Fibre
Side View
Cross Section

Fig. 4.2: Left Half of Cylinder under Bending with Linearized Boundary Conditions.

The boundary condition at the left cylinder end is determined by the end rotation β. The cylinder cross-section at the end is taken to be rigid and rotates as a plane without change in the circular shape. It is assumed that higher orders in the rotation β are negligibly small for a linearized theory. The resulting displacements and rotations at the end section are shown below to first order in β.

$$\begin{aligned} u &= -R\,\beta\cos(\bar{\phi}), \\ v &= 0, \\ w &= 0, \\ \beta x &= \beta\cos(\bar{\phi}), \\ \beta\phi &= 0. \end{aligned} \qquad (4.1)$$

The exact end conditions, including nonlinear terms, are discussed in section 5.5.3.

A closed form solution for the linear bending problem is given by Donnell[22]. After transformation to the coordinate system in Fig. 4.2, it becomes

$$u = 0.50\,\beta\,R\sin(\phi^{\circ})(1 + 4x/L), \qquad (4.2a)$$

$$v = 0.25\,\beta\,L\cos(\phi^{\circ})(3/4 - 2x/L - 4x^2/L^2 + 8\nu R^2/L^2), \qquad (4.2b)$$

$$w = 0.25\,\beta\,L\sin(\phi^{\circ})(3/4 - 2x/L - 4x^2/L^2). \qquad (4.2c)$$

For this solution the top and bottom points at the cylinder end are fixed vertically. The cross-section at the cylinder end is no longer rigid since the last term in

Eq. 4.2b causes displacements tangential to the local circumferential coordinate $\bar{\phi}$.

The corresponding strains are computed using Eq. 2.8:

$$\epsilon_x = 2\,\beta\,R/L\,\sin(\phi^\circ), \tag{4.3a}$$

$$\epsilon_\phi = -\,2\,\nu\,\beta\,R/L\,\sin(\phi^\circ), \tag{4.3b}$$

$$\gamma_{x\phi} = 0, \tag{4.3c}$$

$$k_x = 2\,\beta/L\,\sin(\phi^\circ), \tag{4.3d}$$

$$k_\phi = -\,2\,\nu\,\beta/L\,\sin(\phi^\circ), \tag{4.3e}$$

$$k_{x\phi} = 0. \tag{4.3f}$$

The stresses are then defined with Eq. 3.8.

$$\sigma_x = 2\,E\,\beta\,(R+z)/L\,\sin(\phi^\circ), \tag{4.4a}$$

$$\sigma_\phi = 0, \tag{4.4b}$$

$$\tau_{x\phi} = 0. \tag{4.4c}$$

The relationship between Donnell's solution and the common beam stresses can be clearly seen in the equations above. The stresses are the same as those predicted by beam theory. With $\nu=0$ in the displacement function (Eq. 4.2) the cylinder behaves like a simple beam. That is, the circular cross-section is not deformed.

With zero circumferential stress, the circumferential strain ϵ_ϕ is $-\,\nu\,\epsilon_x$. The strain ϵ_ϕ has its maximum values at the top and bottom of the cylinder and is zero at the cylinder side. The positive circumferential strain in the upper cylinder half and the negative strain in the lower half cause individual points of the cross-section to move circumferentially towards the bottom. These circumferential displacements are zero at the top and bottom fibre and have their maximum value at the side of the cylinder.

For later convenience a measure of the effect of the circumferential stretching is defined. This is the difference between the vertical movement of the cylinder side and the deflection of the top fibre. This difference is denoted as Δv. The Donnell solution predicts the circumferential stretching as

$$\Delta v = (8\ \nu\ R^2/L^2)\ wb,$$

$$wb = \beta\ L/4.$$

For long cylinders Δv is quite small, but it is significant for relatively short cylinders. For a cylinder with the geometry of the cylinder being tested by Stephens[37] ($R/L = 764.5/1829$), Δv is 42 % of wb. A better insight into the effects of Δv is gained if it is expressed as a function of the end rotation β. The rotation at which the classical buckling stress σcr occurs, assuming linear bending theory, is

$$\beta cr = t\ L/2R^2[3(1-\nu^2)\ ]^{-1/2}. \qquad (4.5)$$

$$\Delta v = (2\ \nu\ R^2/L)\ \beta,$$

$$= (\nu\, t\, [3(1-\nu^2)]^{-1/2})\ (\beta/\beta cr). \qquad (4.6)$$

For $\nu=0.3$ and $\beta=\beta cr$, Δv is equal to 0.182 t.

The circumferential strain $\epsilon\phi$ for this Δv is 0.182 t/R at the top fibre when the elastic buckling moment *M*cr has been reached. If Δv is prevented at the ends due to rigid plates then a circumferential compressive stress equal to ν times the longitudinal stress develops. In a structural test this can lead to an outward buckle along the end plate of the cylinder.

4.2.2 Element Approximation of Cylinder under Bending

In the preceding section it was shown that the linear solution for the displacements of a cylinder under bending consists of products of simple trigonometric functions in the coordinate ϕ° (Fig. 4.2) and quadratic polynomials in the longitudinal coordinate x. If the semi-circumference is divided into several elements, the coordinate ϕ° can be expressed by the local element coordinate ϕ and the angle α between the side edge and the origin of the element coordinate:

$$\phi^\circ = \alpha + \phi.$$

With above expression introduced into Eq. 4.2, the addition formulas of trigonometry result in there being a combination of $\sin\phi$ and $\cos\phi$ terms in the displacement fields. Some of these terms in the displacement function cannot be represented exactly by the assumed displacement field (Eqs. 3.1) of the element. A list of terms occuring in the Donnell solution is given in Table 4.3 and compared with the available parameters of the element displacement functions.

Table 4.3: Approximations of the Element Displacement Field.

Displacement	terms in Donnell solution	terms in the element displacement field	Nature of the approximation
u	$\sin\phi$ $x\sin\phi$ $\cos\phi$ $x\cos\phi$	$\alpha_4\sin\phi$ $\alpha_8 x\sin\phi$ $\alpha_2\cos\phi$ $\alpha_7 x$	exact exact exact o.k. for $\cos\phi \cong 1$
v	$\cos\phi$ $x\cos\phi$ $x^2\cos\phi$ $\sin\phi$ $x\sin\phi$ $x^2\sin\phi$ $v\cos\phi$ $v\sin\phi$	$\alpha_3\cos\phi$ $\alpha_4 x\cos\phi$ $\alpha_8 x^2\cos\phi$ $\alpha_1\sin\phi$ $\alpha_2 x\sin\phi$ † α_6 ‡ ‡	exact exact exact exact exact o.k. for $x<<L$ o.k. for $\cos\phi \cong 1$ o.k. for $\sin\phi \cong 0$
w	$\sin\phi$ $x\sin\phi$ $x^2\sin\phi$ $\cos\phi$ $x\cos\phi$ $x^2\cos\phi$	$\alpha_3\sin\phi$ $\alpha_4 x\sin\phi$ $\alpha_8 x^2\sin\phi$ $\alpha_1\cos\phi$ $\alpha_2 x\cos\phi$ $\alpha_{12} x^2$	exact exact exact exact exact o.k. for $\cos\phi \cong 1$

---

† No term appears, because there is no term in the displacement field for v which has a factor of $x^2\sin\phi$.

‡ '$v\cos\phi$' and '$v\sin\phi$' represent the circumferential strain predicted by Donnell which is independent of the displacements for u and w. The parameters α_1 and α_3 occur as rigid motions in the displacement function for w too, and are therefore not suitable for these two terms.

Table 4.3 indicates that the exact functions for *u* and *w* are well represented by the element displacement fields for small angles, and the term '$v\cos\phi$' for *v* can be approximated for shallow elements by the rigid element rotation around the revolution axis. For one element per half circumference the element coordinate ϕ coincides with ϕ°, and *u* and *w* are exactly represented. The boundary conditions for this case force α_4 to zero which thereby causes Δv to be zero.

The approximations of $\cos\phi$ with 1 and $\sin\phi$ with 0 are worst for two elements per semi-circumference ($p = 45°$) and improve with grid refinement.

For the terms '$v\sin\phi$' and '$x^2\sin\phi$' in *v*, there are no corresponding terms in the element displacement functions. This suggests that a large number of elements is needed to keep the error by the approximation for $\sin\phi$ and $\cos\phi$ in an reasonable range. An element refinement in the longitudinal direction reduces the errors arising from the approximation of displacement terms involving x and x^2.

Summarizing the above discussion it can be said that the element should work well for the linear problem of a cylinder under bending. However, one must be careful in selecting an element gridwork to keep the approximations of the displacement field in an reasonable range.

4.2.3 Results of Linear Tests

In order to evaluate the performance of the present finite element and the influence of the boundary conditions, two cylinders are chosen for the linear bending problem. The two different boundary conditions considered are:

1. rigid ends, as described in section 4.2.1 with $v = w = \beta\phi = 0$,
2. semi-rigid ends, which allow the stretching predicted by the Donnell solution to occur at the cylinder end. That is, v, w, and $\beta\phi$ are free which allows a distortion of the cross-section. Nevertheless, the circular cross-section remains plane since out-of-plane forces do not apply.

In addition to a cylinder of the same geometry as that tested (Stephens[37]) another cylinder was also examined. The large L/R ratio was chosen in order to study whether the effects of the boundary conditions at the cylinder end would be less than those of the short cylinder. The data is given in Table 4.4.

Table 4.4: Cylinder Data for Linear Bending Test.

	Long cylinder	Short cylinder
Length (mm)	2500	1829
Radius (mm)	90	764.5
Wall thickness (mm)	1.1	5.13
Ratio L/R	27.7	2.39
Ratio R/t	81.8	149
Young's modulus (MPa)	200000	202016
Poisson's ratio	0.3	0.3
End rotation	0.01	0.000485808
Beam deflection (mm)	6.25	0.222136
Donnell solution Δv(mm)	0.01944	0.093145
Beam moment (kNm)	4.03079	802290

The element meshes chosen for the quarter cylinder modelled range from 1×1 to 10×10 elements, but were concentrated on even numbers for the circumferential division (NP) in order to facilitate calculation of the parameter Δv.

In all cases for NP=1, the results obtained are as indicated earlier in the last chapter. That is, the boundary conditions at the top and bottom prevent any circumferential stretching. If the displacements computed are expressed in terms of the parameters α_i, the deflections can be shown to correspond to the Donnell solution with $\nu=0$. The latter coincides with the beam theory. The moment calculated is found to be 9.89 % higher than the beam theory would predict. This reflects a factor of $1/(1-\nu^2)$, caused by the restriction of Δv. A solution for the long cylinder was also obtained with $\nu=0$ and it gives a bending moment equal to that from beam theory thus verifying the factor of $1/(1-\nu^2)$. The moments calculated are accurate to 5 digits, and for the deflections no difference could be detected from the beam theory.

The first cylinder investigated is the long cylinder, whose maximum bottom fibre deflection, stretching at the mid-section and end moment are shown for different mesh sizes in Tables 4.5 to 4.7.

Table 4.5: Ratio of Bottom Fibre Centre Deflection to Beam Theory for Long Cylinder with Rigid Ends.

NX \ NP	2	4	6	8	10
2	1.18	1.24	1.26	1.27	1.27
4	1.033	1.051	1.052	1.054	1.054
6	1.008	1.014	1.014	1.014	1.014
8	1.0024	1.0050	1.0050	1.0051	1.0051
10	1.0006	1.0019	1.0018	1.0017	1.0017

Table 4.6: Ratio of End Moment to Beam Theory for Long Cylinder with Rigid Ends.

NX \ NP	2	4	6	8	10
2	0.724	0.539	0.510	0.496	0.481
4	0.801	0.828	0.843	0.849	0.851
6	0.857	0.940	0.963	0.971	0.976
8	0.875	0.978	1.004	1.013	1.018
10	0.882	0.994	1.021	1.032	1.035

Table 4.7: Ratio of Computed Δv to Donnell Solution for Long Cylinder with Rigid Ends.

NX \ NP	2	4	6	8	10
2	-6.7	20	20	20	20
4	3.6	4.5	4.6	4.7	4.7
6	2.2	2.4	2.5	2.5	2.5
8	1.6	1.7	1.8	1.8	1.8
10	1.3	1.5	1.5	1.5	1.5

Table 4.5 shows that the deflection for the cylinder middle converges to the beam deflection with an increasing number of elements in the longitudinal direction. A similar convergence is found for the stretching of the mid-section of the cylinder, shown in Table 4.7. The moment converges with finer element divisions in both x and ø direction to a

value above the beam moment, which reflects the stiffening effect of the rigid ends. As mentioned earlier, this restraint results in circumferential stresses, which are relieved by an upward moving of the cylinder and an emphasized stretching near the cylinder ends. Figure 4.3 shows the difference of the variation of slope between the 10×10 element mesh and the beam theory (the differences in deflections are less illustrative), and the variation of circumferential stretching versus the distance from the cylinder end in the longitudinal direction is plotted in Fig. 4.4.

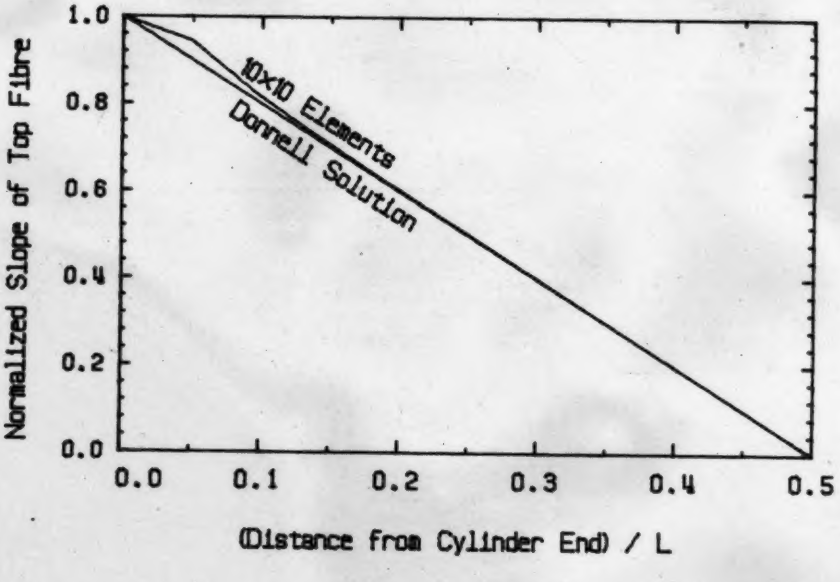

Fig. 4.3: Slope Variation of Long Cylinder with Rigid Ends.

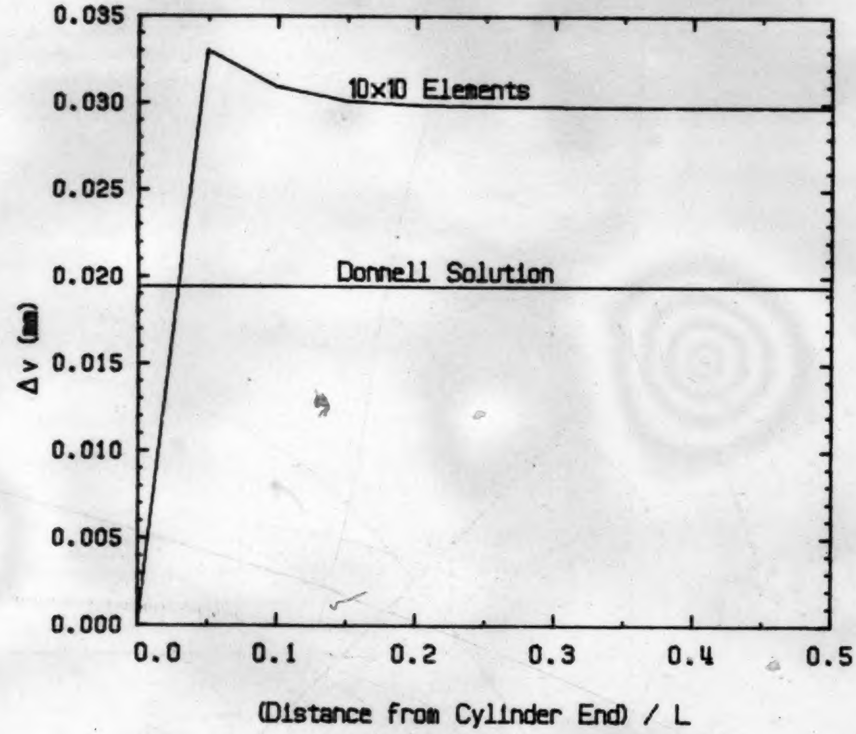

Fig. 4.4: Variation of Parameter Δv for Long Cylinder with Rigid Ends.

The second boundary conditions, referred to earlier as semi-rigid ends, were introduced to see if these boundary conditions would better represent the cylinder behaviour associated with the Donnell solution. The ratios of the resulting end moment and the paramter Δv for the long cylinder are shown in Table 4.8 and 4.9.

Table 4.8: Ratio of End Moment to Beam Theory for Long Cylinder with Semi-Rigid Ends.

NX \ NP	2	4	6	8	10
2	-0.020	-0.200	-0.245	-0.262	-0.269
4	0.632	0.666	0.673	0.676	0.671
6	0.746	0.827	0.844	0.850	0.852
8	0.785	0.883	0.903	0.910	0.914
10	0.804	0.909	0.931	0.939	0.942

Table 4.9: Ratio of Computed Δv to Donnell Solution for Long Cylinder with Semi-Rigid Ends.

NX \ NP	2	4	6	8	10
2	12	14	14	14	14
4	3.6	4.1	4.3	4.3	4.3
6	2.1	2.4	2.4	2.5	2.5
8	1.53	1.75	1.80	1.81	1.82
10	1.28	1.46	1.50	1.52	1.52

A similar table for deflections is not given for this case since the top and bottom fibre deflections are the same as predicted by the beam theory and the Donnell solution. The stretching is found to be constant along the cylinder length as predicted by Donnell and is a little better estimated than for the cylinder with rigid ends. The moment convergences towards the beam solution, but shows quite unexpectedly poor values for less than 6 elements in the longitudinal direction.

For the second cylinder, which has a much lower L/R ratio than the first (2.4 versus 27.8), the circumferential stretching is expected to be more significant than for the long cylinder. The results for deflection, the paramter Δv, and moment of the cylinder with the rigid ends are given in Tables 4.10 to 4.12.

Table 4.10: Ratio of Bottom Fibre Deflection to Beam Theory for Short Cylinder with Rigid Ends.

NP / NX	2	4	6	8	10
2	2.455	0.621	0.549	0.535	0.528
4	1.454	0.640	0.607	0.594	0.588
6	0.998	0.632	0.606	0.596	0.591
8	0.857	0.629	0.605	0.596	0.591
10	0.808	0.627	0.604	0.596	0.592

Table 4.11: Ratio of Computed Δv to Donnell Solution for Short Cylinder with Rigid Ends.

NP NX	2	4	6	8	10
2	-5.67	1.070	1.192	1.197	1.201
4	-1.83	1.000	1.010	1.021	1.025
6	-1.05	0.967	0.994	1.004	1.009
8	0.368	0.961	0.989	0.999	1.003
10	0.546	0.958	0.986	0.996	1.001

Table 4.12: Ratio of End Moment to Beam Theory for Short Cylinder with Rigid Ends.

NP NX	2	4	6	8	10
2	0.902	1.029	1.058	1.069	1.074
4	0.892	1.021	1.049	1.060	1.064
6	0.887	1.015	1.041	1.050	1.055
8	0.883	1.010	1.033	1.042	1.046
10	0.880	1.007	1.027	1.034	1.038

The bending moment is found to converge in a manner similar to that for the long cylinder to a value above the beam moment. The stretching tends to a value near Donnell's prediction. The deflections appear at first to be unusually small since they converge to around 0.585 times the beam deformation. The reason for the relatively small displacements becomes clear from inspection of the deflected shape of the cylinder, shown in Fig. 4.5.

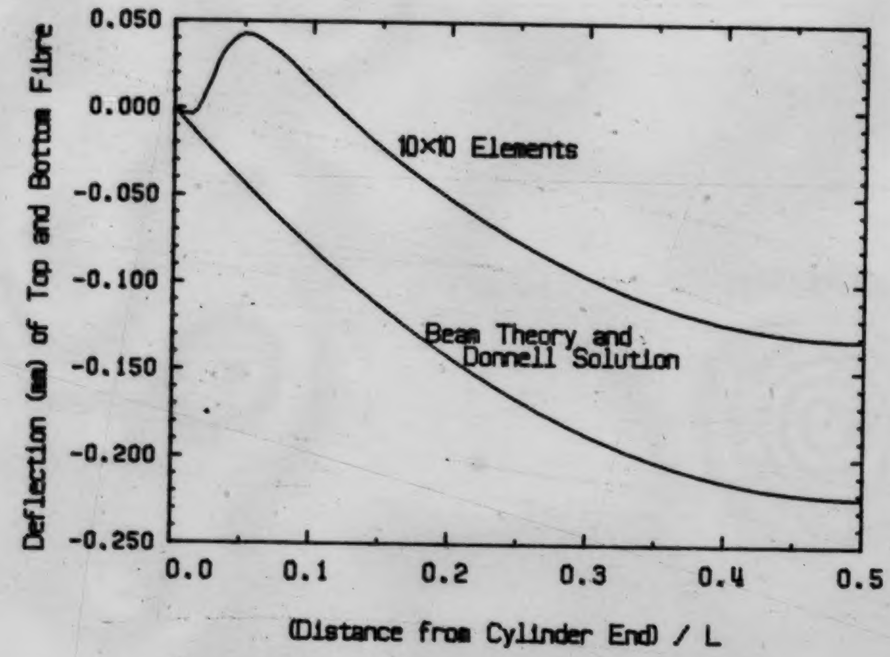

Fig. 4.5: Deflection of Short Cylinder with Rigid Ends.

In addition to the deflection predicted by the beam theory the inner part of the cylinder undergoes essentially a rigid body motion in the direction opposite to the bending deflection. This upward displacement is 0.091 mm and can be attributed to the circumferential stress caused by the restraint of the rigid ends. The similar numerical values for this displacement and for Δv (0.093 mm in Table 4.4) suggests that as the element grid is refined, the magnitude

of this rigid body displacement should approach the value of Δv from the Donnell solution. Flügge[25] predicted a similar outward deformation for the ends of axially compressed cylinders. He showed this disturbance to occur within a distance of circa $(Rt)^{1/2}$, which for the short cylinder is 62 mm. Since for the finest element mesh used, the shell element length is 91 mm, the displacement fields can only approximate the localized curvature. In order to study the upward movement in detail, the end region should be modelled with at least one or two elements. The deflections of the long cylinder are less affected by the rigid ends. However, the induced strains and stresses cannot be neglected.
The use of long elements (125 mm long for a 10×10 element mesh) is not adequate for the region affected by the end constraint (ca. 10 mm). The long elements force the stretching to develop farther away from the cylinder end and therefore influence the deflections of the cylinder over a larger region and increase the rotational stiffness.

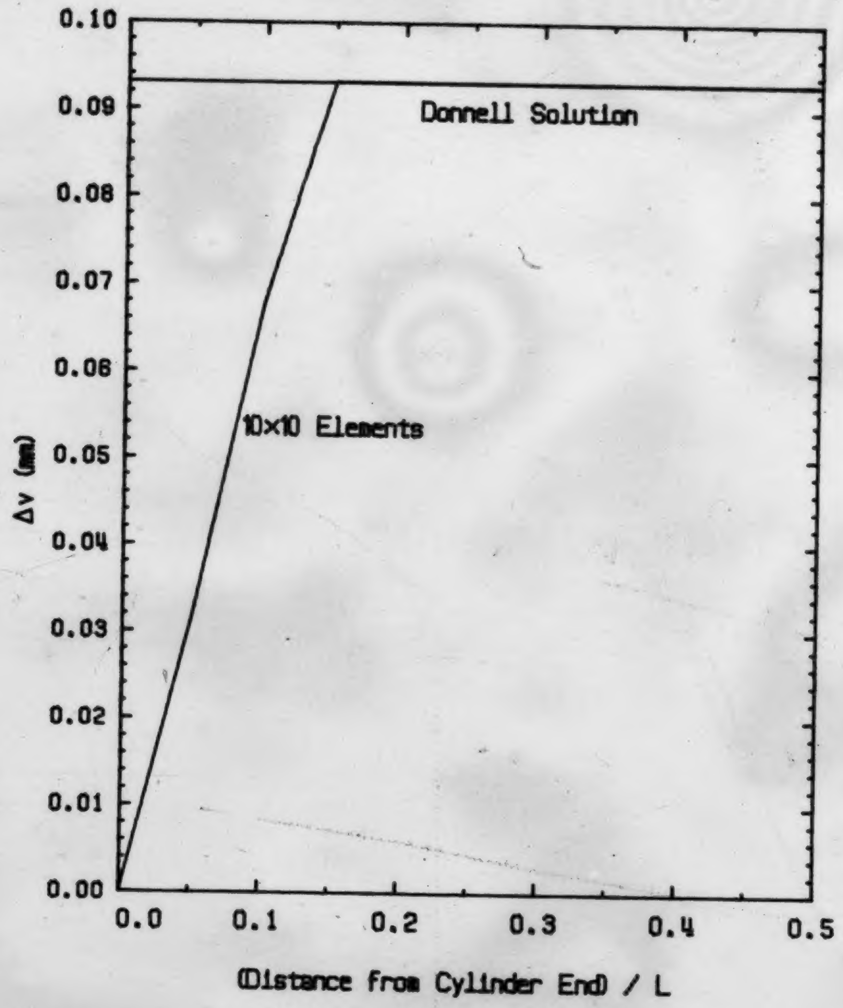

Fig. 4.6: Variation of Δv of Short Cylinder with Rigid Ends.

Fig. 4.6 shows the convergence of Δv to Donnell's prediction: At the cylinder ends Δv is zero and the transition region for Δv encompasses the first three elements in the axial direction.

With the application of the semi-rigid boundary conditions, results similar to those for the long cylinder are obtained: Δv is constant over the cylinder length and the deflections correspond exactly to the beam theory.

The variation of Δv and the end moment with the element mesh are given in Tables 4.13 and 4.14.

Table 4.13: Ratio of Computed Δv to Donnell Solution for Short Cylinder with Semi-Rigid Ends.

NX \ NP	2	4	6	8	10
2	0.917	1.045	1.075	1.085	1.090
4	0.856	0.974	1.002	1.012	1.016
6	0.845	0.961	0.988	0.998	1.003
8	0.841	0.957	0.984	0.993	0.998
10	0.839	0.955	0.982	0.991	0.996

Table 4.14: Ratio of Cylinder Moment to Beam Moment for Short Cylinder with Semi-Rigid Ends.

NX \ NP	2	4	6	8	10
2	.8302	.9465	.9706	.9792	.9833
4	.8348	.9529	.9774	.9862	.9903
6	.8356	.9551	.9787	.9875	.9916
8	.8359	.9546	.9791	.9879	.9920
10	.8360	.9547	.9793	.9881	.9923

As opposed to the long cylinder, the moment, Δv, and the deflections converge to the values of Donnell's solution with an increasing number of elements in the circumferential direction. For a given total number of elements the long and the short cylinders have different 'optimal' mesh sizes. For the long cylinder the best ratio of NX to NP is 10:2, and for the short cylinder NX:NP is around 4:10. For both cases a good mesh seems to be that one when the curved sides of the elements are as long as the longitudinal dimension. The exact mesh-ratios for equilateral elements would be for the long cylinder (NX:NP) 10:2.26 and for the short cylinder 3.81:10.

It is interesting to note that the so called 'optimal' meshes discussed above have the least total inter-element boundary length for a fixed number of elements. If one could assume that the effects of element nonconformity are contributed similarly for circumferential and longitudinal inter-element boundaries and that the total effect is dependent on the total inter-element boundary length, then it follows that meshes with equilateral elements would suffer the least due to nonconformity.

The results discussed above show that grid meshes with equilateral elements give the best results for a given number of elements. Rigid ends cause the circumferential strain predicted by Donnell to be developed by the elements near the cylinder end. Thereby the cylinder undergoes an upward lifting equal to Δv. For short cylinders this effect is large compared with the deflections from beam theory, whereas the deflections of long cylinders are less affected. Unfortunately, the circumferential stretching has not been reported yet from structural tests, so that it could be compared to the results obtained in this study.

In the preceding section it is shown that the element displacement field of the present element approximates the displacements of a cylinder under bending for sufficiently small element dimensions. The best results for the linear bending problem were obtained with about equilateral elements. It is shown that the cylinder is significantly influenced by the boundary conditions at the cylinder end. If the nodal points at the circumference between the top and bottom fibre are free to move along the circumference and to rotate around the local longitudinal axis (semi-rigid cylinder end) the top and bottom fibre deflections of the cylinder correspond exactly to the beam theory and the circumferential stretching is constant with respect to the cylinder length.

Rigid cylinder ends prevent circumferential strain at the cylinder end and thereby cause circumferential stresses which are relieved towards the cylinder middle by an upward movement of the cylinder in a direction opposite to the bending deflections.

In real cylinders, boundary conditions are neither rigid nor 'semi-rigid' but lie somewhere in between and one has to decide which boundary condition comes nearest to structural reality.

5. Nonlinear Problems

5.1 Introduction

The geometric nonlinear behaviour of circular shell elements has been studied mostly using cylindrical arch, panel, and barrel vault problems [24,27-29,35]. The pure bending of finite cylinders, which represents the main part of this chapter, has been analyzed mostly by using half-analytical methods and finite difference techniques [24,25,36,38].

In order to test the program developed for this study and to evaluate the performance of the shell element it is first tested on cylindrical arches and barrel vaults. For simplicity only concentrated loads are considered. Then the rigid body motions occuring in a cylinder under bending are examined and the resulting induced strains for the present element are discussed. Finally the problem of a cylinder under bending is examined and results obtained with the present shell element are discussed.

5.2 The Circular Arch

Sabir and Lock[34] investigated the geometric nonlinear behaviour of a circular arch element on arches with R/t ratios ranging from 43 to 500. The other data for the arches studied are:

$L = 100$ in.,
$E = 10^7$ psi.,
$A = 1$ in.^{2} as area of cross-section,
$I = 1$ in.^{4} as moment of inertia of cross section,

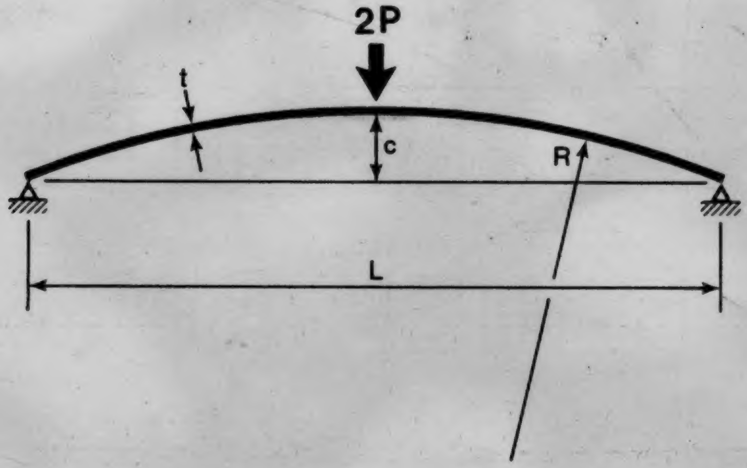

Fig. 5.1: Circular Arch under Concentrated Load.

For one particular arch Sabir and Lock expected horizontal and vertical tangents in the load-deflection curve. In order to follow the equilibrium path through these regions, they employed a procedure which switched automatically from load to displacement control and vice versa. For an arch with R/t=500 Sabir and Lock demonstrated that an increasing number of elements reduces the load significantly. A reason for this is that the element can only represent a linear change of curvature (compare Eq. 3.2e). Localized changes in slope for deep arches (the maximum deflection for the deepest arch was 10 % of the radius) might require a very fine mesh.

In the present study the shell thickness and the element length were chosen to give the same cross-section properties as the arches of Sabir and Lock[34]. In order to simulate the displacement field used by Sabir and Lock the displacements corresponding to the longitudinal axis and Poisson's ratio are set to zero. Neglecting the parameters corresponding to the x-coordinate, the displacement field used by Sabir and Lock is obtained.

For the nonlinear strains Sabir and Lock assumed

$$\epsilon\phi = (v_{,\phi}+w)/R + 1/2\ \beta\phi^2,$$
$$\beta\phi = w_{,\phi}/R. \qquad (5.1)$$

Compared with $\beta\phi=(w_{,\phi}-v)/R$ used in the present study, the expressions above correspond to a more 'shallow' theory. As done by Sabir and Lock, the nonlinear strain terms involving $\beta\phi_2$ and βx_1 are set to zero. Since the circular arch is a plane structure, the strain terms βx_2, βx_3, and

$\beta\phi$, should be zero. However, the displacement field (Eqs. 3.1) causes these strain terms to have nonzero values that are assumed to be negligibly small.

The program developed for this study allows either displacement control or load control. For the arch problem prescribed displacements are used. Thus only part of the equilibrium path can be obtained. The recalculation of the tangent stiffness matrix during the equilibrium iteration is found to take about the same time as the computation of the equilibrium forces, so that the full Newton-Raphson method is used.

Using symmetry, only one half of the arch needs to be modelled for which ten elements were used. The load-deflection curves obtained are given in Fig. 5.2 and 5.3.

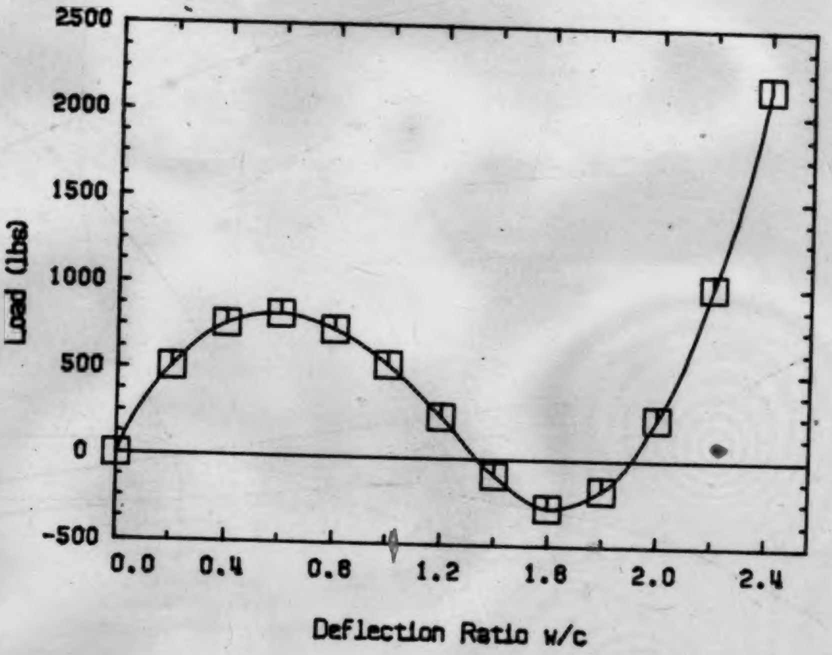

Fig. 5.2: Load Deflection Curve for Cylindrical Arch (R=250 in.) under Concentrated Load.

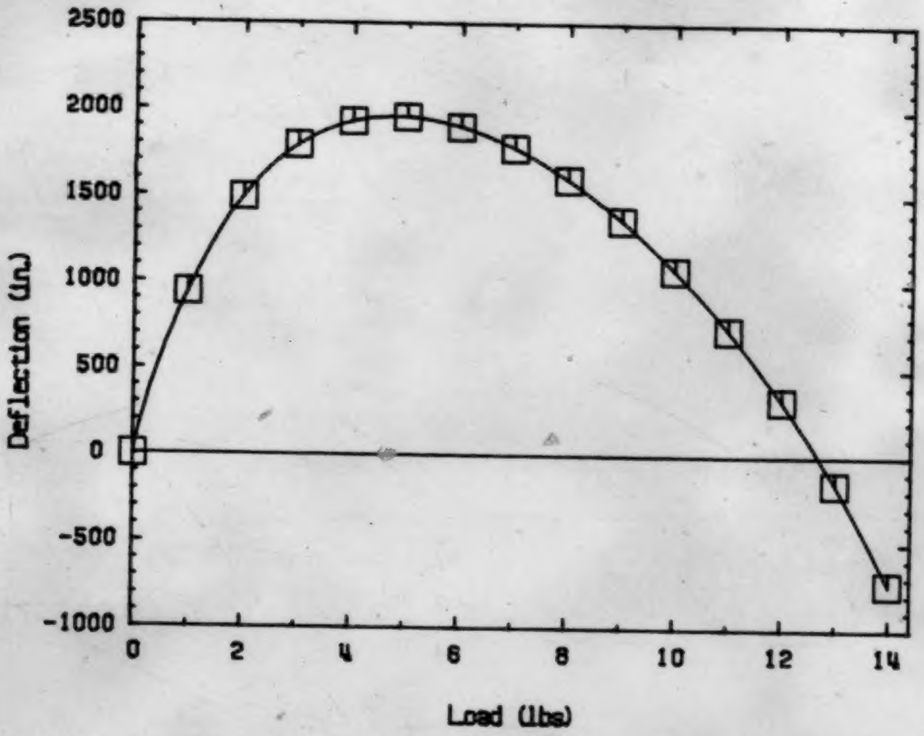

Fig. 5.3: Load Deflection Curve for Cylindrical Arch (R=150 in.) under Concentrated Load.

The results obtained are similar to those of Sabir and Lock except that the equilibrium path is slightly above theirs. This difference can be attributed not only to the more general strain expressions used herein but also to a different element mesh. Unfortunately a conclusive comparison is not possible because Sabir and Lock do not identify the element gridwork used. Due to the high computing costs associated with nonlinear problems, a convergence study with finer element meshes is not done. That study would be necessary to determine the influence, if any, of the different strain displacement expression used here.

Table 5.1: Loads (lbs) for Prescribed Deflections of Two Cylindrical Arches.

Δ (in.) or 5w/c	R=250 in.	R=150 in.
1	939.6	507.8
2	1489	759.7
3	1789	819.3
4	1927	734.3
5	1954	535.0
6	1898	241.2
7	1776	- 94.83
8	1596	-281.1
9	1362	-174.8
10	1074	242.1
11	730.0	1003.6
12	323.2	2159.0
13	-157.6	—
14	-734.5	—

5.3 The Barrel Vault Problem

After Sabir and Lock[34] applied the geometric nonlinear theory to arches, they tested various cylindrical shell formulations for a barrel vault under external pressure. Since the strain element by Ashwell and Sabir[4] showed the best convergence, the element was subsequently used for the problem of a point loaded barrel vault as shown in Fig. 5.4.

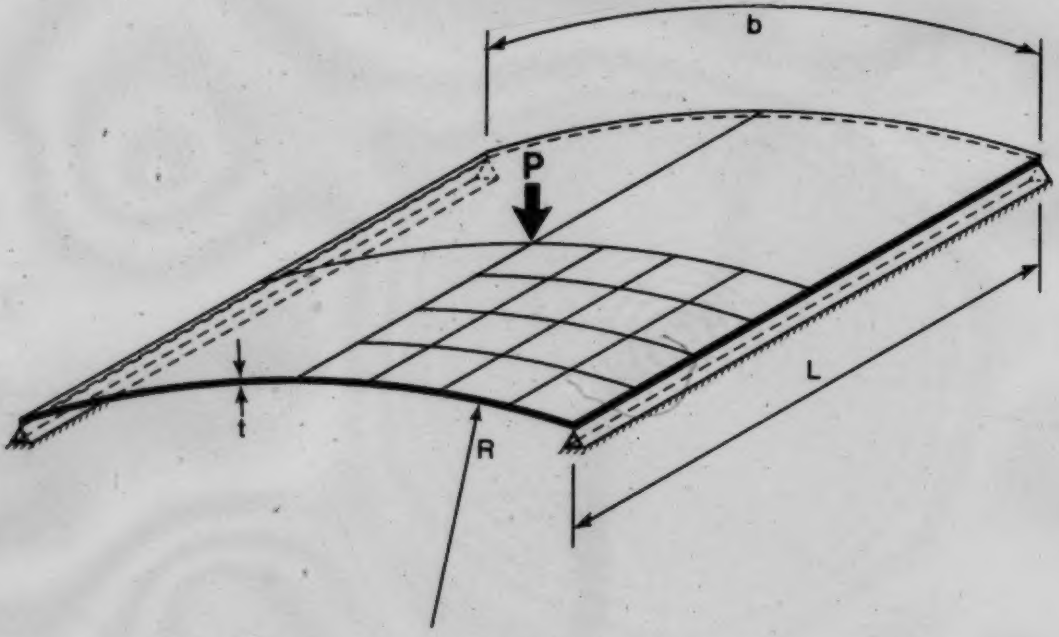

Fig. 5.4: Hinged Barrel Vault under Single Load.

The data for the cylindrical panel are:

L = 20 in.,

R = 100 in.,

b = 20 in.,

$t = 1$ or 0.5 in.,

$E = 450000$ psi,

$\nu = 0.3$.

For the computation, one quarter of the panel is divided into 4×4 elements. The curved edges are free and the longitudinal edges are hinged, with rotation about the longitudinal axis the only movement allowed. Since the load deflection curve is expected to exhibit horizontal tangents, the vertical displacement under the load P is prescribed in steps of 0.1 inches as in Ref. 35.

As in their study, the nonlinear strain terms βx_1, βx_2, $\beta \phi_1$, and $\beta \phi_2$ are assumed to be negligibly small. The load-deflection curves obtained follow the published curves of Sabir and Lock[35]. A more detailed comparison is difficult since the actual numerical results obtained by Sabir and Lock were not published. The results of the present study are given in Table 5.2.

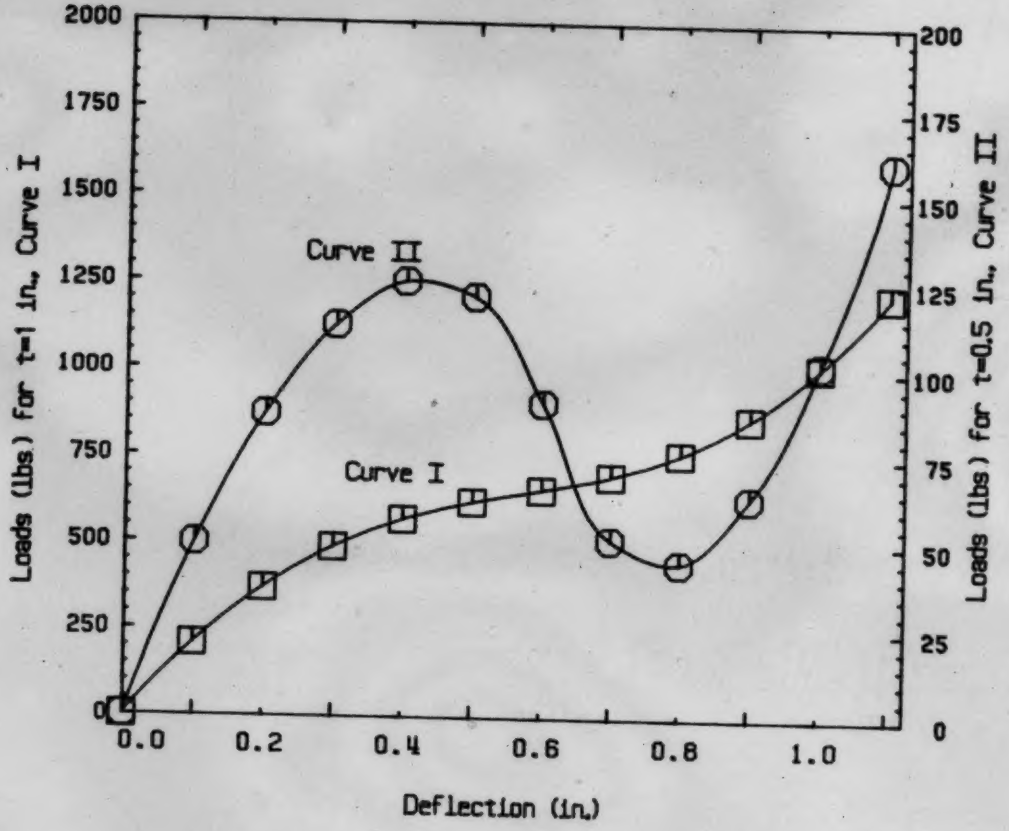

Fig. 5.5: Load Deflection Curve of a Hinged Barrel Vault under Single Load.

Table 5.2: Loads for Prescribed Deflections of a Hinged Barrel Vault under Single Load.

Deflection	Load P (lbs)	
Δ (in.)	t=1 in.	t=0.5 in.
0.1	207.8	49.84
0.2	369.7	87.17
0.3	488.7	112.6
0.4	569.5	125.2
0.5	621.0	121.0
0.6	657.7	90.60
0.7	698.6	51.44
0.8	762.9	44.78
0.9	865.5	63.56
1.0	1016	102.3
1.1	1219	160.1

5.4 Nonlinear Strains and Rigid Body Motions

As shown in the previous chapters the finite element displacement fields used include rigid body motions associated with the linear strain displacement equations. With the inclusion of the nonlinear strain terms certain rigid body motions are no longer properly represented. Introducing rigid translations along any of the $\bar{x}$, $\bar{y}$, or $\bar{z}$ axes (see Fig. 2.2) into Eq. 3.13 gives zero strains. These motions are therefore properly represented.

The rotations around the $\bar{x}$, $\bar{y}$, and $\bar{z}$ axes are discussed for small rotations in section 2.3. With the introduction of the exact displacements some of the rotations cannot be exactly represented by the element and may cause significant strains for even relatively small rotations. This problem is analyzed in further detail below.

5.4.1 Rotation around the $\bar{x}$-Axis

A rotation about the $\bar{x}$-axis occurs for elements at the-side of a cylinder under bending, since the vertical movement of the sides is larger than that at the top or bottom of the cylinder. If the magnitude of the rotation is Δ, then the corresponding displacements are given by

$$u = 0, \tag{5.2a}$$

$$v = R \sin\Delta, \tag{5.2b}$$

$$w = -R(1-\cos\Delta). \tag{5.2c}$$

This motion is represented exactly by the element displacement field and therefore does not induce any strains.

5.4.2 Rotation around the $\bar{y}$-Axis

A rotation about the $\bar{y}$-axis occurs at the top and bottom fibre of a cylinder under bending and is largest at the ends of the cylinder.

The theoretical displacements for a rigid body motion of a cylindrical element are given below for a rotation of magnitude Δ.

$$u = R \sin\Delta \cos\phi - x\,(1-\cos\Delta)\ , \tag{5.3a}$$

$$v = x \sin\Delta \sin\phi + R(1-\cos\Delta)\,[\sin\phi \cos\phi], \tag{5.3b}$$

$$w = -\,x \sin\Delta \cos\phi - R(1-\cos\Delta)\,[\cos^2\phi]. \tag{5.3c}$$

The terms in square brackets cannot be represented by the element displacement fields, since neither v nor w have the required trigonometric terms. The finite element displacement fields determined by setting the nodal displacements to values consistent with Eqs. 5.3, are

$$u = R \sin\Delta \cos\phi - x\,(1-\cos\Delta)\ , \tag{5.4a}$$

$$v = x \sin\Delta \sin\phi + R\,(1-\cos\Delta)\,[\cos(p)\{2\sin\phi-\phi\sin(p)/p\}], \tag{5.4b}$$

$$w = -\,x \sin\Delta \cos\phi - R\,(1-\cos\Delta)[\cos(p)\{2\cos\phi-\cos(p)\}]. \tag{5.4c}$$

It is seen that u is exactly represented, and v and w are quite well approximated for a larger number of elements in the circumferential direction.

With Eqs. 3.13 we obtain for the induced strains:

$$
\begin{aligned}
\epsilon_x &= -(1-\cos\Delta)+1/2(1-\cos\Delta)^2+1/2\,\sin^2\Delta \\
&= 0, \\
\epsilon_\phi &= (1-\cos\Delta)f+1/2\,\sin^2\Delta\sin^2\phi+\,1/2\,[(1-\cos\Delta)f]^2 \\
&\quad +\,1/2\,[(1-\cos\Delta)\sin(p)\,\cos(p)\,\phi/p])^2, \\
\gamma_{x\phi} &= (1-\cos\Delta)\sin\Delta\,[1\,-2/3\,p^2\sin\phi\,-\sin(p)\,\cos^2(p)\phi/p], \\
k_x &= 0, \\
k_\phi &= (1-\cos\Delta)\sin(p)\cos(p)/pR, \\
k_{x\phi} &= 0, \qquad\qquad (5.5)
\end{aligned}
$$

with $f = \cos(p)[p\,\cos(p)-\sin(p)]/p$.

With the assumption that higher terms in Δ are negligibly small relative to other terms the strain expressions are simplified:

$$\epsilon_\phi \cong \Delta^2\,d,$$

where d is a function of ϕ and p.

$$
\begin{aligned}
\gamma_{x\phi} &= O(\Delta^3), \\
k_\phi &= O(\Delta^2).
\end{aligned}
$$

The strain $\gamma_{x\phi}$ is of higher order in Δ and can be therefore neglected if compared to ϵ_ϕ. The curvature k_ϕ gives a maximum circumferental strain of about '$t \cdot \Delta^2/4R$', which can be neglected for large R/t ratios.

Taking the centre rotation of the finite element as the rigid body rotation, the rotation for the top element at the cylinder end is:

$$\Delta = \beta cr \cos(\pi/2NP)\ (1-1/2NX). \qquad (5.6)$$

For a fine element mesh the factor (1-1/2NX) can be approximated by 1.

The strain $\epsilon\phi$ induced by the rigid body motion is denoted by $\epsilon\phi^+$. It is compared to the longitudinal strain which causes the classical buckling stress σcr.

$$\epsilon\phi^+ \cong d/2\ [\beta cr \cos(\pi/2NP)]^2. \qquad (5.7)$$

Assuming ν as 0.3, $\epsilon\phi^+$ can be expressed in terms of the critical buckling strain:

$$\epsilon\phi^+ \cong d\ (tL^2\epsilon cr/13.22R^3)\ [\cos(\pi/2NP)]^2. \qquad (5.8)$$

The induced strain $\epsilon\phi^+$ is largest for $\phi = \pm\phi$ and is computed below for various numbers of elements in the circumferential direction,

Table 5.3: Circumferential Strain Induced by Rotation around the $\bar{y}$-Axis.

NP	2	4	6	8	10
$\frac{-\epsilon_{\phi}^{+}\cdot R^3}{\epsilon_{cr}\cdot tL^2}$	0.0239	0.0106	0.0054	0.0032	0.0021

As shown in Table 5.3 the strain ϵ_{ϕ}^{+} tends to zero for a large number of elements in the circumferential direction. For a thick, long cylinder the longitudinal strain may become so large that a large number of elements is necessary to ensure reasonable results. However, these spurious strains are very localized at the top or bottom of the ends of the cylinder and decay rapidly with increased longitudinal and circumferential distance due to the term 'Δ^2'.

5.4.3 Rotation around the $\bar{z}$-Axis

Rotations about the $\bar{z}$-axis occur at the sides of the cylinder and are largest for the side elements at the cylinder ends. The theoretical rigid body displacements associated with this motion are given below for a rotation of magnitude Δ.

$$u = R \sin\Delta \sin\phi - x\,(1-\cos\Delta), \tag{5.9a}$$

$$v = -\,x \sin\Delta \cos\phi - R\,(1-\cos\Delta)\,[\sin\phi \cos\phi], \tag{5.9b}$$

$$w = -\,x \sin\Delta \sin\phi - R\,(1-\cos\Delta)\,[\sin^2\phi]. \tag{5.9c}$$

The element displacement functions approximate the above functions as shown below.

$$u = R \sin\Delta \sin\phi - x\,(1-\cos\Delta), \tag{5.10a}$$

$$\begin{aligned} v = &- x \sin\Delta \cos\phi \\ &- R\,(1-\cos\Delta)\,[\cos(p)\,\{2\sin\phi-\phi\sin(p)/p\}], \end{aligned} \tag{5.10b}$$

$$\begin{aligned} w = &- x \sin\Delta \sin\phi \\ &- R\,(1-\cos\Delta)\,[\sin^2(p)+2\cos\phi\{\cos(p)-\cos\phi\}]. \end{aligned} \tag{5.10c}$$

Substituting the element displacement field into the strain expressions gives

$$\begin{aligned} \epsilon x &= -(1-\cos\Delta) + 1/2\,(1-\cos\Delta)^2/2 + 1/2\,\sin^2\Delta, \\ &= 0, \\ \epsilon\phi &= -(1-\cos\Delta)(1+f) + 1/2\,(1-\cos\Delta)^2(1+f)^2 \\ &\quad + 1/2[(1-\cos\Delta)\,\sin(p)\,\cos(p)\,\phi/p]^2 \\ &\quad + 1/2\,\sin^2\Delta\,\cos^2\phi, \\ \gamma x\phi &= (1-\cos\Delta)\sin\Delta\,[-\cos\phi + \cos\phi(1+f) \\ &\quad +\sin(p)\cos(p)\phi\sin\phi/p], \\ kx &= 0, \\ k\phi &= (1-\cos\Delta)\,\sin(p)\,\cos(p)\,/pR, \\ kx\phi &= 0. \end{aligned} \tag{5.11}$$

For small rotations Δ, only the lowest powers of Δ for each strain component need to be considered.

$$\begin{aligned} \epsilon\phi &= -\,(\Delta^2/2)\,[\sin^2\phi+\cos(p)\,\{\cos(p)-\sin(p)/p\}], \\ \gamma x\phi &= (\Delta^3/2)\,\cos(p)/p\,[\phi\sin(p)\sin\phi+p\,\cos(p)-\sin(p)], \end{aligned}$$

$$k\phi = (\Delta^2/2)\,\sin(p)\,\cos(p)/pR. \qquad (5.12)$$

It is seen that the strain $\gamma x\phi$ can be neglected with respect to $\epsilon\phi$ and $k\phi$. The curvature $k\phi$ gives a maximum circumferential strain of about '$t\cdot\Delta^2/4R$', which can be neglected for large R/t ratios.

The maximum value of $\epsilon\phi$ occurs at $\phi = \pm p$. The circumferential strain can be expressed by '$d\cdot(-\Delta^2/2)$', where d is a factor depending on NP and the angle ϕ. For example with NP=4, d is 0.36 and converges to zero with increasing NP.

This rotation is equivalent to the derivative of the tangential displacement v with respect to the longitudinal coordinate x, calculated at the element origin. For the side elements at the cylinder ends we obtain:

$$\begin{aligned} \Delta &= \beta\,\cos(\pi/2NP)\,(1-1/2NX) \quad \text{if NP is even,} \\ &\cong \beta\,\cos(\pi/2NP) \qquad \text{for } NX>>1. \qquad (5.13) \end{aligned}$$

Letting β be the critical elastic buckling rotation βcr and $\nu=0.3$ the induced circumferential strain $\epsilon\phi^{+}$ can be defined as

$$\epsilon\phi^{+} = d\ \epsilon cr\ tL^2/13.22R^3\ \cos^2(\pi/2NP),$$

where ϵcr is the longitudinal strain corresponding to the classical buckling stress.

Table 5.4: Circumferential Strain Induced by Rotation around the $\bar{z}$-Axis.

NP	2	4	6	8	10
$\frac{-\epsilon_{\phi}^{+} \cdot R^3}{\epsilon_{cr} \cdot tL^2}$	0.0275	0.0075	0.0034	0.0019	0.0012

5.4.4 Summary of the Rigid Body Rotations

It was demonstrated that a rigid body motion around the $\bar{x}$-axis does not induce spurious strains.

The strains induced by rotations around the other two axes are reduced approximately quadratically for an increase in the number of circumferential elements. Except for the case with NP=2 the strains due to rotations around the $\bar{y}$-axis are larger than those of the $\bar{z}$-axis.

Table 5.5: Maximum of Induced Strains from Rigid Body Motions.

		Long Cylinder	Short Cylinder	Cylinder of Stephens *et al.*
L		2500	1829	2000
R		90	764.5	100
t		1.1	5.13	1
tL^2/R^3		9.43	0.038	4
	NP			
$\frac{\epsilon_{\phi}^{+}}{\epsilon_{cr}}$	2	0.259	0.0011	0.110
	4	0.100	0.0004	0.042
	6	0.051	0.0002	0.022
	8	0.030	0.0001	0.013
	10	0.020	0.0001	0.008

Considering the induced strains described above, the analysis of cylinders with a high ratio tL^2/R^3 should be done with some care using the present element. The short cylinder has a very low tL^2/R^3 ratio when compared to the other cylinders and therefore is less affected by strains from rigid body motions.

The induced negative circumferential strains cause the element to develop compressive stresses in the circumferential direction. These can be relieved by an increase of the circumference (that is an increase of the radius of the cylinder). With a larger radius the bending stiffness of the cylinder is increased. The short cylinder remains essentially unaffected but the induced strains for the long cylinders will tend to reduce the ovalization of the cross-section which thereby limits the reduction of the bending stiffness.

Compared with the arch and the barrel vault problem the geometric nonlinear bending of a cylinder is particularly difficult. The deflections of the barrel vault are in the order of the shell thickness t. The only rigid body rotation occurring for the circular arch is the rotation around the longitudinal axis which can be exactly represented by the element displacement functions. The circular cylinder under bending undergoes deformations in the order of 20 times the thickness and there are significant rigid body motions. In the finite element model these result in induced strains.

Although the induced circumferential strains are small compared to the longitudinal strains from bending they will tend to increase the diameter of the cylinder and thereby alter significantly the behaviour of the cylinder.

15

5.5 Cylinder under Bending

5.5.1 Review of Earlier Investigations

Flügge indicates in Ref. 26 for the buckling problem of a cylinder under bending that the bending stiffness for small displacements agrees with the linear theory of Donnell, but with increasing deflections (end rotation) the mid section of the cylinder ovalizes and the section modulus is reduced. As the end rotation increases the bending moment increases at a decreasing rate until it reaches a maximum (which is referred to as the buckling moment) after which it then decreases.

Stephens *et al.*[38] showed for cylinders with a ratio R/t of 100, that the buckling moment is equal to the classical buckling moment *M*cr and decreases with increasing L/R ratio to Brazier's solution. Using a finite difference technique they showed the buckling mode that occurs to be a combination of longitudinal wrinkles and an ovalization of the cross-section. They defined the buckling moment to be the moment for which large deflections or ovalization occurs with increases in moment of the order of 0.01 %. The ovalization is shown to depend largely on the L/R ratio. Since the development of longitudinal wrinkles is likely to occur only for thin cylinders, the ovalization effect should be studied with thick cylinders since otherwise a combination of both buckling modes may occur.

Fabian[24] investigated the nonlinear bending of infinite cylinders and separated the ovalization from the wrinkling effect by restricting the possible displacement functions. With longitudinal wrinkling prevented the bending moment was found to be linear up to stresses of 25 % of σ_{cr}. Then the moment increased less than proportionally and reached a maximum of around 53 % of M_{cr}. This is only slightly less than predicted by the Brazier solution.

The results of structural tests are largely dependent on imperfections and material nonlinearities. Since most analytical studies include only geometrical nonlinearities and simplified imperfections, a discussion of structural tests is not done in this study. A review of these tests is given in Ref. 37.

5.5.2 Boundary Conditions and Their Representation

In many structures that incorporate cylinders, the cylinders have very complex boundary conditions. The ends are often attached to stiff plates to ensure that the cross-section is maintained. Often longitudinal or circumferential stiffeners are present to increase the load limits.

In most geometric nonlinear studies of cylinders under bending, the cylinder is idealized as a perfect tube. The end condition adopted depends on the type of cylinder investigated and the kind of analysis performed.

For infinitely long cylinders a complete torus has been considered (Flügge[25], Fabian[24]). Seide and Weingarten[36] described the ends of finite cylinders by restricting the radial deflections to zero but allow a warping of the cross-section. Stephens *et al.*[38] investigated finite cylinders by applying stresses on the cylinder ends which were distributed according to the linear beam theory. In order to minimize the warping or distortion of the cross-section the cylinder end was stiffened with two cylindrical rings.

Although they state that a distortion of the cross-section was thereby prevented, the author believes that the rings allow a circumferential stretching as discussed in section 4.2.3. Otherwise an upward buckle near the cylinder end similar to Fig. 4.5 would be expected.

A third way to describe boundary conditions is to prescribe displacements at the cylinder ends, which is discussed in the following sections.

5.5.3 Prescribed Displacements at the Cylinder Ends

In prescribing the displacements at the cylinder ends the circular cross-section is retained and a warping or distortion of the cylinder end is prevented. However, one has to consider that rigid ends present a problem which is different from the infinite cylinder and might give rise to stresses or strains which deform the cylinder unexpectedly at the ends (e.g. Fig. 4.5).

5.5.3.1 Shortening of Cylinder due to Bending

If a cylinder is bent by applied moments (or end rotations as in the present study) the linear beam theory predicts a quadratic displacement function. Under finite deformations the cylinder stretches longitudinally because the deformed neutral axis describes an arc as opposed to a straight line. In the nonlinear analysis of cylinders, large end rotations give rise to a net axial force unless the cylinder ends are allowed to move axially. Using $\bar{L}$ as the new cylinder length and $\bar{R}$ as the radius of the curvature of the bent cylinder the elongation ΔL and the strain ϵx for fixed ends can be expressed.

$$\Delta L = \bar{L} - L, \qquad (5.14)$$

Assuming the form of the bent cylinder is a circular arch, $\bar{R}$ and L can be expressed by the end rotation β and the new cylinder length $\bar{L}$.

$$\begin{aligned} L &= 2\,\bar{R}\,\sin\beta \\ &= \bar{L}\,\sin\beta/\beta. \end{aligned} \qquad (5.15)$$

Inserting this into Eq. 5.14 we get

$$\begin{aligned} \Delta L &= \bar{L}\,(1-\sin\beta/\beta), \\ \epsilon x &\doteq \Delta L/\bar{L} = 1 - \sin\beta/\beta \\ &\doteq \beta^2/6 \quad \text{for } \beta \ll 1. \end{aligned} \qquad (5.16)$$

A better insight of the effect of ϵ_x is gained if the induced stress $\bar{\sigma}$ is compared to the critical stress σ_{cr}.

$$\bar{\sigma} = E\,\beta^2/6,$$

$$\sigma_{cr} = \beta_{cr}\,E\,R/2L,$$

$$\beta_{cr} = (t\,L/2R^2)\cdot[3(1-\nu^2)]^{-1/2}. \qquad (5.17)$$

Substituting β_{cr} for β we obtain:

$$\max \bar{\sigma}/\sigma_{cr} = tL^2/24R^3[3(1-\nu^2)]^{-1/2}.$$

$$= tL^2/39.65\,R^3 \qquad \text{for } \nu=0.3.$$

The ratio of max $\bar{\sigma}/\sigma_{cr}$ is given for three cylinders in Table 5.6.

Table 5.6: Ratio of max $\bar{\sigma}/\sigma_{cr}$ for Three Cylinders.

	Long Cylinder	Short Cylinder	Cylinder of Stephens *et al*.
L	2500	1829	2000
R	90	764.5	100
t	1.1	5.13	1
L/R	27.18	2.392	20
t/R	0.0122	0.0067	0.01
max $\bar{\sigma}/\sigma_{cr}$	0.238	0.001	0.101

As shown in Table 5.6 the axial stress $\bar{\sigma}$ is significant for large (L/R) and (t/R), that is for long thick cylinders. Therefore, for these problems care must be taken in dealing with axial boundary conditions.

In the program used for the present study, the axial force arising due to end restraint is treated similarly to an equilibrium force during the equilibrium iteration. Since the displacements at the cylinder end are prescribed, the application of nodal forces at the end is not possible. Instead, displacements are applied to the cylinder ends which approximate the displacements for free cylinder ends.

5.5.3.2 Nonlinear Boundary Conditions for End Rotation

The displacements prescribed at the cylinder end consist of two parts. First, the cross-section is rotated around the longitudinal axis with angle β, and second, if wanted, the circumferential stretching may be applied. The displacements and rotations at the cylinder end for a rotation about a horizontal axis while maintaining a rigid cross-section are given below.

$$u = -R \sin\beta \cos\bar{\phi}, \tag{5.18a}$$

$$v = R\,(1-\cos\beta) \sin\bar{\phi} \cos\bar{\phi}, \tag{5.18b}$$

$$w = -R\,(1-\cos\beta) \cos^2\bar{\phi}, \tag{5.18c}$$

$$\beta x = \sin\beta \cos\bar{\phi}, \tag{5.18d}$$

$$\beta\phi = (1-\cos\beta) \sin\bar{\phi} \cos\bar{\phi}. \tag{5.18e}$$

The angle $\bar{\phi}$ is the circumferential coordinate measured from the top fibre (Fig. 4.2) and β is the angular rotation of the cross-section.

For small rotations the trigonometric functions in β are approximated by the first term of the corresponding Taylor's series. This results in the following linear expressions which were used for the linear bending problem.

$$u = -R\,\beta\cos\bar{\phi}, \tag{5.19a}$$

$$v = 0, \tag{5.19b}$$

$$w = 0, \tag{5.19c}$$

$$\beta x = \beta\cos\bar{\phi}, \tag{5.19d}$$

$$\beta\phi = 0. \tag{5.19e}$$

In order to simulate the cylinder by Stephens *et al.*[38] points on the cylinder ends should be allowed to move in the circumferential direction. Otherwise stresses in the circumferential direction occur at the cylinder end, and an outward buckle similar to Fig. 4.5 would occur. In the linear analysis this effect was avoided by allowing v and $\beta\phi$ to be free.

In a nonlinear analysis, however, v and $\beta\phi$ cannot be let free since these degrees of freedom are needed to prescribe the rotation of the cylinder end (Eq. 5.18). Therefore displacements are applied which approximate a cylinder end with no circumferential stresses. The Donnell equation (Eq. 4.2) for zero circumferential stress is derived from the linear bending theory of cylinders. It is assumed that the nonlinear circumferential stretching is about as much as in the linear range.

In section 4.2 it is shown that the maximum displacement Δv for $\sigma x = \sigma cr$ is only 0.182 times the shell thickness t. For the derivation of the displacements it is therefore permissable, that $\sin(\Delta v/R)$ and $\cos(\Delta v/R)$ are approximated by $\Delta v/R$ and 1, respectively, for large R/t ratios.

The displacements due to this prescribed circumferential strain are as follows:

$$u = \bar{D}\ \beta \sin\beta \sin^2\bar{\phi}, \tag{5.20a}$$

$$v = \bar{D}\ \beta \sin\bar{\phi}, \tag{5.20b}$$

$$w = 0, \tag{5.20c}$$

$$\beta x = 0, \tag{5.20d}$$

$$\beta\phi = -\ \bar{D}\ \beta \sin\bar{\phi}/R, \tag{5.20e}$$

where $\bar{D}$ equals to $2\nu R^2/L$.

5.5.4 Discussion of Test Results

The cylinders considered are the long cylinder by Stephens *et al.*[38] and the short cylinder by Stephens[37], whose data are given in Table 5.6. As in the preceding nonlinear analysis the full Newton-Raphson-Method is used. The step size of the rotation of the cylinder end is chosen as 10 % of βcr. The equilibrium iterations are stopped when the norm of the incremental displacements is smaller than 10^{-6} times the norm of the first displacements of the current load step. The CPU-time required for each load step is found to be approximately 0.9 seconds per element. The calculation of the three stiffness matrices takes about 48 seconds for one element type. This calculation is done only once. Due to these high computing costs only a limited number of runs were possible.

5.5.4.1 Rigid and Semi-Rigid Cylinder Ends

In order to study the effect of axial fixed ends and prescribed circumferential strain, three tests of the long cylinder (L/R/t=2000/100/1) were done with 4×2 elements. The results are given in Table 5.7 and are compared with the deflection and end moment of the linear beam theory.

Table 5.7: Effects of Axially Fixed Ends and Prescribed Circumferential Strain on the Long Cylinder by Stephens *et al.*[38] with 4×2 Elements and $\beta = \beta cr$.

	axial fixed	axial free, no Donnell strain	axial free, prescribed Donnell strain
w / *w* beam †	1.028	1.050	1.034
M / *M* beam	0.865	0.827	0.699
Δw(mm) ‡	7.27	7.50	7.35
(axial shortening or axial force) / beam theory	1.67	1.51	1.013
σx(top)/beam theory cylinder end cylinder middle	 -1.28 -1.26	 -1.50 -1.47	 -1.35 -1.57
σx(bottom)/beam theory cylinder end cylinder middle	 1.71 1.38	 1.63 1.26	 1.43 1.27

Comparing the two columns with no circumferential strain at the end, the following can be said: The axial force due to fixed ends increases the longitudinal strains in the cylinder and increases the end moment by about 5 %. The deflection is reduced by 3 % and the ovalization by 2.2 %. In prescribing Donnell's circumferential strain at the ends the deflection *w* and the ovalization Δw are slightly reduced. The bending moment drops by 16 % when compared to the cylinder with rigid ends. A similar effect has been observed already in section 4.2.3 where deflections and moments of a long cylinder decreased when circumferential strains were allowed to develop.

---

† The deflection *w* is the mean of top and bottom deflection.
‡ The ovalization or flattening Δw is measured as the difference of top and bottom fibre deflection.

The longitudinal strains vary significantly. For the cylinder with Donnell's strain the stresses vary less than in the two other cases. A significant improvement is the calculation of the axial shortening which shows only a 1.3 % difference from the beam solution. Because of the effect of the prescribed Donnell strain on the computation of the axial shortening and the increased bending stiffness for axial fixed ends the next tests are done with axial free ends and the prescription of Donnell's circumferential strain at the cylinder ends.

5.5.4.2 The Short Cylinder

The finite element gridwork chosen for the cylinder by Stephens[37] is NP×NX = 3×8 elements. It was chosen to have approximately equilateral elements. The cylinder data are given in Table 5.6. For the first load step ($\Delta\beta = 0.1\ \beta cr$) four equilibrium iterations were needed and only two iterations were neccessary for further loadings. This fast convergence is possible because of the small displacements of the cylinder. The calculation could not however be continued beyond the first iteration of the fifth load step since the determinant of the tangent stiffness matrix was found to be negative. The results of Stephens *et al.*[38] indicate that the buckling moment for the present cylinder would be around 0.98 Mcr. The results of the present study are given in the table below.

Table 5.8: Nonlinear Results of Short Cylinder under Bending.

Load Step, ($\beta/\beta cr$)	$\frac{\lvert K^{T}{}_{i} \rvert}{\lvert K^{T}{}_{0} \rvert}$	Δw (mm)	Mean Deflection (mm)	Shortening of Cylinder (mm)
0.0	1.0000	0.0000	0.0000	0.000000
0.1	0.8669	0.0018	0.2194	0.000145
0.2	0.6289	0.0072	0.4388	0.000580
0.3	0.3041	0.0164	0.6583	0.001305
0.4	0.0359	0.0288	0.8779	0.002321
0.5	-0.1031	—	—	—

The mean value of the top and bottom deflection is almost proportional to the end rotation β and is 1.2 % less than predicted by beam theory (w=0.222136 mm). The bending moments found are almost proportional to the rotation β. The increase in the bending moment between the third and fourth load step is only 0.005 % smaller than the value of the first load step. The insignificant nonlinearities for deflection and the bending moment can be explained by the very small geometric differences between the loaded and the unloaded cylinder. The ovalization, for example, at β = 0.4 βcr is only 3.3 % of the deflections or 0.56 % of the thickness t. The flattening Δw increases quadratically with respect to the end rotation. The results by Stephens *et al.*[38] show the same trend; the ovalization grows approximately quadratically to the bending moment, which is, as found in the present study, almost proportional to the end rotation. A numerical comparison is difficult, since the smallest L/R ratio in Ref. 38 is 3.4 (as opposed to 2.4 in the present study) and the paramter Δw is hardly visible in the graphical representation of the results. Unfortunately Stephens *et al*. did not give the end rotation, shortening, or the circumferential stresses, which should be compared with the results obtained in this study.

The shortening of the cylinder is about double as much as Eq. 5.17 predicts. This discrepancy may be due to the small number of elements in the longitudinal direction and the relative low L/R ratio. However, a satisfactory explanation is still not available.

The stresses of the mid-section after the fourth load step are shown in Fig. 5.6. The stresses of the cylinder end are omitted since the differences are too small to be shown.

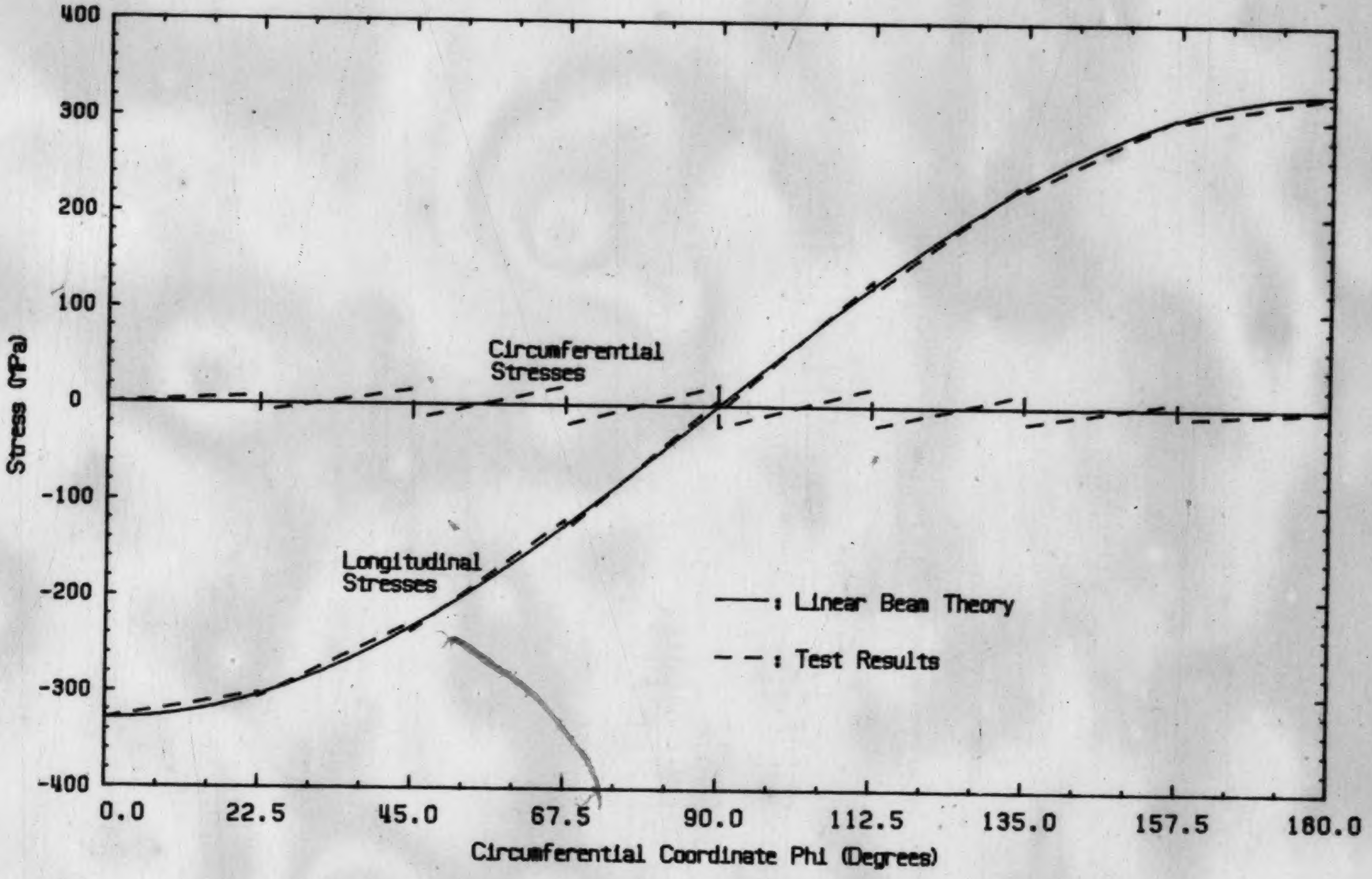

Fig. 5.6: Stresses for Short Cylinder at Mid-Section for $\beta = 0.4\ \beta cr$.

The longitudinal stresses approximate the beam solution quite well, since the deflections are very close to the beam theory.

The circumferential stresses approximate Donnell's theory that σ_ϕ should be zero. The stress σ_ϕ for each element (p=22.5°) varies almost linearly, which is an effect of the lack of a continuous ϕ-term in the strain function for ϵ_ϕ.

At the cylinder middle the longitudinal stress of the top fibre is 0.05 % above the beam stress and the bottom stress is 0.03 % less than the beam theory. At the top fibre of the cylinder end σ_x has about the same value as predicted by the beam theory, while the longitudinal stress at the bottom fibre is about 0.4 % larger.

5.5.4.3 The Long Cylinder

The data for this cylinder are:

$L = 2000$ mm,

$R = 100$ mm,

$t = 1$ mm,

$E = 6895$ MPa,

$\nu = 0.3$.

Stephens *et al.* found the buckling moment to be 0.636 M_{cr} and observed a maximum ovalization of about 16 times the cylinder thickness. As in the preceding problem the cylinder is tested with prescribed circumferential strain at the ends and axial free ends. The finite element mesh chosen is NX×NP = 13×4 elements, which gives an element aspect ratio of 0.98. The cylinder is tested up to an end rotation of $\beta = \beta_{cr}$ with a load step size of $\beta = 0.1\ \beta_{cr}$. The results are given in Table 5.9 below.

Table 5.9: Nonlinear Results of Long Cylinder under Bending.

Load Step	Increase of Moment (Nmm)	Increase in Mean Deflection (mm)	Increase in Δw (mm)
1	123156	3.0331	0.33
2	122158	3.0735	0.92
3	120650	3.1075	1.17
4	119235	3.1125	1.16
5	117974	3.1125	1.08
6	116819	3.1110	0.98
7	115699	3.1090	0.83
8	114659	3.1082	0.77
9	113743	3.1100	0.77
10	112739	3.1045	0.73

Despite a recalculation of the tangent stiffness matrix, the convergence was rather slow. Four to five equilibrium iterations were necessary for each load step. The axial movement of the cylinder end was found to be in good agreement with the prediction by Eq. 5.17. The difference lies between 1.1 % for $\beta = 0.1\ \beta cr$ and 4.2 % for $\beta = 1.0\ \beta cr$. The moment for the first load step is 93.9 % of the beam theory and for the tenth load step 86.0 %. The decrease in the difference between the moments at two successive load steps has an average of 0.8 % and is largest at the third load step. After the third load step the change in moment per load step decreases at a slower rate. It is interesting to note that the rate of increase in ovalization decreases after the third load step and that the additional mean deflections have their maximum at the fourth load step.

If one compares the end rotation with the ovalization and the deflection, a geometric stiffening of the cylinder after $\beta = 0.3\ \beta_{cr}$ is observed. An explanation for this stiffening is that the induced stresses reduce the ovalization and thereby limit the reduction of the bending stiffness.

The relative increase of the bending stiffness is especially seen in the determinant $| K^{T} |$ which increases steadily from 1.5×10^{1002} at $\beta = 0.1\ \beta_{cr}$ to 1.2×10^{1023} after the last load step.

Table 5.10 shows the ovalizations calculated by Stephens *et al.* and the present study.

Table 5.10: Ovalization of Long Cylinder under Bending

Moment / *M*cr	Ovalization $\Delta w/t$ Stephens *et al.* †	Ovalization $\Delta w/t$ present study
0.1	0.3	0.4
0.2	1.0	1.4
0.3	2.3	2.7
0.4	4.5	4.0
0.5	8.7	5.1
0.6	13.5	6.1
0.636	16.0	6.5

Up to a moment of 0.3 *M*cr the present study gives a larger ovalization than Stephens *et al.*. This can be partly explained by the calculation of the bending moment which for $\beta = 0.1\ \beta_{cr}$ is 6 % lower than predicted by beam theory

---

† Approximate values obtained from graphical results.

(131000 Nmm). The present results compare reasonably well with those of Stephens up to 0.3 M_{cr}. Beyond that moment, Stephens' solution predicts a much larger rate of increase in Δw.

To illustrate the development of cross-section ovalization the incremental deflections for the first three and the last load step are illustrated in Fig 5.7. The curves above the dashed line are the deflections for the bottom fibre, and the deflections of the top fibre are shown below the dashed line. The fourth increment, which is almost identical with the third one and the increments of step 5 to 9 are omitted for clarity of the other curves.

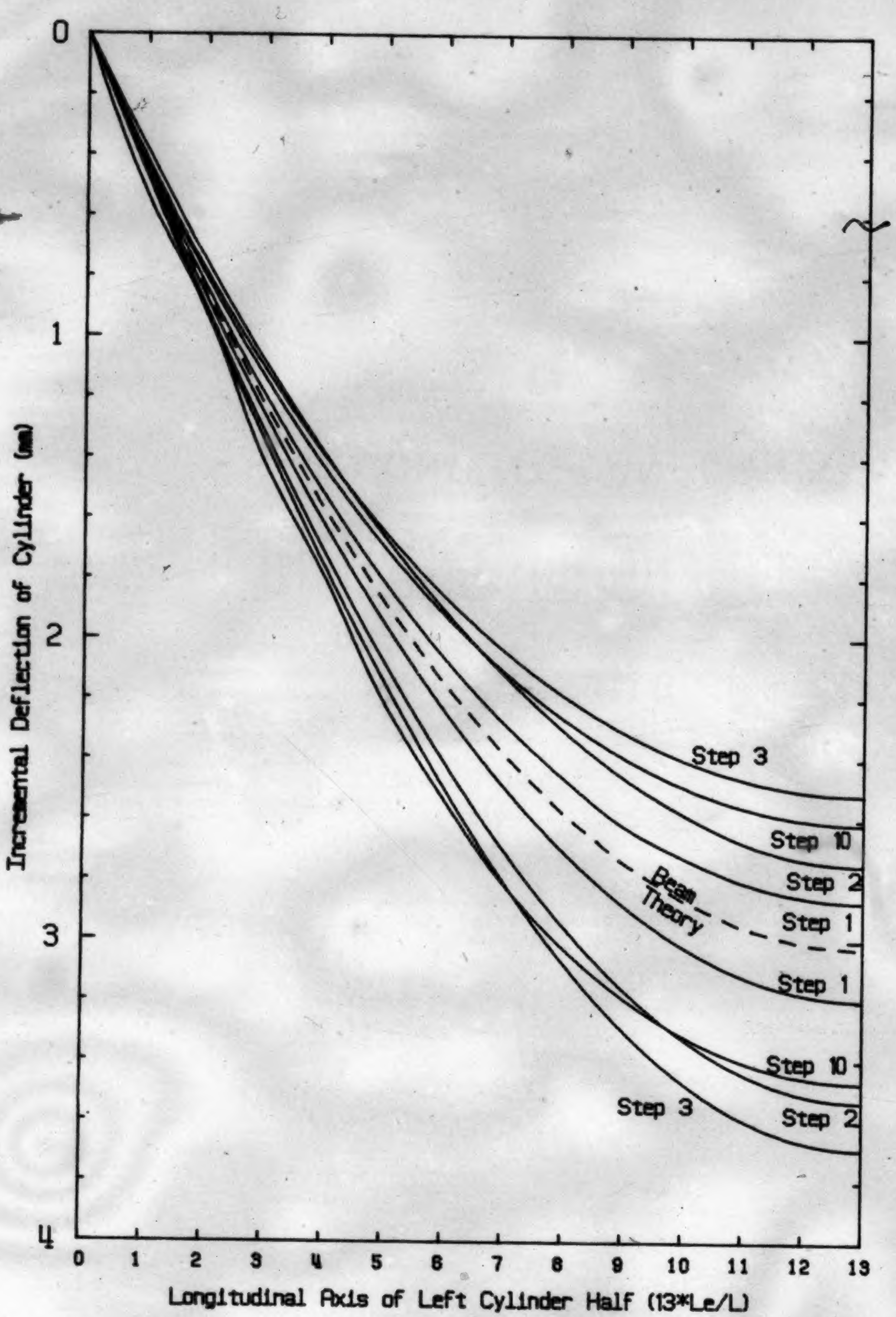

Fig. 5.7 : Incremental Deflections of Long Cylinder under Bending.

With increasing end rotation the ovalization is reduced at the cylinder middle but still increases near the cylinder end. The wave-like differences of the tenth step might be interpreted as the beginning of a longitudinal wrinkling. In order to find the buckling mode occuring an element refinement in the circumferential direction is appropriate so that the stresses induced by rigid body motions are kept small. Unfortunately Stephens *et al*. did not present the moment end rotation and moment-deflection relationship which should be compared to the present results.

Lastly the longitudinal and circumferential stresses for $\beta = 0.3\ \beta cr$ are presented in Fig. 5.8 and compared to the beam theory and the results of Stephens *et al*..

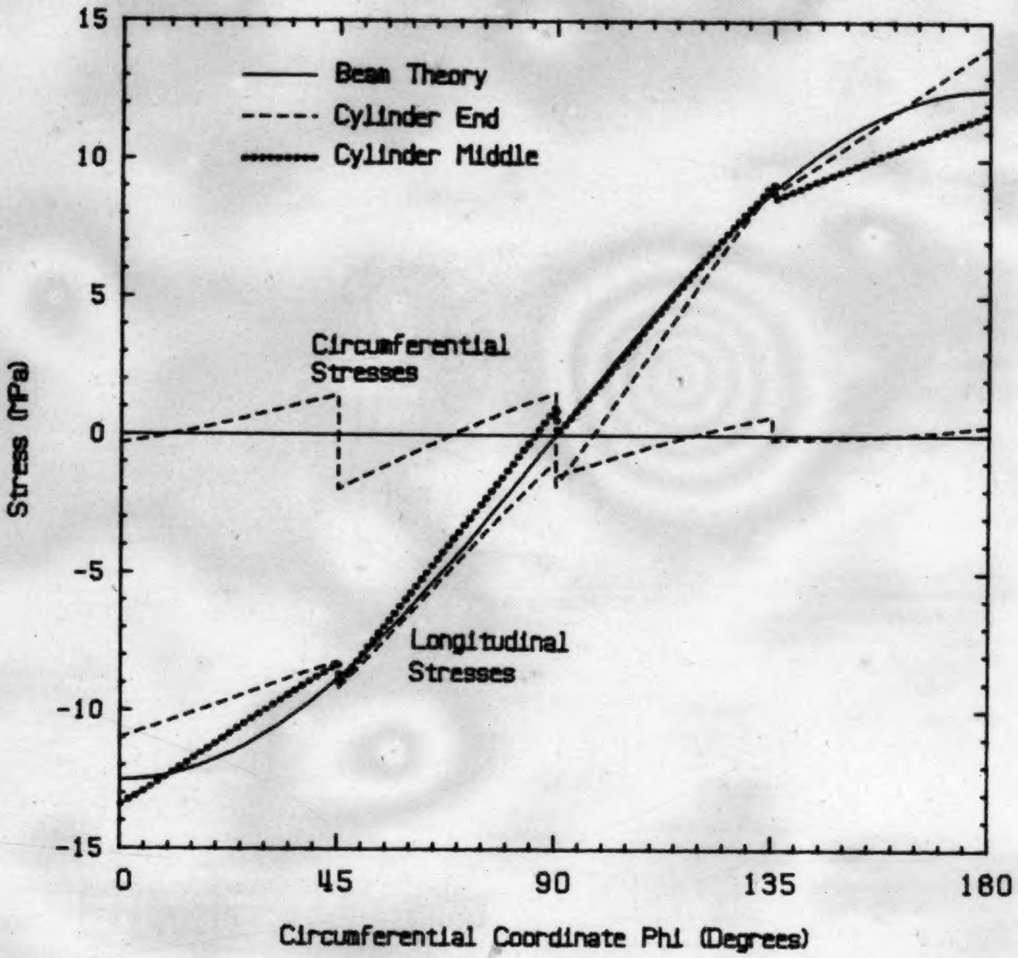

Fig. 5.8: Stresses of Long Cylinder at $\beta = 0.3\ \beta cr$.

Despite the surprisingly coarse stress distribution an effect is observed which Stephens *et al*. found also. In the middle of the bent cylinder the stresses at the top and the bottom fibre decreases. In order to maintain equilibrium of horizontal forces the neutral axis shifts by about 5° towards the top fibre.

The stresses at the cylinder end are shifted in the reverse sense. The neutral axis is about 7.5° lower than the middle fibre of the beam. The circumferential stresses at the cylinder end are in the average about zero. The more positive σ_ϕ from the top fibre to 45° is in accordance with the quite low σ_x: The circumferential strains prescribed are based on the longitudinal stresses of the beam theory. A positive increase in σ_x without changing the circumferential strain results in an increase in σ_ϕ. Near the bottom fibre the longitudinal stresses approximate the beam theory quite well; correspondingly the circumferential stress tends towards zero as expected.

6. Summary and Conclusions

In the foregoing a modified finite element is developed for geometric nonlinear behaviour of thin cylindrical shells. The element is proven to be at least equal in performance when compared to other elements for the linear pinched cylinder problem. The bending of a cylinder under end moments shows that the element gives the exact beam deflection if points at the cylinder ends are allowed to move in the circumferential direction. Otherwise an upward lifting is observed. Despite the good results for deflections the cylinder moment and the circumferential strain predicted are very poor unless approximately equilateral elements are used.

In the nonlinear range the element is successfully applied to the barrel vault problem with concentrated loads and successfully follows the nonlinear load-deflection path with horizontal tangents. In another test problem, the pinched circular arch, the element gives loads slightly higher than the results by Sabir and Lock. One reason for the different performance is the difference in the magnitude of the deflections in the two problems. The barrel vault was tested up to w=0.011 R while the circular arch had a deflection of 0.137 R.

In the context of nonlinear problems, the element is tested for spurious strains arising from rigid body motions. It is shown that the element remains strain-free for translations in all directions as well as for a rotation around the longitudinal axis. However, rotations around the two other axes induce strains in the element. In the nonlinear bending problem, cylinders with a high ratio tL^2/R^3 are apt to develop compressive circumferential stresses as a result. These stresses enlarge the diameter of the cylinder and reduce the flattening or ovalization of the cross-section.

Due to high computing costs only a limited number of runs were done for the nonlinear bending problem. It was shown that the ends of the cylinder move axially due to second order effects and that a rigid cross-section at the cylinder end causes circumferential stresses which in turn influence the middle of the cylinder. In order to assess the influence of various boundary conditions it seems necessary that the element be refined near the cylinder end and that there be enough elements in the circumferential direction to obtain a uniform stress distribution for σ_x.

Two cylinders with quite different values of tL^2/R^3 were tested. The short cylinder showed good results except that the determinant of the tangent stiffness matrix became negative at the fifth load step. The reason for this behaviour is not clear. With an element gridwork of 3×8 elements the representation of the bent cylinder might be too coarse and might cause numerical problems during the triangularization of the stiffness matrix.

A very long cylinder showed the problem with induced strains. After a rotation of $\beta = 0.3\ \beta cr$ the ovalization and the deflection did not increase very much and neither the determinant of the stiffness matrix nor the displacements indicated a buckling behaviour.

The success of the element for nonlinear problems with small deflections suggests that the element works best when strains arising from rigid body motions are kept small compared the to the strains due to the structural loading. The rigid body motions which rotate perpendicular to the longitudinal axis are responsible for these strains.

In order to avoid these induced stresses one should either change the tangent stiffness matrix of an element by a subtraction of rigid body motions or change the displacement functions to include the rigid element displacements.

As shown, the element works well for most linear and nonlinear problems. However, the bending of cylinders appears to be particularly difficult. Besides the problems of representing the boundary conditions at the cylinder end, the element itself can only approximate the displacements of a cylinder under bending. With restrictions due to the high computing time involved, a detailed study of the various problems with the cylinder under bending has been only started and further research is necessary to solve the problem adequately.

References

1. B. O. Almroth and J. H. Starnes, Jr.,
"The Computer in Shell Stability Analysis",
ASCE Journal, Vol. 101, EM6, 1975, pp. 837-888.

2. J. H. Argyris and P. C. Dunne,
"Post-Buckling Finite Element Analysis of Circular Cylinders under End Load",
Acta Technica, Vol. 87, 1978, Nr. 1-2, pp. 5-16.

3. D. G. Ashwell and R. H. Gallagher,
Finite Elements for Thin Shells and Curved Members,
John Wiley & Sons, 1976.

4. D. G. Ashwell and A. B. Sabir,
"A New Cylindrical Shell Element Based on Simple Independent Strain Functions", *International Journal of Mechanical Science*, Vol. 4, 1972, pp. 171-183.

5. D. G. Ashwell and A. B. Sabir,
"A Corrected Assessment of the Cylindrical Shell Element of Bogner, Fox and Schmidt when Applied to Arches", *International Journal of Mechanical Sciences*, Vol. 15, 1973, pp. 325-327.

6. D. G. Ashwell, A. B. Sabir and T. M. Roberts,
"Further Studies in the Application of Curved Finite Elements to Circular Arches",
International Journal of Mechanical Sciences, Vol. 13, 1971, pp. 507-517.

7. K.-J. Barthe und E. L. Wilson,
Numerical Methods in Finite Element Analysis,
Prentice-Hall, 1976.

8. Budiansky (Editor),
Buckling of Structures, Symposium Cambridge (USA), June 17-21 1974, Springer Verlag, Berlin, 1976.

9. F. K. Bogner, R. L. Fox and L. A. Schmidt, "A Cylindrical Shell Discrete Element", *AIAA Journal*, Vol. 5, 1967, Part 1, pp. 745-756.

10. L. G. Brazier, "On the Flexure of Thin Cylindrical Shells and Other "Thin" Sections", *Proceedings of the Royal Society*, London, Series A, Vol. 116, 1927, pp. 104-114.

11. F. A. Brogan and B. O. Almroth, "Practical Methods for Elastic Collapse Analysis for Shell Structures", *AIAA Journal*, Vol. 9, Part 2, 1971, pp. 2321-2325.

12. D. O. Brush and B. O. Almroth, Buckling of Bars, Plates and Shells, McGraw-Hill, 1975.

13. G. Cantin, "Rigid Body Motions in Curved Finite Elements", *AIAA Journal*, Vol. 8, 1970, Part 2, pp. 1252-1255.

14. G. Cantin and R. W. Clough, "A Curved, Cylindrical-Shell, Finite Element", *AIAA Journal*, Vol 6., 1968, pp. 1057-1062.

15. G. F. Carey, "A Unified Approach to Three Finite Element Theories for Geometric Nonlinearity", *Computer Methods in Applied Mechanics and Engineering*, Vol. 4, 1974, pp. 69-79.

16. Y. K. Cheung, Finite Strip Method in Structural Analysis, Pergamon Press, New-York, 1976.

17. J. J. Connor and C. Brebbia, "Stiffness Matrix for Shallow Rectangular Shell Element", *ASCE Proceedings, Engineering Mechanics Division*, Vol. 93, 1967, EM5, pp. 43-65.

18. G. R. Cowper, G. M. Lindberg and M. D. Olson,
"A Shallow Shell Finite Element of Trianglular Shape", *International Journal of Solids and Structures*, Vol. 6, 1970, Part 2, pp. 1133-1156.

19. M. A. Crisfield,
"A Faster Modified Newton-Raphson Iteration", *Computer Methods in Applied Mechanics and Engineering*, Vol. 20, 1979, pp. 267-278.

20. D. J. Dawe,
"High Order Triangular Finite Element for Shell Analysis", *International Journal of Solids and Structures*, Vol. 11, 1975, pp. 1097-1110.

21. D. J. Dawe,
"Static Analysis of Diaphragm-Supported Cylindrical Shells Using a Curved Finite Strip", *International Journal for Numerical Methods in Engineering*, Vol. 11, 1977, pp. 1347-1364.

22. L. H. Donnell,
Beams, Plates, and Shells,
McGraw-Hill, New-York, 1976.

23. C. L. Dym,
Introduction to the Theory of Shells,
Pergamon Press, Glasgow, 1974.

24. O. Fabian,
"Collapse of Cylindrical, Elastic Tubes under Combinded Bending, Pressure and Axial Loads", *International Journal of Solids and Structures*, Vol. 13, 1977, Part 2, pp. 1257-1270.

25. W. Flügge,
"Die Stabilität der Kreiszylinderschale", *Ingenieurarchiv*, Bd. 3, 1932, pp. 463-506.

26. W. Flügge,
Stresses in Shells, 2nd Edition,
Springer Verlag, New-York, 1973.

27. R. H. Gallagher,
"A Discrete Element Procedure for Thin-Shell Instability Analysis", *AIAA Journal*, Vol. 5, Part 1, 1967, pp. 138-145.

28. G. Horrigmoe,
"Hybrid Stress Finite Element Model for Non-linear Shell Problems", *International Journal of Numerical Methods in Engineering*, Vol. 12, 1978, pp. 1819-1838.

29. T. M. Hrudey,
"The Application of a Refined Shallow Shell Finite Element to Geometric Nonlinear Structures", *C.A.S.I. Transactions*, Vol. 6, No. 2, Sept. 1973.

30. W. Kanok-Nukulchai,
"A Simple and Efficient Finite Element for General Shell Analysis", *International Journal for Numerical Methods in Engineering*, Vol. 14, 1979, pp. 179-200.

31. E. Ramm,
Strategies for Tracing Nonlinear Response Near Limit Points, Europe - US Workshop: Nonlinear Finite Element Analysis in Structural Mechanics, July 28-31 1980, Bochum.

32. E. Ramm,
Geometrisch nichtlineare Elastostatik und finite Elemente, Bericht Nr. 76-2, Institut für Baustatik der Universität Stuttgart, 1976.

33. A. B. Sabir and A. C. Lock,
"A Curved Cylindrical Shell Finite Element", *International Journal of Mechanical Sciences*, Vol. 14, 1972, pp. 125-135.

34. A. B. Sabir and A. C. Lock,
"Large Deflection, Geometrically Non-linear Finite Element Analysis of Circular Arches", *International Journal of Mechanical Sciences*, Vol. 15, 1973, Part 1, pp. 37-47.

35. A. B. Sabir and A. C. Lock,
"The Application of Finite Elements to the Large Deflection Geometrically Non-linear Behaviour of Cylindrical Shells", Variational Methods in Engineering, Vol. 2, Department of Civil Engineering, University of Southampton, Southampton University Press, 1973, pp. 7/66-7/75.

36. P. Seide and V. I. Weingarten,
"On the Buckling of Circular Cylindrical Shells under Pure Bending", *Journal of Applied Mechanics*, Vol. 28, 1961, pp. 112-116.

37. M. Stephens,
"The Local Buckling of Thin-Walled Tubular Steel Members", thesis, Spring Convocation 1982, University of Alberta, Edmonton, Canada.

38. W. B. Stephens, J. H. Starnes, Jr., and B. O. Almroth,
"Collapse of Long Cylindrical Shells under Combined Bending and Pressure Loads", *AIAA Journal*, Vol. 13, 1975, Part 1, pp. 20-25.

39. J. R. Tillerson, J. A. Stricklin and W. C. Haisler,
Numerical Methods for the Solution of Nonlinear Problems in Structural Engineering,
published in: Numerical Solutions of Nonlinear Structural Problems, pp. 67-101, edited by R. H. Hartung.

40. S. Timoshenko and S. Woinoisky-Kreiger,
Theory of Plates and Shells,
Maple Press, York (Pa.), 1959.

41. S. Timoshenko and J. M. Gere,
Theory of Elastic Stability,
McGraw-Hill, New-York, 1961.

42. J. R. Westlake,
A Handbook of Numerical Matrix Inversion and Solution of Linear Equations,
John Wiley & Sons, New-York, 1968.

43. R. H. Wu and E. A. Witmer,
Analytical and Experimental Studies of Nonlinear Transient Responses of Stiffened Cylindrical Panels, *AIAA Journal*, Vol. 13, 1975, pp. 1171-1178.

44. O. C. Zienkiewizc,
The Finite Element Method, 3rd Edition, McGraw-Hill, London, 1977.

45. O. C. Zienkiewicz and E. Hinton,
"Reduced Integration, Function Smoothing and Non-conformity in Finite Element Analysis (with Special Reference to Thick Plates)", *Journal of the Franklin Institute*, 302, Nos 5 & 6, Nov./Dec. 1976, pp. 443-461.

Appendix A.1

Inverse of the Matrix [T]

0	A4	0	0	E1	0	A4	0	0	E1	0	-A4	0	0	-E1	0	-A4	0	0	-E1
0	A6	0	0	E2	0	-A6	0	0	-E2	0	A6	0	0	E2	0	-A6	0	0	-E2
D4	D8	A5	0	E3	-D4	D8	A5	0	E3	D4	D8	-A5	0	E3	-D4	D8	-A5	0	E3
0	D9	B3	0	E4	0	-D9	-B3	0	-E4	0	-D9	B3	0	-E4	0	D9	-B3	0	E4
A1	E5	0	0	E8	A1	-E5	0	0	-E8	A1	E5	0	0	E8	A1	-E5	0	0	-E8
E6	E9	F1	E7	F2	-E6	E9	F1	-E7	F2	E6	E9	-F1	E7	F2	-E6	E9	-F1	-E7	F2
A3	0	0	0	0	-A3	0	0	0	0	-A3	0	0	0	0	A3	0	0	0	0
A6	0	0	0	0	-A6	0	0	0	0	A6	0	0	0	0	-A6	0	0	0	0
0	C1	A2	D3	C8	0	C1	A2	-D3	C8	0	-C1	A2	-D3	-C8	0	-C1	A2	D3	-C8
0	C2	B5	B4	C9	0	-C2	-B5	B4	-C9	0	C2	-B5	B4	C9	0	-C2	B5	B4	-C9
A7	D1	F3	D7	F4	A7	-D1	-F3	D7	-F4	-A7	-D1	F3	-D7	-F4	-A7	D1	-F3	-D7	F4
0	0	0	-A3	0	0	0	0	A3	0	0	0	0	A3	0	0	0	0	-A3	0
0	0	B6	B7	0	0	0	-B6	B7	0	0	0	-B6	B7	0	0	0	B6	B7	0
A9	0	0	A8	0	-A9	0	0	-A8	0	A9	0	0	A8	0	-A9	0	0	-A8	0
0	0	B8	B9	0	0	0	-B8	B9	0	0	0	B8	-B9	0	0	0	-B8	-B9	0
0	0	0	0	-A7	0	0	0	0	-A7	0	0	0	0	A7	0	0	0	0	A7
0	0	0	0	A9	0	0	0	0	-A9	0	0	0	0	A9	0	0	0	0	-A9
D5	C4	C3	D6	C5	-D5	C4	C3	-D6	C5	D5	C4	-C3	D6	C5	-D5	C4	-C3	-D6	C5
0	C6	F5	B1	C7	0	-C6	-F5	B1	-C7	0	-C6	F5	-B1	-C7	0	C6	-F5	-B1	C7
B2	D2	F6	F7	F8	B2	-D2	-F6	F7	-F8	-B2	-D2	F6	-F7	-F8	-B2	D2	-F6	-F7	F8

$s = \sin(p)$
$c = \cos(p)$
$\alpha = cp-s$

$A1 = 0.25$
$A2 = 1/4R$
$A3 = 1/4l$
$A4 = 1/4s$
$A5 = 1/4\alpha$
$A6 = 1/4ls$
$A7 = 1/4Rp$
$A8 = -1/4lp$
$A9 = -1/4lRp$
$B1 = 1/8R^2p$
$B2 = -1/16R^2p$
$B3 = 1/4l\alpha$
$B4 = -1/8R$
$B5 = 3/8Rl$
$B6 = 3/4l^3$
$B7 = -3/4l^2$
$B8 = 3/4pl^3$
$B9 = -3/4pl^2$
$C1 = c/4Rs$
$C2 = c/4lRs$
$C3 = -c/4R^2\alpha$
$C4 = s/4R^2\alpha$
$C5 = s/4R\alpha$
$C6 = s/4lR^2\alpha$
$C7 = s/4Rl\alpha$
$C8 = \alpha/4ps$
$C9 = \alpha/4lps$
$D1 = -p^2s/12l\alpha$
$D2 = -p^2s/9.6Rl\alpha$
$D3 = -1/8R$
$D4 = -1/8Rs$
$D5 = 1/8R^3p$
$D6 = 1/8R^2p$
$D7 = -p/24$
$D8 = -p/4\alpha$
$D9 = -p/4l\alpha$
$E1 = R/4s$
$E2 = R/4ls$
$E3 = -pR/4\alpha$
$E4 = -pR/4l\alpha$
$E5 = -Rc/4ls$
$E6 = -pl/16R$
$E7 = -pl/16$
$E8 = -R^2(2c+sp)/8sl$
$E9 = -s(2+p^2)/8\alpha$

$F1 = c(2+p^2)/8\alpha$
$F2 = -pR(2c+sp)/8\alpha$
$F3 = [(6\alpha+p^2(3cp-s)]/24lp\alpha$
$F4 = -R(3\alpha+sp^2)/12l\alpha$
$F5 = (s-3cp)/8lR^2p\alpha$
$F6 = [5p^2(3cp-s)-18\alpha]/96lRp\alpha$
$F7 = (12-5p^2)/96pR$
$F8 = (-5p^2s-9\alpha)/48l\alpha$

Appendix A.2

Linear Strain Fields in Terms of Nodal Displacements

$$\begin{bmatrix} \langle \theta x \rangle \\ \langle \theta ø \rangle \\ \langle \theta x ø \rangle \\ \langle \alpha x \rangle \\ \langle \alpha ø \rangle \\ \langle \alpha x ø \rangle \end{bmatrix} =$$

(s+$\underline{s}$)K1	K2	K8	(p$\underline{s}$-øs)/4L	L7	-(4x+1)N4
0	K3(1+x)	-K9	0	(1+x)/L8	N5
0	K4(21+3x)-K5(p+ø)	L1	3x(p+ø)L5	-L9-N1	N6
0	K6(x+1)	-L2	-(p+ø)(1+3x)L6	(1+x)N3	N8-(21+3x)N7
0	K7(1+x)	-L3	0	(1+x)(øps-α)N2	-N9+M1
-(s+$\underline{s}$)K1	-K2	K8	-(p$\underline{s}$-øs)/4L	-L7	(4x-1)N4
0	K3(1-x)	K9	0	(1-x)/L8	-N5
0	-K4(21-3x)+K5(p+ø)	-L1	-3x(p+ø)L5	-L9+N1	-N6
0	K6(x-1)	-L2	(p+ø)(1-3x)L6	-(1-x)N3	N8+(21-3x)N7
0	K7(1-x)	L3	0	(1-x)(øps-α)N2	N9-M1
-(s-$\underline{s}$)K1	-K2	-K8	(p$\underline{s}$-øs)/4L	L7	-(4x-1)N4
0	-K3(1-x)	K9	0	(1-x)/L8	-N5
0	K4(21-3x)-K5(p-ø)	L1	-3x(p-ø)L5	L9-N1	N6
0	K6(x-1)	L2	(p-ø)(1-3x)L6	(1-x)N3	-N8-(21-3x)N7
0	-K7(1-x)	L3	0	(1-x)(øps+α)N2	-N9-M1
(s-$\underline{s}$)K1	K2	-K8	-(p$\underline{s}$-øs)/4L	-L7	(4x+1)N4
0	-K3(1+x)	-K9	0	(1+x)/L8	N5
0	K4(21+3x)-K5(p-ø)	-L1	3x(p-ø)L5	L9+N1	-N6
0	K6(x+1)	L2	-(p-ø)(1+3x)L6	-(1-x)N3	-N8+(21+3x)N7
0	-K7(1+x)	-L3	0	(1+x)(øps+α)N2	N9+M1

$s = \sin(p)$
$c = \cos(p)$
$\underline{s} = \sin(\phi)$
$\alpha = cp-s$

$K1 = 1/4ls$
$K2 = x^2\phi/8lpR^2$
$K3 = c/4lRs$
$K4 = 1/8Rl$
$K5 = x^3/8Rpl^3$
$K6 = (x^2-l^2)/8Rl^2+\phi x^2/8Rpl^2$
$K7 = \alpha/4lsp$
$K8 = 1/4Rp$
$K9 = sp^2/12l\alpha$

$L1 = 1/4pl+p(3cp-s)/24l\alpha$
$L2 = p/24$
$L3 = R(sp^2+3\alpha)/12l\alpha$
$L4 = 1/4Rlps$
$L5 = 1/4pl^3$
$L6 = 1/4pl^2$
$L7 = x\phi/8R^3\phi$
$L8 = s\phi/4R^2l\alpha$
$L9 = c\phi/4R^2\alpha$

$N1 = x\phi(3cp-s)/8R^2pl\alpha$
$N2 = \phi/8R^2p$
$N3 = l\phi/8R^3p$
$N4 = 1/4R^2pl$
$N5 = s(6\phi^2-5p^2)/48Rl\alpha$
$N6 = (3cp-s)(5p^2-6\phi^2)+18(2x^2-l^2)$
$N7 = x/8Rpl^2$
$N8 = (6\phi+12-5p^2)/96Rp$
$N9 = \phi/4lp$
$M1 = (6s\phi^2-9\alpha-5p^2s)/48l\alpha$

Appendix B.1

Listing of the Finite Element Program

The finite element program used is given with subroutines ordered alphabetically. All computations were done at the Computing Centre of the University of Alberta on an Amdahl 470/V7 and later on Amdahl 470/V8. The equation solver VBSOLV is not given as it was not developed during this study. The functions COST and GUINFO are utility functions of the Department of Computing Services.

```
C     ***************************************************************
C     *                                                             *
C     *        FINITE ELEMENT PROGRAM FOR GEOMETRIC NONLINEAR       *
C     *         ANALYSIS OF THIN-WALLED CIRCULAR STRUCTURES         *
C     *                                                             *
C     ***************************************************************
C
C     ( THIS PROGRAM CALLS THE PROGRAMS MAIN1 OR MAIN4 )
C
      IMPLICIT REAL*8(A-H,O-Z)
      READ(5,10) M
   10 FORMAT(G5)
      IF (M.EQ.1) CALL MAIN1
      IF (M.EQ.2) CALL ASTART
C     IF (M.EQ.4) CALL MAIN4
      STOP
      END
      SUBROUTINE ASOKT(NOEL,OD,OKT,IX)
C
C     ASSEMBLAGE OF THE (TANGENT) STIFFNESS MATRIX
C
      IMPLICIT REAL*8(A-H,O-Z)
      COMMON / EIK   /E2K(20,20),E3K(1540),E4K(8855)
      COMMON / WHOLE /IBC(2),INR,IN(50),IS,IT,IXCH,LCH,NBAND,NEC,
     1 NEL,NINTP,NINTS,NINTX,NL,NMAX,NN,NNC,NN5,NPD,NX,NX1,NP,NP1,
     2 N2P,N2X,NX2
      COMMON / ETANK /ETK(20,20),V(20)
      DIMENSION NOEL(4,NEL),OD(NN5),OKT(NBAND,NN5),IX(NN5),INS(121)
C
      DO 10 J=1,NN5
      DO 10 I=1,NBAND
   10 OKT(I,J)=0.D0
      DO 40 I=1,NEL
      IF (IN(12).EQ.0) GOTO 30
      DO 20 J=1,4
      J5=(NOEL(J,I)-1)*5
      L=(J-1)*5
      DO 20 K=1,5
   20 V(L+K)=OD(J5+K)
   30 CALL KT
   40 CALL STUFF(OKT,NBAND,NN5,INS,ETK,NOEL,NEL,NN,I,IX)
      IF (IN(7).EQ.1) CALL PRTMAT(OKT,NBAND,1,1,NBAND,NN5,'OKT.FREE')
      RETURN
      END
      SUBROUTINE ASSEM(NOEL,OKT,IX,OD)
C
C     STIFFNESS MATRICES
C
      IMPLICIT REAL*8(A-H,O-Z)
      COMMON / EIK   /E2K(20,20),E3K(1540),E4K(8855)
      COMMON / WHOLE /IBC(2),INR,IN(50),IS,IT,IXCH,LCH,NBAND,NEC,
     1 NEL,NINTP,NINTS,NINTX,NL,NMAX,NN,NNC,NN5,NPD,NX,NX1,NP,NP1,
     2 ISTART,IHALF,IDUMMY(7),NCONV
      COMMON / PART  /BETA,BETA2,CBETA,CED,DB,DEG,DELTA,DELTAT,E,ED,
     1 EN,E2,FLEX,PEL,PEL2,PI,R,RL,RM,RN,RNU,DNORM,PREC,TH,XEL,TIME,
     2 XD,REDUCE,FLOAD,FSTEP
      DIMENSION OKT(NBAND,NN5),OD(NN5),NOEL(4,NEL),IX(NN5)
C
      DAS=COST(0)
      WRITE(7,10) DAS
   10 FORMAT(/' BEFORE ASSEM:',F10.2)
      IS=IS+1
      FLOAD=FLOAD+FSTEP
      IT=-1
      IF ((IS+IHALF).GT.1) GOTO 40
      CALL GTCPL(TIME)
      IF (IN(12).EQ.0) IS=-1
      CALL TMAT
      DO 20 I=1,NN5
   20 OD(I)=0.D0
      WRITE(12) OD
      IF (IN(11).NE.1) GOTO 30
      READ(11) E2K
      IF (IN(12).EQ.0) GOTO 40
      READ(11) E3K,E4K
      GOTO 40
   30 CALL CYLSTF
      IN(11)=1
   40 CALL ASOKT(NOEL,OD,OKT,IX)
      RETURN
      END
      SUBROUTINE ASTART
C
C     ARRANGING ARRAYS FOR SUBROUTINE RSTART
C
      IMPLICIT REAL*8(A-H,O-Z)
      COMMON / WHOLE /IBC(2),INR,IN(50),IS,IT,IXCH,LCH,NBAND,NEC,
     1 NEL,NINTP,NINTS,NINTX,NL,NMAX,NN,NNC,NN5,NPD,NX,NX1,NP,NP1,
     2 ISTART,IHALF,NEXTIT,LCAUSE,NEXTIS,NEXTOV,ITOVAL,ITOVIT,NOVA
      DIMENSION OKT(65,605),NOEL(4,100),P(605),IV(605),IH(605),
     1 IX(605),OD(605),DV(53),ID(605),OF(605),VL(605),NPL(605),
     2 IXNEW(605)
C
      READ(10) IBC,INR,IN,IS,IT,IXCH,LCH,NBAND,NEC,NEL,NEXTIT,
     1 LCAUSE,NINTP,NINTS,NINTX,NL,NMAX,NN,NNC,NN5,NPD,NX,NX1,NP,
     2 NP1,IHALF,NEXTIS,NEXTOV,ITOVAL,ITOVIT,NOVA
      ISTART=1
      CALL RSTART(OKT,P,OD,NOEL,OF,IX,DV,IV,IH,VL,NPL,IXNEW)
      STOP
      END
      SUBROUTINE BC1(IX)
C
C     GENERATION OF BOUNDARY CONDITIONS FOR (A-)SYMMETRY OF THE
C     TOP AND BOTTOM EDGE AND THE MID-SECTION OF THE CYLINDER
C
      IMPLICIT REAL*8(A-H,O-Z)
      COMMON / WHOLE /IBC(2),INR,IN(50),IS,IT,IXCH,LCH,NBAND,NEC,
     1 NEL,NINTP,NINTS,NINTX,NL,NMAX,NN,NNC,NN5,NPD,NX,NX1,NP,NP1,
     2 N2P,N2X,NX2
      DIMENSION IX5(5,121),N(5),IX(NN5)
C
      DO 10 J=1,NN
      DO 10 I=1,5
   10 IX5(I,J)=1
      IF (IBC(1)-1) 30,30,20
   20 N(1)=2
      N(2)=5
      GOTO 40
   30 N(1)=3
      N(2)=4
   40 IF (IBC(2)-1) 60,60,50
   50 K=4
      N(3)=1
      N(4)=4
      GOTO 70
   60 K=5
      N(3)=2
      N(4)=3
      N(5)=5
   70 CONTINUE
      DO 80 I=1,2
      DO 80 J=1,NX1
      IX5(N(I),J*NP1)=0
   80 IX5(N(I),J*NP1-NP)=0
      J1=NX*NP1+1
      J2=J1+NP
      DO 90 I=3,K
      DO 90 J=J1,J2
   90 IX5(N(I),J)=0
      DO 100 I=1,NN
      K=5*(I-1)
      DO 100 J=1,5
  100 IX(K+J)=IX5(J,I)
      RETURN
      END
      SUBROUTINE BXP(X,P)
C
C     COEFFICIENTS OF 'B,X', 'B,PHI', 'B3', AND 'B4'.
C     (BX3,BP3,BX2,BP1)
C
      IMPLICIT REAL*8(A-H,O-Z)
      COMMON / WHOLE /IBC(2),INR,IN(50)
      COMMON / PART  /BETA,BETA2,CBETA,CED,DB,DEG,DELTA,DELTAT,E,ED,
     1 EN,E2,FLEX,PEL,PEL2,PI,R,RL,RM,RN,RNU,RNU1,SIGMA,TH,XEL
      COMMON / TMINUS/T(20,20)
      COMMON / BF    /BPF(20),BXF(20),B3F(20),B4F(20)

      DS=DSIN(P)
      DC=DCOS(P)
      R2=R*R
      X2=X*X/2.DO
      XDR=X/R
      P2=P*P/2.DO
      XP=X*P
      XDR4=XDR/4.DO
      XDRS=XDR*DS
      RP=R*P
      X2DR=X2/R
      X3DR=X2*XDR/3.DO
      RXP=RP*X
      R1=R*(1.DO+P2)
      RXP2=R*X*P2
      PX2=P*X2
      PR2=P*R2
      DO 10 I=1,20
      BXF(I)=-T(2,I)*DC-T(4,I)*DS-T(8,I)*XDRS+T(10,I)*R-T(12,I)*X-
     1 T(13,I)*X2-T(14,I)*XP-T(15,I)*PX2-T(17,I)*R2-T(19,I)*PR2
   10 BPF(I)=-T(6,I)/R-T(11,I)*XDR4-T(14,I)*X2DR-T(15,I)*X3DR-
     1 T(16,I)*RP-T(17,I)*RXP-T(18,I)*R1-T(19,I)*RXP2-T(20,I)*X
      IF (IN(31).LT.1) RETURN
C
      DO 20 I=1,20
      B3F(I)=T(2,I)*DS-T(4,I)*DC-T(8,I)*XDR*DC+T(11,I)/4.DO+
     1 T(17,I)*PR2+T(19,I)*R2*(P2-1.DO)+T(20,I)*R
   20 B4F(I)=-T(2,I)*DS+T(4,I)*DC+T(8,I)*XDR*DC+T(11,I)*0.75DO-
     1 T(17,I)*PR2-T(19,I)*R2*(P2-1.DO)-T(20,I)*R
      RETURN
      END
      SUBROUTINE CHANGE(IXNEW,IX,NPL,VL)
C
C     INPUT OF LOAD, DISPLACEMENTS AND CORESPONDING FLAGS,
C     SHOWING IF A LOAD (DISPLACEMENT) IS TO BE HELD CONSTANT,
C     OR TO BE INCREASED AFTER EACH LOAD STEP
C
C     INPUT
C             K: DEGREE OF FREEDOM TO BE CHANGED
C             L: NEW BOUNDARY CONDITION (1 TO 6)
C             F: APPLYING FORCE OR DISPLACEMENT
C
      IMPLICIT REAL*8(A-H,O-Z)
      COMMON / WHOLE /IBC(2),INR,IN(50),IS,IT,IXCH,LCH,NBAND,NEC,
     1 NEL,NINTP,NINTS,NINTX,NL,NMAX,NN,NNC,NN5,NPD,NX,NX1,NP,NP1,
     2 N2P,N2X,NX2
      COMMON / PART  /BETA,BETA2,CBETA,CED,DB,DEG,DELTA,DELTAT,E,ED,
     1 EN,E2,FLEX,PEL,PEL2,PI,R,RL,RM,RN,RNU,RNU1,SIGMA,TH,XEL,TIME
      DIMENSION IX(NN5),VL(NN5),NPL(NN5),IXNEW(605)
C
      NPD=2*NNC
      IF (IXCH.EQ.0) GOTO 30
      DO 20 I=1,IXCH
      READ(5,10) K,L
   10 FORMAT(3G20.10)
      IF (IX(K).EQ.2) NPD=NPD-1
      IF (L.EQ.2) NPD=NPD+1
   20 IX(K)=L
   30 NL=6
```

```
      IF (LCH.EQ.0) GOTO 60
      DO 40 I=1,6
      NPL(I)=0
   40 IXNEW(I)=0
      DO 50 I=1,LCH
      READ(5,10) K,L,F
      IF (IX(K).EQ.0) CALL ERROR(7,K,K)
      NL=NL+1
      NPL(L)=NPL(L)+1
      IXNEW(NL)=L
      NPL(NL)=K
   50 VL(NL)=F
      NPL(1)=NPL(3)+NPL(4)
      NPL(2)=NPL(5)+NPL(6)
   60 READ (5,10,END=70)L
      CALL ERROR(4,L,L)
   70 RETURN
      END
      SUBROUTINE CYLSTF
C
C     CALCULATION OF THE THREE STIFFNESS MATRICES
C
      IMPLICIT REAL*8(A-H,O-Z)
      COMMON / WHOLE /IBC(2),INR,IN(50),IS,IT,IXCH,LCH,NBAND,NEC,
     1 NEL,NINTP,NINTS,NINTX,NL,NMAX,NN,NNC,NN5,NPD,NX,NX1,NP,NP1,
     2 N2P,N2X,NX2
      COMMON / PART  /BETA,BETA2,CBETA,CED,DB,DEG,DELTA,DELTAT,E,ED,
     1 EN,E2,FLEX,PEL,PEL2,PI,R,RL,RM,RN,RNU,DNORM,SIGMA,TH,XEL,TIME
      COMMON / EIK   /E2K(20,20),E3K(1540),E4K(8855)
      COMMON / AF    /AXF(20),APF(20),APXF(20)
      COMMON / TF    /TXF(20),TPF(20),TPXF(20)
      COMMON / BF    /BPF(20),BXF(20),B3F(20),B4F(20)
      DIMENSION X(24),WX(24),P(24),WP(24),T1(20),T2(20),
     1 BX2(20,20),BP2(20,20),BXBP(20,20),B32(20,20),B42(20,20),
     2 BX32(20,20),BP42(20,20),B342(20,20),B432(20,20),
     3 BX31(20,20),BP41(20,20)
C
      IF (IN(31).NE.2) GOTO 10
      CALL NEWCYL
      RETURN
   10 CONTINUE
      CALL GAUSS(X,WX,24,XEL,NINTX)
      CALL GAUSS(P,WP,24,PEL,NINTP)
      IF (IN(25).EQ.1) CALL TMAT
      DO 20 I=1,20
      DO 20 J=1,20
   20 E2K(J,I)=0.D0
      DO 30 I=1,1540
   30 E3K(I)=0.D0
      DO 40 I=1,8855
   40 E4K(I)=0.D0
C
      C=E*TH/(1.D0-RNU*RNU)
      D=C*TH*TH/12.D0
      RNU1=(1.D0-RNU)/2.D0
      RNU2=RNU1+RNU1
      RNU4=RNU2+RNU2
C
      DO 150 INX=1,NINTX
      DO 150 INP=1,NINTP
      CALL SALF(X(INX),P(INP))
      CALL STH(X(INX),P(INP))
      DO 50 I=1,20
      T1(I)=TXF(I)+RNU*TPF(I)
   50 T2(I)=TPF(I)+RNU*TXF(I)
C
C     STIFFNESS MATRIX OF SECOND ORDER
C
      WXWPR=WX(INX)*WP(INP)*R
      W2C=WXWPR*C
      W2D=WXWPR*D
      DO 60 I=1,20
      DO 60 J=I,20
   60 E2K(I,J)=E2K(I,J)+
     1 W2C*(TXF(I)*T1(J)+TPF(I)*T2(J)+RNU1*TPXF(I)*TPXF(J))+
     2 W2D*(AXF(I)*(AXF(J)+RNU*APF(J))+APF(I)*(APF(J)+RNU*AXF(J))+
     3 RNU4*APXF(I)*APXF(J))
      IF (IN(12).EQ.0) GOTO 150
C
C     PRECALCULATIONS FOR NONLINEAR TERMS
C
      CALL BXP(X(INX),P(INP))
      DO 80 I=1,20
      DO 70 J=1,20
      BX2(J,I)=BXF(I)*BXF(J)
   70 BP2(J,I)=BPF(I)*BPF(J)
      DO 80 J=1,20
   80 BXBP(J,I)=BXF(J)*BPF(I)
      DO 90 J=1,20
      DO 90 I=1,20
      BX31(I,J)=BX2(I,J)
   90 BP41(I,J)=BP2(I,J)
      IF (IN(31).NE.1) GOTO 110
C
C     PRECALCULATIONS FOR EXTENDED STRAIN EXPRESSIONS
C
      DO 100 J=1,20
      DO 100 I=1,20
      B32(I,J)=B3F(I)*B3F(J)
      B42(I,J)=B4F(I)*B4F(J)
      BX31(I,J)=BX31(I,J)+B32(I,J)
      BP41(I,J)=BP41(I,J)+B42(I,J)
      B342(I,J)=B32(I,J)+RNU*B42(I,J)
      B432(I,J)=B42(I,J)+RNU*B32(I,J)
      BX32(I,J)=2.D0*BX2(I,J)+B32(I,J)
  100 BP42(I,J)=2.D0*BP2(I,J)+B42(I,J)
C
C     STIFFNESS MATRIX OF THIRD ORDER
C
  110 CONTINUE
      W3=W2C
      W4=W2C*1.5D0
      N=0
      DO 120 I=1,20
      N=N+1
      E3K(N)=E3K(N)+W3*3.D0*(T1(I)*BX31(I,I)+T2(I)*BP41(I,I)+
     1 RNU2*(TPXF(I)*BXBP(I,I)))
      IF (I.EQ.20) GOTO 120
      I1=I+1
      DO 120 J=I1,20
      N=N+1
      E3K(N)=E3K(N)+W3*(2.D0*T1(I)*BX31(I,J)+T1(J)*BX31(I,I)+
     1 2.D0*T2(I)*BP41(I,J)+T2(J)*BP41(I,I)+
     2 RNU2*(TPXF(I)*(BXBP(I,J)+BXBP(J,I))+TPXF(J)*BXBP(I,I)))
      N=N+1
      E3K(N)=E3K(N)+W3*(2.D0*T1(J)*BX31(I,J)+T1(I)*BX31(J,J)+
     1 2.D0*T2(J)*BP41(I,J)+T2(I)*BP41(J,J)+
     2 RNU2*(TPXF(J)*(BXBP(I,J)+BXBP(J,I))+TPXF(I)*BXBP(J,J)))
      IF (J.EQ.20) GOTO 120
      J1=J+1
      DO 120 K=J1,20
      N=N+1
      E3K(N)=E3K(N)+W3*(T1(I)*BX31(J,K)+T1(J)*BX31(I,K)+T1(K)*BX31(I,J)
     1 +T2(I)*BP41(J,K)+T2(J)*BP41(I,K)+T2(K)*BP41(I,J)+
     2 RNU1*(TPXF(I)*(BXBP(J,K)+BXBP(K,J))+TPXF(J)*(BXBP(I,K)+
     3 BXBP(K,I))+TPXF(K)*(BXBP(I,J)+BXBP(J,I))))
  120 CONTINUE
C
C     STIFFNESS MATRIX OF FOURTH ORDER
C
      N=0
      DO 130 I=1,20
      N=N+1
      E4K(N)=E4K(N)+W4*(BX2(I,I)+BP2(I,I))*(BX2(I,I)+BP2(I,I))
      IF (I.EQ.20) GOTO 130
      I1=I+1
      DO 130 J=I1,20
      N=N+1
      E4K(N)=E4K(N)+W4*(BX2(I,I)+BP2(I,I))*(BX2(I,J)+BP2(I,J))
      N=N+1
      E4K(N)=E4K(N)+W4*(BX2(I,I)*BX2(J,J)+BP2(I,I)*BP2(J,J)+
     1 (BX2(I,I)*BP2(J,J)+BX2(J,J)*BP2(I,I)+4.D0*BX2(I,J)*
     2 BP2(I,J))/3.D0)
      N=N+1
      E4K(N)=E4K(N)+W4*(BX2(I,J)+BP2(I,J))*(BX2(J,J)+BP2(J,J))
      IF (J.EQ.20) GOTO 130
      J1=J+1
      DO 130 K=J1,20
      N=N+1
      E4K(N)=E4K(N)+W4*(BX2(I,I)*BX2(J,K)+BP2(I,I)*BP2(J,K)+
     1 (BX2(I,I)*BP2(J,K)+2.D0*BX2(I,J)*BP2(I,K)+
     2 2.D0*BX2(I,K)*BP2(I,J)+BX2(J,K)*BP2(I,I))/3.D0)
      N=N+1
      E4K(N)=E4K(N)+W4*(BX2(I,J)*BX2(J,K)+BP2(I,J)*BP2(J,K)+
     1 (2.D0*BX2(I,J)*BP2(J,K)+BX2(J,J)*BP2(I,K)+
     2 2.D0*BX2(J,K)*BP2(I,J)+BX2(I,K)*BP2(J,J))/3.D0)
      N=N+1
      E4K(N)=E4K(N)+W4*(BX2(I,J)*BX2(K,K)+BP2(I,J)*BP2(K,K)+
     1 (BX2(I,J)*BP2(K,K)+2.D0*BX2(I,K)*BP2(J,K)+
     2 2.D0*BX2(J,K)*BP2(I,K)+BX2(K,K)*BP2(I,J))/3.D0)
      IF (K.EQ.20) GOTO 130
      K1=K+1
      DO 130 L=K1,20
      N=N+1
      E4K(N)=E4K(N)+W4*(BX2(I,J)*BX2(K,L)+BP2(I,J)*BP2(K,L)+
     1 (BX2(I,J)*BP2(K,L)+BX2(I,K)*BP2(J,L)+BX2(I,L)*BP2(J,K)+
     2 BX2(J,K)*BP2(I,L)+BX2(J,L)*BP2(I,K)+BX2(K,L)*BP2(I,J))/3.D0)
  130 CONTINUE
      IF (IN(31).NE.1) GOTO 150
C
C     CONTRIBUTIONS OF EXTENDED STRAIN EXPRESSION FOR EK4(I,J,K,L)
C
      N=0
      DO 140 I=1,20
      N=N+1
      E4K(N)=E4K(N)+W4*(B342(I,I)*BX32(I,I)+B432(I,I)*BP42(I,I))
      IF (I.EQ.20) GOTO 140
      I1=I+1
      DO 140 J=I1,20
      N=N+1
      E4K(N)=E4K(N)+W4*((B342(I,I)*BX32(I,J)+B432(I,I)*BP42(I,J))+
     1 B342(I,J)*BX32(I,I)+B432(I,J)*BP42(I,I))/2.D0
      N=N+1
      E4K(N)=E4K(N)+W4*(B342(I,I)*BX32(J,J)+B432(I,I)*BP42(J,J)+
     1 B342(J,J)*BX32(I,I)+B432(J,J)*BP42(I,I)+
     2 (B342(I,J)*BX32(I,J)+B432(I,J)*BP42(I,J))*4.D0)/6.D0
      N=N+1
      E4K(N)=E4K(N)+W4*(B342(I,J)*BX32(J,J)+B432(I,J)*BP42(J,J)+
     1 B342(J,J)*BX32(I,J)+B432(J,J)*BP42(I,J))/2.D0
      IF (J.EQ.20) GOTO 140
      J1=J+1
      DO 140 K=J1,20
      N=N+1
      E4K(N)=E4K(N)+W4*(B342(I,I)*BX32(J,K)+B432(I,I)*BP42(J,K)+
     1 B342(J,K)*BX32(I,I)+B432(J,K)*BP42(I,I)+
     2 (B342(I,J)*BX32(I,K)+B432(I,J)*BP42(I,K)+
     3 B342(I,K)*BX32(I,J)+B432(I,K)*BP42(I,J))*2.D0)/6.D0
      N=N+1
      E4K(N)=E4K(N)+W4*((B342(I,J)*BX32(J,K)+B432(I,J)*BP42(J,K))*2.D0+
     1 B342(I,K)*BX32(J,J)+B432(I,K)*BP42(J,J)+
     2 (B342(J,K)*BX32(I,J)+B432(J,K)*BP42(I,J))*2.D0+
     3 B342(J,J)*BX32(I,K)+B432(J,J)*BP42(I,K))/6.D0
      N=N+1
      E4K(N)=E4K(N)+W4*(B342(I,J)*BX32(K,K)+B432(I,J)*BP42(K,K)+
     1 B342(K,K)*BX32(I,J)+B432(K,K)*BP42(I,J)+
     2 (B342(I,K)*BX32(J,K)+B432(I,K)*BP42(J,K)+
     3 B342(J,K)*BX32(I,K)+B432(J,K)*BP42(I,K))*2.D0)/6.D0
      IF (K.EQ.20) GOTO 140
      K1=K+1
      DO 140 L=K1,20
      N=N+1
      E4K(N)=E4K(N)+W4*(B342(I,J)*BX32(K,L)+B432(I,J)*BP42(K,L)+
     1 B342(I,K)*BX32(J,L)+B432(I,K)*BP42(J,L)+
     2 B342(I,L)*BX32(J,K)+B432(I,L)*BP42(J,K)+
     3 B342(J,K)*BX32(I,L)+B432(J,K)*BP42(I,L)+
     4 B342(J,L)*BX32(I,K)+B432(J,L)*BP42(I,K)+
     5 B342(K,L)*BX32(I,J)+B432(K,L)*BP42(I,J))/6.D0
  140 CONTINUE
C
C     STORAGE OF STIFFNESS MATRICES
C
  150 CONTINUE
      WRITE(11) E2K
      IF (IN(12).EQ.0) GOTO 160
      WRITE(11) E3K,E4K
  160 IF (IN(25).EQ.1) STOP
      REWIND 11
      RETURN
      END
      SUBROUTINE DATA(TITLE)
C
C     INPUT OF: GEOMETRY, MATERIAL PROPERTIES,
C               ELEMENT SUBDIVISON,
C               SYMMETRY AND ASYMMETRY,
C               ORDER OF INTEGRATION,
C               ANGLE AT ENDS,
C               OUTPUT AND ITERATION PARAMETERS.
C
      IMPLICIT REAL*8(A-H,O-Z)
      COMMON / WHOLE /IBC(2),INR,IN(50),IS,IT,IXCH,LCH,NBAND,NEC,
     1 NEL,NINTP,NINTS,NINTX,NL,NMAX,NN,NNC,NN5,NPD,NX,NX1,NP,NP1,
     2 N2P,N2X,NX2
      COMMON / PART  /BETA,BETA2,CBETA,CED,DB,DEG,DELTA,DELTAT,E,ED,
     1 EN,E2,FLEX,PEL,PEL2,PI,R,RL,RM,RN,RNU,RNU1,PREC,TH,XEL,TIME
      REAL TITLE(50)
C
      READ(5,10) TITLE
   10 FORMAT(50A4)
      READ(5,20) RL,R,TH,E,RNU
      READ(5,20) NX,NP
      READ(5,20) (IBC(I),I=1,2)
      READ(5,20) NINTX,NINTP,NINTS
      READ(5,20) CBETA,CED
      READ(5,20) INL,INL1,INN
      READ(5,20) (IN(I),I=1,INL)
      READ(5,20) (IN(I),I=INL1,INN)
      READ(5,20) IXCH,LCH
   20 FORMAT(20G20)
      RETURN
      END
      SUBROUTINE EQ(OD,OF,NOEL)
C
C     CALCULATION OF NEGATIVE INTERNAL EQUILIBRIUM FORCES
C
      IMPLICIT REAL*8(A-H,O-Z)
      COMMON / EIK   /E2K(20,20),E3K(1540),E4K(8855)
      COMMON / WHOLE /IBC(2),INR,IN(50),IS,IT,IXCH,LCH,NBAND,NEC,
     1 NEL,NINTP,NINTS,NINTX,NL,NMAX,NN,NNC,NN5,NPD,NX,NX1,NP,NP1,
     2 N2P,N2X,NX2
      DIMENSION V(20),F(20),OF(NN5),NOEL(4,NEL),VV(20,20),OD(NN5)
C
      DO 10 I=1,NN5
   10 OF(I)=0.D0
      DO 80 M=1,NEL
      DO 20 I=1,4
      K=5*(NOEL(I,M)-1)
      I5=(I-1)*5
      DO 20 J=1,5
      F(I5+J)=0.D0
   20 V(I5+J)=OD(K+J)
C
C     QUADRATIC PART
C
      DO 30 I=1,20
      F(I)=F(I)+E2K(I,I)*V(I)
      IF (I.EQ.20) GOTO 30
      I1=I+1
      DO 30 J=I1,20
      F(I)=F(I)+E2K(I,J)*V(J)
      F(J)=F(J)+E2K(I,J)*V(I)
   30 CONTINUE
C
C     QUBIC PART
C
      DO 40 I=1,20
      DO 40 J=I,20
   40 VV(I,J)=V(I)*V(J)
      N=0
      DO 50 I=1,20
      N=N+1
      F(I)=F(I)+E3K(N)*VV(I,I)/2.D0
      IF (I.EQ.20) GOTO 50
      I1=I+1
      DO 50 J=I1,20
      N=N+1
      W=E3K(N)
      F(I)=F(I)+W*VV(I,J)
      F(J)=F(J)+W*VV(I,I)/2.D0
      N=N+1
      W=E3K(N)
      F(I)=F(I)+W*VV(J,J)/2.D0
      F(J)=F(J)+W*VV(I,J)
      IF (J.EQ.20) GOTO 50
      J1=J+1
      DO 50 K=J1,20
      N=N+1
      W=E3K(N)
      F(I)=F(I)+W*VV(J,K)
      F(J)=F(J)+W*VV(I,K)
      F(K)=F(K)+W*VV(I,J)
   50 CONTINUE
C
C     QUARTIC PART
C
      N=0
      DO 60 I=1,20
      N=N+1
      F(I)=F(I)+E4K(N)*VV(I,I)*V(I)/3.D0
      IF (I.EQ.20) GOTO 60
      I1=I+1
      DO 60 J=I1,20
      N=N+1
      W=E4K(N)
      F(I)=F(I)+W*VV(I,I)*V(J)
      F(J)=F(J)+W*VV(I,I)*V(I)/3.D0
      N=N+1
      W=E4K(N)
      F(I)=F(I)+W*VV(I,J)*V(J)
      F(J)=F(J)+W*VV(I,I)*V(J)
      N=N+1
      W=E4K(N)
      F(I)=F(I)+W*VV(J,J)*V(J)/3.D0
      F(J)=F(J)+W*VV(I,J)*V(J)
      IF (J.EQ.20) GOTO 60
      J1=J+1
      DO 60 K=J1,20
      N=N+1
      W=E4K(N)
      F(I)=F(I)+W*VV(I,J)*V(K)*2.D0
      F(J)=F(J)+W*VV(I,I)*V(K)
      F(K)=F(K)+W*VV(I,I)*V(J)
      N=N+1
      W=E4K(N)
      F(I)=F(I)+W*VV(J,J)*V(K)
      F(J)=F(J)+W*VV(I,J)*V(K)*2.DO
      F(K)=F(K)+W*VV(I,J)*V(J)
      N=N+1
      W=E4K(N)
      F(I)=F(I)+W*VV(J,K)*V(K)
      F(J)=F(J)+W*VV(I,K)*V(K)
      F(K)=F(K)+W*VV(I,J)*V(K)*2.DO
      IF (K.EQ.20) GOTO 60
      K1=K+1
      DO 60 L=K1,20
      N=N+1
      W=2.DO*E4K(N)
      F(I)=F(I)+W*VV(J,K)*V(L)
      F(J)=F(J)+W*VV(I,K)*V(L)
      F(K)=F(K)+W*VV(I,J)*V(L)
      F(L)=F(L)+W*VV(I,J)*V(K)
   60 CONTINUE
      DO 70 I=1,4
      I5=(I-1)*5
      K=5*(NOEL(I,M)-1)
      DO 70 J=1,5
   70 OF(K+J)=OF(K+J)-F(I5+J)
   80 CONTINUE
      RETURN
      END
      SUBROUTINE ERROR(I,K,L)
C
C     ERROR DIAGNOSIS OF INPUT
C
      IF (I.EQ.1) WRITE(6,10) K,L
   10 FORMAT(' '/' NUMBER OF ELEMENTS =',I5,' ALLOWED ONLY',I4)
      IF (I.EQ.2) WRITE(6,20) K,L
   20 FORMAT(' '/' NUMBER OF CHANGES IN BOUNDARY CONDITIONS =',
     1 I5/' POSSIBLE ONLY',I4)
      IF (I.EQ.3) WRITE(6,30) K,L
   30 FORMAT(' '/' NUMBER OF LOAD CHANGES =',I5,' POSSIBLE ONLY',I4)
      IF (I.EQ.4) WRITE(6,40) K
   40 FORMAT(' '/' NOT ALL DATA IN UNIT 5 IS NEEDED; FIRST SURPLUS
     1 DATA IS',I5)
      IF (I.EQ.5) WRITE(6,50) K,L
   50 FORMAT(' '/' NUMBER OF ELEMENTS IN THE LONGITUDINAL DIRECTION
     1  =',I5/' ALLOWED ONLY',I3)
      IF (I.EQ.6) WRITE(6,60) L,K
   60 FORMAT(' '/' NUMBER OF ELEMENTS IN THE CIRCUMFERENTIAL
     1 DIRECTION =',I5/' ALLOWED ONLY',I3)
      IF (I.EQ.7) WRITE(6,70) K
   70 FORMAT(' '/' DISPLACEMENT NUMBER',I4,' IS ASSIGNED LOAD,
     1 BUT DEFINED AS FIXED')
      IF (I.EQ.8) WRITE(6,80) K
   80 FORMAT(' '/' NUMBER OF LOAD STEPS =',I4,'. ALLOWED ONLY',I4)
      IF (I.EQ.9) WRITE(6,90) K,L
   90 FORMAT(' '/' NO SUCCESS IN VBSOLV AT LOAD STEP',I3,
     1 ' , ITERATON',I3)
      IF (I.EQ.10) WRITE(6,100) L,K
  100 FORMAT(' '/' DISPLACEMENT NORM OF ITERATION',I3,' IN LOAD',
     1 ' STEP',I3,' IS GREATER THAN'/' 1.001 TIMES THE FIRST',
     2 ' DISPLACEMENT NORM OF THE CURRANT LOAD STEP.')
      IF (I.EQ.11) WRITE(6,110) K
  110 FORMAT(' '/' CYLINDER FORCES CANNOT BE COMPUTED BY NODAL
     1 FORCES'/' WHEN CROSS SECTION IS ALLOWED TO DISTORT.')
      STOP
      END
      SUBROUTINE FORCE1(NOEL,OD)
C
C     CALCULATION OF AXIAL FORCE AND BENDING MOMENT OF CYLINDER
C     BY CONSIDERING ELEMENT STRESSES
C
      IMPLICIT REAL*8(A-H,O-Z)
      COMMON / TMINUS/T(20,20)
      COMMON / WHOLE /IBC(2),INR,IN(50),IS,IT,IXCH,LCH,NBAND,NEC,
     1 NEL,NINTP,NINTS,NINTX,NL,NMAX,NN,NNC,NN5,NPD,NX,NX1,NP,NP1
      COMMON / PART  /BETA,BETA2,CBETA,CED,DB,DEG,DELTA,DELTAT,E,ED,
     1 EN,E2,FLEX,PEL,PEL2,PI,R,RL,RM,RN,RNU,RNU1,PREC,TH,XEL,TIME
      COMMON / AF    /AXF(20),APF(20),APXF(20)
      COMMON / TF    /BX1(20),BP2(20),TPXF(20)
      COMMON / BF    /BP3(20),BX3(20),BX2(20),BP1(20)
      COMMON / DELVW /RV(20),RW(20)
      DIMENSION V(20),NOEL(4,NEL),PS(24),WS(24),OD(NN5)
C
      RN=0.D0
      RM=0.D0
      PHI=PEL
      X=XEL
      IA=1
      IE=NEC
      IF (IN(16).EQ.2) GOTO 10
      CALL GAUSS(PS,WS,24,XEL,NINTS)
      X=PS(NINTS)
   10 IF (IN(30).EQ.0) GOTO 20
      X=-X
      IA=NEL-NP+1
      IE=NEL
   20 CALL GAUSS(PS,WS,24,PEL,NINTS)
C
C     LINEAR STRESSES
C
      DO 110 I=IA,IE
      DO 30 J=1,4
      L1=(J-1)*5
      L2=(NOEL(J,I)-1)*5
      DO 30 L=1,5
   30 V(L1+L)=OD(L2+L)
      DO 100 J=1,NINTS
      S=PS(J)
      PT=PHI+S
      DS=DSIN(PT)
      DC=DCOS(PT)
      DCOSN=DC
      DCOSM=DC
      CALL STH(X,S)
      CALL SALF(X,S)
      VM=0.D0
      VN=0.D0
      T1=0.D0
      T2=0.D0
      T3=0.D0
      T4=0.D0
      DO 40 K=1,20
      W=V(K)
      T1=T1+BX1(K)*W
      T2=T2+BP2(K)*W
      T3=T3+AXF(K)*W
   40 T4=T4+APF(K)*W
      VN=T1+RNU*T2
      VM=T3+RNU*T4
      IF (IN(15).EQ.0) GOTO 90
C
C     NONLINEAR STRESS CONTRIBUTIONS
C
      BETAX3=0.D0
      BETAP3=0.D0
      BETAX2=0.D0
      BETAP1=0.D0
      BETAX1=0.D0
      BETAP2=0.D0
      CALL BXP(X,S)
      DO 50 K=1,20
      BETAX3=BETAX3+BX3(K)*V(K)
   50 BETAP3=BETAP3+BP3(K)*V(K)
      IF (IN(31).LT.1) GOTO 70
```

```
C
      DO 60 K=1,20
      BETAX2=BETAX2+BX2(K)*V(K)
   60 BETAP1=BETAP1+BP1(K)*V(K)
      IF (IN(31).NE.2) GOTO 70
C
      BETAX1=T1
      BETAP2=T2
C
   70 VN=VN+(BETAX1*BETAX1+BETAX2*BETAX2+BETAX3*BETAX3+
     1 RNU*(BETAP1*BETAP1+BETAP2*BETAP2+BETAP3*BETAP3))/2.D0
      IF (IN(30).EQ.0) GOTO 90
C
C     INFLUENCE OF OVALIZATION OR STRETCHING
C           OF CYLINDER CROSS SECTION
C
      CALL UVW(X,S)
      TV=0.D0
      TW=0.D0
      DO 80 K=1,20
      W=V(K)
      TV=TV+RV(K)*W
   80 TW=TW+RW(K)*W
      WB=(OD(NN5-2)-OD(NN5-NP*5-2))/2.D0
      DCOSM=DCOSM+DS*BETAP3
      DCOSN=DC+(TW*DC+WB-TV*DS)/R
C
   90 RN=RN+VN*WS(J)
  100 RM=RM-WS(J)*(VN*DCOSN+VM*DCOSM*E2)
  110 PHI=PHI+PEL2
      RN=RN*EN
      RM=RM*EN*R
      IF (IN(30).EQ.0) RN=RN*DCOS(BETA2)
      IF (IN(1).EQ.0) RETURN
      RM=RM+RM
      RN=RN+RN
      RETURN
      END
      SUBROUTINE FORCE2(OF,OD)
C
C     CALCULATION OF AXIAL FORCE AND BENDING MOMENT OF CYLINDER
C     BY CONSIDERING THE NODAL FORCES
C
      IMPLICIT REAL*8(A-H,O-Z)
      COMMON / WHOLE /IBC(2),INR,IN(50),IS,IT,IXCH,LCH,NBAND,NEC,
     1 NEL,NINTP,NINTS,NINTX,NL,NMAX,NN,NNC,NN5,NPD,NX,NX1,NP,NP1,
     2 N2P,N2X,NX2
      COMMON / PART  /BETA,BETA2,CBETA,CED,DB,DEG,DELTA,DELTAT,E,ED,
     1 EN,E2,FLEX,PEL,PEL2,PI,R,RL,RM,RN,RNU,RNU1,PREC,TH,XEL,TIME
      DIMENSION OF(NN5),OD(NN5)
C
      IF (IN(30).GT.0) CALL ERROR(11,IN(30),0)
      RN=0.D0
      RM=0.D0
      PHI=0.D0
      DC=DCOS(BETA2)
      DO 10 I=1,NNC
      I5=I*5-4
      RN=RN+OF(I5)
      RM=RM+DCOS(PHI)*(OD(I5)*OF(I5+2)+OF(I5+3)-OF(I5)*R*DC)
   10 PHI=PHI+PEL2
      IF (IN(1).EQ.0) GOTO 20
      RN=RN+RN
      RM=RM+RM
   20 CONTINUE
      RETURN
      END
      SUBROUTINE GAUSS(X,WT,NDIM,A,NORDER)
C
C***********************************************************************
C
C     THIS SUBROUTINE RETURNS TO THE CALLING PROGRAM THE ABSCISSAS
```

```
C      AND WEIGHT FACTORS FOR VARIOUS ORDERS OF GAUSSIAN INTEGRATION.
C
C      INPUT:
C          NORDER= THE ORDER OF THE GAUSSIAN INTEGRATION FORMULA WHICH
C                  IS WANTED.  VALUES WHICH NORDER CAN TAKE ARE 2 TO
C                  10,12, AND 16.
C          A= THE LOWER AND UPPER LIMIT FOR THE INTEGRATION VARIABLE X
C     OUTPUT:
C           X= A VECTOR CONTAINING THE X COORDINATES OF THE INTEGRATION
C              POINTS
C          WT= A VECTOR CONTAINING THE WEIGHT FACTORS
C          NDIM= THE DIMENSION OF X AND WT
C
C       THE INTEGRAL OF F(X) FROM X=-A TO X=A IS THUS EQUAL TO
C           SUM( WT(I)*F(X(I)) ),I=1, NORDER
C
C*********************************************************************
      IMPLICIT REAL*8 (A-H,O-Z)
      DIMENSION X(NDIM),WT(NDIM),XX(24,24),WWT(24,24)
      DATA WWT/24*O.DO,1.DO,23*O.DO,
     1 O.8888888888888889DO,O.5555555555555556DO,22*O.DO,
     2 O.652145154862546DO,O.347854845137454DO,22*O.DO,
     3 O.5688888888888889DO,O.478628670499366DO,O.236926885056189DO,
     4 21*O.DO,O.467913934572691DO,O.360761573048139DO,
     5 O.171324492379170DO,21*O.DO,O.417959183673469DO,
     6 O.381830050505119DO,O.279705391489277DO,O.129484966168870DO,
     7 20*O.DO,O.362683783378362DO,O.313706645877887DO,
     8 O.222381034453374DO,O.101228536290376DO,20*O.DO,
     9 O.330239355001260DO,O.312347077040003DO,O.260610696402935DO,
     * O.180648160694857DO,O.081274388361574DO,19*O.DO,
     1 O.295524224714753DO,O.269266719309996DO,O.219086362515982DO,
     2 O.149451349150581DO,O.066671344308688DO,43*O.DO,
     3 O.2491470458134027800,O.2334925365383548ODO,
     4 O.2031674267230659200,O.1600783285433462200,
     5 O.1069393259953184300,O.0471753363865118200,
     6 90*O.DO,O.1894506104550685ODO,O.1826034150449235900,
     7 O.1691565193950025400,O.1495959888165767300,
     8 O.1246289712555338700,O.0951585116824927800,
     9 O.0622535239386478900,O.0271524594117540900,208*O.DO/
      DATA XX/24*O.DO,O.577350269189626DO,23*O.DO,
     1 O.DO,O.774596669241483DO,22*O.DO,
     2 O.339981043584856DO,O.861136311594053DO,22*O.DO,
     3 O.DO,O.538469310105683DO,O.906179845938664DO,21*O.DO,
     4 O.238619186083197DO,O.661209386466265DO,O.932469514203152DO,
     5 21*O.DO,O.DO,O.405845151377397DO,O.741531185599394DO,
     6 O.949107912342759DO,20*O.DO,O.183434642495650DO,
     7 O.525532409916329DO,O.796666477413627DO,O.960289856497536DO,
     8 21*O.DO,O.324253423403809DO,O.613371432700590DO,
     9 O.836031107326636DO,O.968160239507626DO,19*O.DO,
     * O.148874338981631DO,O.433395394129247DO,O.679409568299024DO,
     1 O.865063366688985DO,O.973906528517172DO,43*O.DO,
     2 O.12523340851146916DO,O.36783149899818020DO,
     3 O.58731795428661744DO,O.76990267419430468DO,
     4 O.90411725637047486DO,O.98156063424671926DO,
     5 90*O.DO,O.09501250983763744ODO,O.28160355077925891DO,
     6 O.45801677765722739DO,O.61787624440264375DO,
     7 O.75540440835500303DO,O.86563120238783174DO,
     8 O.94457502307323258DO,O.98940093499164993DO,208*O.DO/
      IF (NDIM.GE.NORDER) GOTO 20
      WRITE(3,10)
   10 FORMAT('ODIMENSION FOR X AND WT IN SUBROUITNE GAUSS IS TOO SMALL
     1 FOR THE SPECIFIED VALUE OF NORDER')
      STOP
   20 XORDER=NORDER
      IODD=O
      IF ((XORDER/2.DO).GT.(NORDER/2)) IODD=1
      N=NORDER/2
      IF (IODD.EQ.1) N=(NORDER+1)/2
      DO 40 I=1,N
      IF (I.EQ.IODD) GOTO 30
      N1=N+1-I
      N2=N+I
      IF (IODD.EQ.1) N2=N2-1
      X(N1)=-XX(I,NORDER)*A
      X(N2)=-X(N1)
      WT(N1)=WWT(I,NORDER)*A
      WT(N2)=WT(N1)
      GOTO 40
   30 X(N)=0.D0
      WT(N)=WWT(1,NORDER)*A
   40 CONTINUE
      RETURN
      END
      SUBROUTINE GTCPL(TIME)
C
C     REMAINING SECONDS OF CPU-TIME
C
      REAL*8 TIME
      CALL GUINFO('LOCCPUT ',K1)
      CALL GUINFO('GLOBCPUT',K2)
      TIME=(DFLOAT(MIN0(K1,K2)))/76800.D0
      RETURN
      END
      SUBROUTINE INOUT(NOEL,P,TITLE,L,IX,NPL,VL,IXNEW)
C
C     OUTPUT OF INPUT INFORMATION
C
      IMPLICIT REAL*8(A-H,O-Z)
      COMMON / WHOLE /IBC(2),INR,IN(50),IS,IT,IXCH,LCH,NBAND,NEC,
     1 NEL,NINTP,NINTS,NINTX,NL,NMAX,NN,NNC,NN5,NPD,NX,NX1,NP,NP1,
     2 N2P,N2X,NX2
      COMMON / PART  /BETA,BETA2,CBETA,CED,DB,DEG,DELTA,DELTAT,E,ED,
     1 EN,E2,FLEX,PEL,PEL2,PI,R,RL,RM,RN,RNU,RNU1,PREC,TH,XEL
      DIMENSION NOEL(4,NEL),IX(NN5),P(NN5),NPL(NN5),VL(NN5),LT(5),
     1 IXNEW(NL)
      REAL TITLE(50)
C
C     OUTPLUT OF GEOMETRY AND CYLINDER IDEALIZATION
C
      CALL TIME(6,0,LT)
      IF (L.EQ.2) GOTO 120
      IF (IN(26).GT.0) IN(26)=1
      WRITE(7,10) LT,TITLE,RL,R,TH,E,RNU,(IN(I),I=1,35),NX,NP,PEL2,
     1 BETA,NBAND
   10 FORMAT('1',5A4/50A4//,'INPUT DATA'/10('*')////'LENGTH',F13.3,
     1 ' MM'/'RADIUS',F13.3,' MM'/'THICKNESS',F10.3,' MM'/
     2 /'YOUNG',1H','S MODULUS',F11.3,' MPA',
     3 /'POISSON',1H','S RATIO',F11.3,
     4 /'PARAMETER LIST',7(/,5I4),
     5 ///'NUMBER OF ELEMENTS',
     6 //'LONGITUDINAL:',I6,
     7 /'CIRCUMFERENTIAL:',I3,
     8 /'ANGLE PRESCRIBED PER ELEMENT =',F9.6,' RAD',
     9 /'ANGLE (STEPSIZE) AT ENDS DUE TO MOMENT =',E14.8,
     * /'HALF BANDWIDTH =',I3//
     1 /'SYMMETRY PROPERTIES'//,'X-Z PLANE:')
      DO 100 I=1,2
      IF (IBC(I)-1) 20,40,60
   20 WRITE(7,30)
   30 FORMAT('+',11X,'NOT SPECIFIED')
      GOTO 80
   40 WRITE(7,50)
   50 FORMAT('+',11X,'ASYMMETRY')
      GOTO 100
   60 WRITE(7,70)
   70 FORMAT('+',11X,'SYMMETRY')
   80 IF (I.EQ.1) WRITE(7,90)
   90 FORMAT(' Y-Z PLANE:')
  100 CONTINUE
      WRITE(7,110) NINTX,NINTP,NINTS
  110 FORMAT(' '///'ORDER OF GAUSSIAN INTEGRATION FOR STIFFNESS ',
     1 'MATRIX'///,
     2 ' DIRECTION  ORDER'//5X,'X',I9/4X,'PHI',I8///,
     3 'ORDER OF GAUSSIAN INTEGRATION FOR STRESS CALCULATION =',I3)
```

```
      RETURN
C
C     OUTPUT OF NODE ELEMENT CONNECTION
C
  120 WRITE(7,130)
  130 FORMAT(' '///'NODE ELEMENT CONNECTIONS'
     1 ///'ELEMENT             NODES'/)
      DO 140 I=1,NEL
  140 WRITE(7,150) I,(NOEL(J,I),J=1,4)
  150 FORMAT(' ',I5,6X,4I4)
C
C     OUTPUT OF NODAL BOUNDARY CONDITIONS
C
      WRITE(7,160)
  160 FORMAT(' '///'FREEDOM OF DISPLACEMENTS (O=CONSTRAINT TO O,',
     1 ' 1=FREE, 2=PRESCRIBED BY ANGLE AT END)'
     2 ///'    NODE   U   V   W  W,X (W,PHI -V)/R'/)
      DO 170 I=1,NN
  170 WRITE(7,180) I,(IX((I-1)*5+J),J=1,5)
  180 FORMAT(' ',I6,1X,4I4,I8)
      IF (LCH.EQ.O) RETURN
  190 WRITE(7,200) ((NPL(I),IXNEW(I),VL(I)),I=7,NL)
  200 FORMAT(' '///' PRESCRIBED LOADS AND DISPLACEMENTS',
     1 //,'  NR. IXNEW   VALUE (N OR NMM)'//(I5,I4,E21.10))
      RETURN
      END
      SUBROUTINE INPUT1(NOEL,P,IX,VL,NPL,IXNEW)
C
C     INPUT OF CYLINDER DATA AND INITIALIZING OF LOADING VARIABLES
C
      IMPLICIT REAL*8(A-H,O-Z)
      COMMON / WHOLE /IBC(2),INR,IN(50),IS,IT,IXCH,LCH,NBAND,NEC,
     1 NEL,NINTP,NINTS,NINTX,NL,NMAX,NN,NNC,NN5,NPD,NX,NX1,NP,NP1,
     2 ISTART,IHALF,NEXTIT,LCAUSE,NEXTIS,NEXTOV,ITOVAL,ITOVIT,NOVA,
     3 NCONV
      COMMON / PART  /BETA,BETA2,CBETA,CED,DB,DEG,DELTA,DELTAT,E,ED,
     1 EN,E2,FLEX,PEL,PEL2,PI,R,RL,RM,RN,RNU,DNORM,PREC,TH,XEL,TIME,
     2 XD,REDUCE,FLOAD,FSTEP,FDELTA,DONM
      DIMENSION IX(605),NOEL(4,100),P(605),NPL(605),VL(605),
     1 IXNEW(605)
      REAL TITLE(50)
C
      CALL DATA(TITLE)
      NEL=NX*NP
C     IF (NX.GT.10)      CALL ERROR(5,NX,10)
      IF (IN(17).GT.50) CALL ERROR(8,IN(18),50)
      IF (NEL.GT.100)    CALL ERROR(1,NEL,100)
      NN5=(NX+1)*(NP+1)*5
      IF (IXCH.GT.NN5)  CALL ERROR(2,IXCH,NN5)
      IF (LCH.GT.NN5)   CALL ERROR(3,LCH,NN5)
C
C     INITIALIZATION OF VARIABLES AND FLAGS
C
      ISTART=O
      LCAUSE=O
      PI=3.141592653589793DO
      NX1=NX+1
      NP1=NP+1
      NN=NX1*NP1
      NBAND=(NP1+2)*5
      NEC=NP
      NNC=NP1
      XEL=RL/(4.DO*NX)
      PEL=PI/(2.DO*NP)
      IF (IN(26).NE.O) PEL=DFLOAT(IN(26))/1000000000.DO
      PEL2=PEL+PEL
      EN=E*TH*R/(1.DO-RNU*RNU)
      E2=TH*TH/R/12.DO
      WUR=DSQRT(3.DO*(1.DO-RNU*RNU))
      BETA=RL*TH/R/R/2.DO/WUR*CBETA
      DB=BETA
      ED=CED*(DMIN1((PI*PI*R*R/RL/2.DO),(RL*TH/WUR/R)))/2.DO
      DONM=2*RNU*R*R/RL
      IF (IN(30).EQ.0) DONM=0.D0
      IF (IN(25).EQ.1) CALL CYLSTF
C
C     INITIALIZATIONS FOR NONLINEAR PROBLEM
C
      FLEX=-RL/EN/12.56637D0
      DELTA=0.D0
      IS=0
      RM=0.D0
      RN=0.D0
      IHALF=0
      FLOAD=0.D0
      FSTEP=1.D0
      REDUCE=0.56234D0
      IF (IN(29).GT.0) REDUCE=DFLOAT(IN(29))/10000.D0
      NEXTOV=0
      NCONV=0
C
C     DETERMINATION OF BOUNDARY CONDITIONS
C
      CALL BC1(IX)
      IF (IN(12).EQ.1) GOTO 10
      CALL LINEND(P,IX)
      GOTO 30
   10 DO 20 I=1,NP1
      I5=(I-1)*5
      DO 20 J=1,5
   20 IX(I5+J)=2
   30 CALL CHANGE(IXNEW,IX,NPL,VL)
      IF (IN(22).EQ.1) CALL NORMD(DNORM,IX)
C
C     DETERMINATION OF ELEMENT NODE CONNECTIONS
C
      DO 40 I=1,NX
      K=(I-1)*NP
      L=K+I-1
      DO 40 J=1,NP
      KJ=K+J
      LJ=L+J
      NOEL(1,KJ)=LJ+1
      NOEL(2,KJ)=LJ+NP1+1
      NOEL(3,KJ)=LJ+NP1
   40 NOEL(4,KJ)=LJ
C
      IF (IN(5).EQ.1) CALL INOUT(NOEL,P,TITLE,1,IX,NPL,VL,IXNEW)
      IF (IN(6).EQ.1) CALL INOUT(NOEL,P,TITLE,2,IX,NPL,VL,IXNEW)
      RETURN
      END
      SUBROUTINE INPUT2
C
C     DATA CHANGES DURING RESTART
C
      IMPLICIT REAL*8(A-H,O-Z)
      COMMON / WHOLE /IBC(2),INR,IN(50),IS,IT,IXCH,LCH,NBAND,NEC,
     1 NEL,NINTP,NINTS,NINTX,NL,NMAX,NN,NNC,NN5,NPD,NX,NX1,NP,NP1,
     2 ISTART,IHALF,NEXTIT,LCAUSE,NEXTIS,NEXTOV,ITOVAL,ITOVIT,NOVA,
     3 NCONV
      COMMON / PART  /BETA,BETA2,CBETA,CED,DB,DEG,DELTA,DELTAT,E,ED,
     1 EN,E2,FLEX,PEL,PEL2,PI,R,RL,RM,RN,RNU,DNORM,PREC,TH,XEL,TIME,
     2 XD,REDUCE,FLOAD,FSTEP,FDELTA,DONM,XDN
C
C     (IF NOT ENOUGH DATA IN FIRST INPUT LINE, NO CHANGES ARE MADE)
C
      READ(5,10,END=50) NCHIN,NED,NDB,NREDUC,NEWIX,NLOAD
   10 FORMAT(10G20)
   20 IF (NCHIN.EQ.0) GOTO 30
      READ(5,10) I,J
      IN(I)=J
      NCHIN=NCHIN-1
      GOTO 20
   30 CONTINUE
```

```
      EDNEW=1.D0
      DBNEW=1.D0
      IF (NED.EQ.1)    READ(5,10) EDNEW
      IF (NDB.EQ.1)    READ(5,10) DBNEW
      ED=ED*EDNEW
      DB=DB*DBNEW
      FSTEP=FSTEP*(DMIN1(EDNEW,DBNEW))
      IF (NREDUC.EQ.1) READ(5,10) REDUCE
      IF ((NEWIX+NLOAD).EQ.0) GOTO 40
C
C     CHANGE OF LOADS AND BOUNDARY CONDITIONS NOT YET IMPLEMENTED
C
   40 READ(5,10,END=50) L
      CALL ERROR(4,L,L)
   50 NCONV=0
      IF (XDN.LT.XD*10.D0**IN(19)) NCONV=1
      RETURN
      END
      SUBROUTINE ITERA(INDEX,DV,OD,VL)
C
C     REDUCTION OF LOAD STEP
C
      IMPLICIT REAL*8(A-H,O-Z)
      COMMON / WHOLE /IBC(2),INR,IN(50),IS,IT,IXCH,LCH,NBAND,NEC,
     1 NEL,NINTP,NINTS,NINTX,NL,NMAX,NN,NNC,NN5,NPD,NX,NX1,NP,NP1,
     2 ISTART,IHALF
      COMMON / PART  /BETA,BETA2,CBETA,CED,DB,DEG,DELTA,DELTAT,E,ED,
     1 EN,E2,FLEX,PEL,PEL2,PI,R,RL,RM,RN,RNU,DNORM,PREC,TH,XEL,TIME,
     2 XD,REDUCE,FLOAD,FSTEP,FDELTA
      DIMENSION DV(53),OD(NN5),VL(NL)
C
      IF (INDEX.GT.1) GOTO 10
      REWIND 12
      WRITE(12) OD
      FDELTA=(DV(IS+2)-DELTAT)/2.D0
      IF (IHALF.GT.0) GOTO 30
      FDELTA=DELTA
      FLOAD=DFLOAT(IS)
      RETURN
C
   10 IS=IS-1
      BETA2=BETA2-DB
      FLOAD=FLOAD-FSTEP
      IF (IHALF.EQ.0) WRITE(7,20)
   20 FORMAT('1',9('**'),' START OF LOAD STEP REFINEMENT ',9('**'))
   30 IHALF=IHALF+1
      REWIND 12
      READ(12) OD
      DB=DB*REDUCE
      ED=ED*REDUCE
      FSTEP=FSTEP*REDUCE
      IF (IS.EQ.0 .OR. IN(13).NE.2) FDELTA=0.D0
      FDELTA=FDELTA*REDUCE
      DELTA=FDELTA
      IF (LCH.EQ.0) GOTO 50
      DO 40 I=1,NL
   40 VL(I)=VL(I)*REDUCE
   50 WRITE(7,60)
   60 FORMAT(' ',//,' LOAD STEP IS REDUCED')
      RETURN
      END
      SUBROUTINE KT
C
C     CALCULATION OF THE ELEMENT TANGENT STIFFNESS MATRIX
C     ( STORED IN A UPPER TRIANGLE )
C
      IMPLICIT REAL*8(A-H,O-Z)
      COMMON / WHOLE /IBC(2),INR,IN(50),IS,IT,IXCH,LCH,NBAND,NEC
      COMMON / EIK   /E2K(20,20),E3K(1540),E4K(8855)
      COMMON / ETANK /ETK(20,20),V(20)
      DIMENSION VV(20,20)
C
```

```fortran
C     QUADRATIC PART
C
      DO 10 I=1,20
      DO 10 J=I,20
   10 ETK(I,J)=E2K(I,J)
      IF (IS.EQ.(-1)) GOTO 50
C
C     QUBIC PART
C
      N=0
      DO 20 I=1,20
      N=N+1
      ETK(I,I)=ETK(I,I)+E3K(N)*V(I)
      IF (I.EQ.20) GOTO 20
      I1=I+1
      DO 20 J=I1,20
      N=N+1
      W=E3K(N)
      ETK(I,I)=ETK(I,I)+W*V(J)
      ETK(I,J)=ETK(I,J)+W*V(I)
      N=N+1
      W=E3K(N)
      ETK(I,J)=ETK(I,J)+W*V(J)
      ETK(J,J)=ETK(J,J)+W*V(I)
      IF (J.EQ.20) GOTO 20
      J1=J+1
      DO 20 K=J1,20
      N=N+1
      W=E3K(N)
      ETK(I,J)=ETK(I,J)+W*V(K)
      ETK(I,K)=ETK(I,K)+W*V(J)
      ETK(J,K)=ETK(J,K)+W*V(I)
   20 CONTINUE
C
C     QUARTIC PART
C
      DO 30 I=1,20
      DO 30 J=I,20
   30 VV(I,J)=V(I)*V(J)
      N=0
      DO 40 I=1,20
      N=N+1
      ETK(I,I)=ETK(I,I)+E4K(N)*VV(I,I)
      IF (I.EQ.20) GOTO 40
      I1=I+1
      DO 40 J=I1,20
      N=N+1
      W=E4K(N)
      ETK(I,I)=ETK(I,I)+W*VV(I,J)*2.D0
      ETK(I,J)=ETK(I,J)+W*VV(I,I)
      N=N+1
      W=E4K(N)
      ETK(I,I)=ETK(I,I)+W*VV(J,J)
      ETK(I,J)=ETK(I,J)+W*VV(I,J)*2.D0
      ETK(J,J)=ETK(J,J)+W*VV(I,I)
      N=N+1
      W=E4K(N)
      ETK(I,J)=ETK(I,J)+W*VV(J,J)
      ETK(J,J)=ETK(J,J)+W*VV(I,J)*2.D0
      IF (J.EQ.20) GOTO 40
      J1=J+1
      DO 40 K=J1,20
      N=N+1
      W=E4K(N)*2.D0
      ETK(I,I)=ETK(I,I)+W*VV(J,K)
      ETK(I,J)=ETK(I,J)+W*VV(I,K)
      ETK(I,K)=ETK(I,K)+W*VV(I,J)
      ETK(J,K)=ETK(J,K)+W*VV(I,I)/2.D0
      N=N+1
      W=E4K(N)*2.D0
      ETK(I,J)=ETK(I,J)+W*VV(J,K)
      ETK(I,K)=ETK(I,K)+W*VV(J,J)/2.D0
      ETK(J,J)=ETK(J,J)+W*VV(I,K)
      ETK(J,K)=ETK(J,K)+W*VV(I,J)
      N=N+1
      W=E4K(N)*2.D0
      ETK(I,J)=ETK(I,J)+W*VV(K,K)/2.D0
      ETK(I,K)=ETK(I,K)+W*VV(J,K)
      ETK(J,K)=ETK(J,K)+W*VV(I,K)
      ETK(K,K)=ETK(K,K)+W*VV(I,J)
      IF (K.EQ.20) GOTO 40
      K1=K+1
      DO 40 L=K1,20
      N=N+1
      W=E4K(N)*2.D0
      ETK(I,J)=ETK(I,J)+W*VV(K,L)
      ETK(I,K)=ETK(I,K)+W*VV(J,L)
      ETK(I,L)=ETK(I,L)+W*VV(J,K)
      ETK(J,K)=ETK(J,K)+W*VV(I,L)
      ETK(J,L)=ETK(J,L)+W*VV(I,K)
      ETK(K,L)=ETK(K,L)+W*VV(I,J)
   40 CONTINUE
   50 CONTINUE
      RETURN
      END
      SUBROUTINE LINEND(P,IX)
C
C     BOUNDARY CONDITIONS FOR LINEAR CYLINDER PROBLEM
C
      IMPLICIT REAL*8(A-H,O-Z)
      COMMON / WHOLE /IBC(2),INR,IN(50),IS,IT,IXCH,LCH,NBAND,NEC,
     1 NEL,NINTP,NINTS,NINTX,NL,NMAX,NN,NNC,NN5,NPD,NX,NX1,NP,NP1,
     2 N2P,N2X,NX2
      COMMON / PART  /BETA,BETA2,CBETA,CED,DB,DEG,DELTA,DELTAT,E,ED,
     1 EN,E2,FLEX,PEL,PEL2,PI,R,RL,RM,RN,RNU,RNU1,PREC,TH,XEL
      DIMENSION P(NN5),IX(NN5)
C
      DO 10 I=1,NN5
   10 P(I)=0.D0
      BETA2=BETA
      PHI=0.D0
      K=NN5-NNC*5
      DO 30 I=1,NNC
      L=(I-1)*5
      BC=BETA*DCOS(PHI)
      IX(L+1)=2
      P(L+1)=-R*BC+ED
      IX(L+2)=0
      IX(L+3)=0
      IX(L+4)=2
      P(L+4)=BC
      IX(L+5)=0
      IF (IN(1).EQ.1) GOTO 30
      LK=L+K
      DO 20 J=1,5
      IX(LK+J)=0
   20 P(LK+J)=-P(L+J)
   30 PHI=PHI+PEL2
      RETURN
      END
      SUBROUTINE LOADS(IX,IV,P,OKT,VL,NPL,IXNEW,DD)
C
C     COMPUTATION OF LOAD VECTOR AND CHANGE OF STIFFNESS MATRIX
C
      IMPLICIT REAL*8(A-H,O-Z)
      COMMON / WHOLE /IBC(2),INR,IN(50),IS,IT,IXCH,LCH,NBAND,NEC,
     1 NEL,NINTP,NINTS,NINTX,NL,NMAX,NN,NNC,NN5,NPD,NX,NX1,NP,NP1,
     2 ISTART,IHALF,NEXTIT,LCAUSE,NEXTIS,NEXTOV,ITOVAL
      COMMON / PART  /BETA,BETA2,CBETA,CED,DB,DEG,DELTA,DELTAT,E,ED,
     1 EN,E2,FLEX,PEL,PEL2,PI,R,RL,RM,RN,RNU,RNU1,SIGMA,TH,XEL,TIME
      DIMENSION OKT(NBAND,NN5),IV(NN5),IH(605),P(NN5),IX(NN5),
     1 H(605),VL(NL),NPL(NL),IXNEW(NL),DD(NN5),ID(605),IF(4)
      LOGICAL SUCCES
C
```

```
C     COMPUTATION OF LOAD VECTOR
C
      IF (IS.GT.1 .OR. IT.GE.0) GOTO 20
   10 CALL SPARSE(IV,IH)
      IF (IN(12).EQ.0) GOTO 60
      GOTO 30
   20 REWIND 13
      READ(13) IV,(IH(I),I=1,NN5)
   30 DO 40 I=1,NN5
   40 P(I)=0.D0
      XED=ED+DELTA
      IF (IT.EQ.-1) CALL NONEND(P,XED,DB)
      IF (IN(13).NE.2 .OR. IT.LT.2) GOTO 60
      IF (NEXTOV.EQ.0) CALL NONEND(H,DELTA,0.D0)
      IF (NEXTOV.EQ.1) CALL OVAL(H,DD)
      DO 50 I=1,NN5
   50 P(I)=P(I)+H(I)
   60 IF (IT.EQ.-1 .AND. NPL(2).GT.0) CALL LOADS2(VL,P,NPL,IXNEW,2)
      IF (IN(22).NE.2) GOTO 170
C
C     COMPUTATION OF DETERMINANT WITHOUT NONZERO PRESCRIBED
C     DISPLACEMENTS
C
      WRITE(8) OKT,IV
      DO 70 I=1,NN5
      IF(IX(I).GT.0) GOTO 70
      IV(I)=1
      IH(I)=1
   70 CONTINUE
      DO 80 I=1,NN5
   80 H(I)=0.D0
      CALL VBSOLV(NBAND-1,NN5,0.1D-15,NN5,H,OKT,ID,NBAND,DET,
     1 IEXDET,IV,.TRUE.,SUCCES)
      IF (.NOT.SUCCES) CALL ERROR(9,IS,IT)
C
C     OUTPUT OF THE DETERMINANT AND ITS RELATIVE CONDITION
C
      KK=IDINT(DLOG10(DFLOAT(IABS(IEXDET))))+1
      WRITE(9,90) KK
   90 FORMAT(13H(    1H+,32X,I,I2,')')
      REWIND 9
      READ(9,100) IF(1),IF(2),IF(3),IF(4)
  100 FORMAT(4A4)
      WRITE(7,110) DET
  110 FORMAT(' DETERMINANT =',F10.6,' * 10 **')
      WRITE(7,IF) IEXDET
      IF (IN(22).EQ.1) CALL TEST(OKT,DET,IEXDET,DNORM)
      INN5=NN5
      DO 120 I=1,NN5
  120 INN5=INN5-ID(I)
      IF (INN5.EQ.0) GOTO 160
      WRITE(7,130)
  130 FORMAT(' NEGATIVE DIAGONAL ELEMENTS IN FOLLOWING ROWS:'/)
      DO 140 I=1,NN5
  140 IF (ID(I).EQ.-1) WRITE (7,150) I
  150 FORMAT(' ',I4)
  160 READ(8) OKT,IV
C
C     CHANGE OF STIFFNESS MATRIX
C
  170 CONTINUE
      DO 180 I=1,NN5
  180 H(I)=P(I)
      DO 240 I=1,NN5
      IF (IX(I)-1) 230,240,190
  190 I1=IV(I)
      I2=I-1
      IF (I2.LT.I1) GOTO 210
      DO 200 J=I1,I2
      IZ=NBAND-I+J
      P(J)=P(J)-H(I)*OKT(IZ,I)
  200 OKT(IZ,I)=0.D0
  210 OKT(NBAND,I)=1.D0
      J1=I+1
      J2=IH(I)
      IF (J2.LT.J1) GOTO 230
      DO 220 J=J1,J2
      IZ=NBAND+I-J
      P(J)=P(J)-H(I)*OKT(IZ,J)
  220 OKT(IZ,J)=0.D0
  230 IV(I)=I
      IH(I)=I
  240 CONTINUE
      DO 250 I=1,NN5
  250 IF (IX(I).NE.1) P(I)=H(I)
      IF (IN(8).EQ.1 .OR. IN(8).EQ.3)
     1 CALL PRTMAT(OKT,NBAND,1,1,NBAND,NN5,'OKT,LOAD')
      RETURN
      END
      SUBROUTINE LOADS2(VL,OF,NPL,IXNEW,LD)
C
C     ADDITION OF LOADS AND DISPLACEMENTS DESCRIBED IN INPUT-FILE
C
      IMPLICIT REAL*8(A-H,O-Z)
      COMMON / WHOLE /IBC(2),INR,IN(50),IS,IT,IXCH,LCH,NBAND,NEC,
     1 NEL,NINTP,NINTS,NINTX,NL,NMAX,NN,NNC,NN5,NPD,NX,NX1,NP,NP1,
     2 N2P,N2X,NX2
      DIMENSION VL(NL),NPL(NL),IXNEW(NL),OF(NN5)
C
C     ADDITIONAL LOADS
C
      IF (LD.NE.1 .OR. NPL(1).EQ.0) GOTO 40
      IE=6+NPL(3)
      IF (IE.EQ.6 .OR. (IT.EQ.0.AND.IS.GT.1)) GOTO 20
      DO 10 I=7,IE
      J=NPL(I)
   10 OF(J)=OF(J)+VL(I)
   20 IF (NPL(4).EQ.0) RETURN
      DIS=DFLOAT(IS)
      IF (IT.EQ.0) DIS=1.D0
      IA=IE+1
      IE=IA-1+NPL(4)
      DO 30 I=IA,IE
      J=NPL(I)
   30 OF(J)=OF(J)+VL(I)*DIS
      RETURN
C
C     ADDITIONAL DISPLACEMENTS
C
   40 IF (IT.GE.0) RETURN
      IF (NPL(2).EQ.0) RETURN
      IF (NPL(5).EQ.0 .OR. IS.GE.2) GOTO 60
      IA=7+NPL(1)
      IE=IA-1+NPL(5)
      DO 50 I=IA,IE
   50 OF(NPL(I))=VL(I)
   60 IF (NPL(6).EQ.0) RETURN
      IA=7+NPL(1)+NPL(5)
      IE=IA-1+NPL(6)
      DO 70 I=IA,IE
   70 OF(NPL(I))=VL(I)
      RETURN
      END
      SUBROUTINE LONGER(OD,DELTA)
C
C     APPROXIMATE NODAL DISPLACEMENTS FOR AXIAL FORCE CA. ZERO
C
      IMPLICIT REAL*8(A-H,O-Z)
      COMMON / WHOLE /IBC(2),INR,IN(50),IS,IT,IXCH,LCH,NBAND,NEC,
     1 NEL,NINTP,NINTS,NINTX,NL,NMAX,NN,NNC,NN5,NPD,NX,NX1,NP,NP1,
     2 N2P,N2X,NX2
      DIMENSION OD(NN5)
C
      DO 10 I=1,NX
      K=(I-1)*NNC-4
      DR=DELTA*DFLOAT(NX1-I)/DFLOAT(NX)
      DO 10 J=1,NNC
   10 OD(J*5+K)=OD(J*5+K)+DR
      IF (IN(1).NE.0) GOTO 30
      NX2=NX+2
      N2X=NX+NX
      DO 20 I=NX2,N2X
      K=(I-1)*NNC-4
      DR=DELTA*DFLOAT(I-NX1)/DFLOAT(NX)
      DO 20 J=1,NNC
   20 OD(J*5+K)=OD(J*5+K)-DR
   30 CONTINUE
      RETURN
      END
      SUBROUTINE MAIN1
C
C     ONE QUARTER OF THE CYLINDER IS CONSIDERED
C
      IMPLICIT REAL*8(A-H,O-Z)
      COMMON / WHOLE /IBC(2),INR,IN(50),IS,IT,IXCH,LCH,NBAND,NEC,
     1 NEL,NINTP,NINTS,NINTX,NL,NMAX,NN,NNC,NN5,NPD,NX,NX1,NP,NP1,
     2 ISTART,IHALF,NEXTIT,LCAUSE,NEXTIS
      DIMENSION OKT(65,605),NOEL(4,100),P(605),IV(605),IX(605),
     1 OD(605),DV(53),OF(605),VL(605),NPL(605),IXNEW(605)
C
      CALL INPUT1(NOEL,P,IX,VL,NPL,IXNEW)
C
   10 CALL ASSEM(NOEL,OKT,IX,OD)
C
      CALL LOADS(IX,IV,P,OKT,VL,NPL,IXNEW,OD)
C
      CALL SOLVE(OKT,P,IV,OD,NOEL,IX,DV,OF,VL,NPL,IXNEW)
C
      IF (NEXTIS.GT.0) GOTO 10
C
      STOP
      END
      SUBROUTINE MAINR(OKT,P,OD,NOEL,OF,IX,DV,IV,VL,NPL,IXNEW)
C
C     MAIN SUBROUTINE FOR RESTART FACILITY
C
      IMPLICIT REAL*8(A-H,O-Z)
      COMMON / WHOLE /IBC(2),INR,IN(50),IS,IT,IXCH,LCH,NBAND,NEC,
     1 NEL,NINTP,NINTS,NINTX,NL,NMAX,NN,NNC,NN5,NPD,NX,NX1,NP,NP1,
     2 ISTART,IHALF,NEXTIT,LCAUSE,NEXTIS
      DIMENSION OKT(NBAND,NN5),NOEL(4,NEL),P(NN5),IV(NN5),
     1 IX(NN5),OD(NN5),DV(53),OF(NN5),VL(NL),NPL(NL),IXNEW(NL)
C
      CALL INPUT2
C
      GOTO 20
C
   10 CALL ASSEM(NOEL,OKT,IX,OD)
C
      CALL LOADS(IX,IV,P,OKT,VL,NPL,IXNEW,OD)
C
   20 CALL SOLVE(OKT,P,IV,OD,NOEL,IX,DV,OF,VL,NPL,IXNEW)
C
      IF (NEXTIS.GT.0) GOTO 10
C
      STOP
      END
      SUBROUTINE NEWCYL
C
C     CALCULATION OF THE THREE STIFFNESS MATRICES
C
      IMPLICIT REAL*8(A-H,O-Z)
      COMMON / WHOLE /IBC(2),INR,IN(50),IS,IT,IXCH,LCH,NBAND,NEC,
     1 NEL,NINTP,NINTS,NINTX,NL,NMAX,NN,NNC,NN5,NPD,NX,NX1,NP,NP1,
     2 N2P,N2X,NX2
      COMMON / PART  /BETA,BETA2,CBETA,CED,DB,DEG,DELTA,DELTAT,E,ED,
     1 EN,E2,FLEX,PEL,PEL2,PI,R,RL,RM,RN,RNU,DNORM,SIGMA,TH,XEL,TIME
      COMMON / EIK   /E2K(20,20),E3K(1540),E4K(8855)
      COMMON / AF    /AXF(20),APF(20),APXF(20)
      COMMON / TF    /BX1(20),BP2(20),TPXF(20)
      COMMON / BF    /BP3(20),BX3(20),BX2(20),BP1(20)
      DIMENSION X(24),WX(24),P(24),WP(24),T1(20),T2(20),
     1 BX12(20,20),BX22(20,20),BX32(20,20),BXX(20,20),
     2 BP12(20,20),BP22(20,20),BP32(20,20),BPP(20,20),
     3 BXP2(20,20),BXNBP(20,20),BPNBX(20,20)
C
      CALL GAUSS(X,WX,24,XEL,NINTX)
      CALL GAUSS(P,WP,24,PEL,NINTP)
      IF (IN(25).EQ.1) CALL TMAT
      DO 10 I=1,20
      DO 10 J=1,20
   10 E2K(J,I)=0.D0
      DO 20 I=1,1540
   20 E3K(I)=0.D0
      DO 30 I=1,8855
   30 E4K(I)=0.D0
C
      C=E*TH/(1.D0-RNU*RNU)
      D=C*TH*TH/12.D0
      RNU1=(1.D0-RNU)/2.D0
      RNU2=RNU1+RNU1
      RNU4=RNU2+RNU2
      RNU4D3=RNU4/3.D0
C
      DO 110 INX=1,NINTX
      DO 110 INP=1,NINTP
      CALL SALF(X(INX),P(INP))
      CALL STH(X(INX),P(INP))
      DO 40 I=1,20
      T1(I)=BX1(I)+RNU*BP2(I)
   40 T2(I)=BP2(I)+RNU*BX1(I)
C
C     STIFFNESS MATRIX OF SECOND ORDER
C
      WXWPR=WX(INX)*WP(INP)*R
      W2C=WXWPR*C
      W2D=WXWPR*D
      DO 50 I=1,20
      DO 50 J=I,20
   50 E2K(I,J)=E2K(I,J)+
     1 W2C*(BX1(I)*T1(J)+BP2(I)*T2(J)+RNU1*TPXF(I)*TPXF(J))+
     2 W2D*(AXF(I)*(AXF(J)+RNU*APF(J))+APF(I)*(APF(J)+RNU*AXF(J))+
     3 RNU4*APXF(I)*APXF(J))
      IF (IN(12).EQ.0) GOTO 110
C
C     PRECALCULATIONS FOR NONLINEAR TERMS
C
      CALL BXP(X(INX),P(INP))
      DO 70 I=1,20
      DO 60 J=1,20
      BX12(I,J)=BX1(I)*BX1(J)
      BX22(I,J)=BX2(I)*BX2(J)
      BX32(I,J)=BX3(I)*BX3(J)
      BP12(I,J)=BP1(I)*BP1(J)
      BP22(I,J)=BP2(I)*BP2(J)
      BP32(I,J)=BP3(I)*BP3(J)
      BXX(I,J)=BX12(I,J)+BX22(I,J)+BX32(I,J)
      BPP(I,J)=BP12(I,J)+BP22(I,J)+BP32(I,J)
      BXP2(I,J)=BX1(I)*BP1(J)+BX2(I)*BP2(J)+BX3(I)*BP3(J)
      BXNBP(I,J)=BXX(I,J)+RNU*BPP(I,J)
      BPNBX(I,J)=BPP(I,J)+RNU*BXX(I,J)
   60 CONTINUE
   70 CONTINUE
      DO 80 I=1,19
      I1=I+1
      DO 80 J=I1,20
   80 BXP2(I,J)=(BXP2(I,J)+BXP2(J,I))/2.D0
```

```
C
C     STIFFNESS MATRIX OF THIRD ORDER
C
      W3=W2C
      W4=W2C*1.5DO
      N=O
      DO 90 I=1,20
      N=N+1
      E3K(N)=E3K(N)+W3*3.DO*(BX1(I)*BXNBP(I,I)+BP2(I)*BPNBX(I,I)+
     1 RNU2*(TPXF(I)*BXP2(I,I)))
      IF (I.EQ.20) GOTO 90
      I1=I+1
      DO 90 J=I1,20
      N=N+1
      E3K(N)=E3K(N)+W3*(2.DO*BX1(I)*BXNBP(I,J)+BX1(J)*BXNBP(I,I)+
     1 2.DO*BP2(I)*BPNBX(I,J)+BP2(J)*BPNBX(I,I)+
     2 RNU2*(TPXF(I)*BXP2(I,J)*2.DO+TPXF(J)*BXP2(I,I)))
      N=N+1
      E3K(N)=E3K(N)+W3*(2.DO*BX1(J)*BXNBP(I,J)+BX1(I)*BXNBP(J,J)+
     1 2.DO*BP2(J)*BPNBX(I,J)+BP2(I)*BPNBX(J,J)+
     2 RNU2*(TPXF(J)*BXP2(I,J)*2.DO+TPXF(I)*BXP2(J,J)))
      IF (J.EQ.20) GOTO 90
      J1=J+1
      DO 90 K=J1,20
      N=N+1
      E3K(N)=E3K(N)+W3*
     1 (BX1(I)*BXNBP(J,K)+BX1(J)*BXNBP(I,K)+BX1(K)*BXNBP(I,J)
     2 +BP2(I)*BPNBX(J,K)+BP2(J)*BPNBX(I,K)+BP2(K)*BPNBX(I,J)+
     3 RNU2*(TPXF(I)*BXP2(J,K)+TPXF(J)*BXP2(I,K)+TPXF(K)*BXP2(I,J)))
   90 CONTINUE
C
C     STIFFNESS MATRIX OF FOURTH ORDER
C
      N=O
      DO 100 I=1,20
      N=N+1
      E4K(N)=E4K(N)+W4*(BXX(I,I)*BXNBP(I,I)+BPP(I,I)*BPNBX(I,I)+
     1 RNU4*BXP2(I,I)*BXP2(I,I))
      IF (I.EQ.20) GOTO 100
      I1=I+1
      DO 100 J=I1,20
      N=N+1
      E4K(N)=E4K(N)+W4*((BXX(I,I)*BXNBP(I,J)+BPP(I,I)*BPNBX(I,J)+
     1 BXX(I,J)*BXNBP(I,I)+BPP(I,J)*BPNBX(I,I))/2.DO+
     2 RNU4*BXP2(I,I)*BXP2(I,J))
      N=N+1
      E4K(N)=E4K(N)+W4*((BXX(I,I)*BXNBP(J,J)+BPP(I,I)*BPNBX(J,J)+
     1 BXX(J,J)*BXNBP(I,I)+BPP(J,J)*BPNBX(I,I)+
     2 (BXX(I,J)*BXNBP(I,J)+BPP(I,J)*BPNBX(I,J))*4.DO)/6.DO+
     3 RNU4D3*(BXP2(I,I)*BXP2(J,J)+BXP2(I,J)*BXP2(I,J)*2.DO))
      N=N+1
      E4K(N)=E4K(N)+W4*((BXX(I,J)*BXNBP(J,J)+BPP(I,J)*BPNBX(J,J)+
     1 BXX(J,J)*BXNBP(I,J)+BPP(J,J)*BPNBX(I,J))/2.DO+
     2 RNU4*BXP2(I,J)*BXP2(J,J))
      IF (J.EQ.20) GOTO 100
      J1=J+1
      DO 100 K=J1,20
      N=N+1
      E4K(N)=E4K(N)+W4*((BXX(I,I)*BXNBP(J,K)+BPP(I,I)*BPNBX(J,K)+
     1 BXX(J,K)*BXNBP(I,I)+BPP(J,K)*BPNBX(I,I)+
     2 (BXX(I,J)*BXNBP(I,K)+BPP(I,J)*BPNBX(I,K)+
     3 BXX(I,K)*BXNBP(I,J)+BPP(I,K)*BPNBX(I,J))*2.DO)/6.DO+
     4 RNU4D3*(BXP2(I,I)*BXP2(J,K)+BXP2(I,J)*BXP2(I,K)*2.DO))
      N=N+1
      E4K(N)=E4K(N)+W4*(((BXX(I,J)*BXNBP(J,K)+BPP(I,J)*BPNBX(J,K)+
     1 BXX(J,K)*BXNBP(I,J)+BPP(J,K)*BPNBX(I,J))*2.DO+
     2 BXX(I,K)*BXNBP(J,J)+BPP(I,K)*BPNBX(J,J)+
     3 BXX(J,J)*BXNBP(I,K)+BPP(J,J)*BPNBX(I,K))/6.DO+
     4 RNU4D3*(BXP2(J,J)*BXP2(I,K)+BXP2(I,J)*BXP2(J,K)*2.DO))
      N=N+1
      E4K(N)=E4K(N)+W4*((BXX(I,J)*BXNBP(K,K)+BPP(I,J)*BPNBX(K,K)+
     1 BXX(K,K)*BXNBP(I,J)+BPP(K,K)*BPNBX(I,J)+
     2 (BXX(I,K)*BXNBP(J,K)+BPP(I,K)*BPNBX(J,K)+
     3 BXX(J,K)*BXNBP(I,K)+BPP(J,K)*BPNBX(I,K))*2.D0)/6.D0+
     4 RNU4D3*(BXP2(I,J)*BXP2(K,K)+BXP2(I,K)*BXP2(J,K)*2.D0))
      IF (K.EQ.20) GOTO 100
      K1=K+1
      DO 100 L=K1,20
      N=N+1
      E4K(N)=E4K(N)+W4*((BXX(I,J)*BXNBP(K,L)+BPP(I,J)*BPNBX(K,L)+
     1 BXX(I,K)*BXNBP(J,L)+BPP(I,K)*BPNBX(J,L)+
     2 BXX(I,L)*BXNBP(J,K)+BPP(I,L)*BPNBX(J,K)+
     3 BXX(J,K)*BXNBP(I,L)+BPP(J,K)*BPNBX(I,L)+
     4 BXX(J,L)*BXNBP(I,K)+BPP(J,L)*BPNBX(I,K)+
     5 BXX(K,L)*BXNBP(I,J)+BPP(K,L)*BPNBX(I,J))/6.D0+
     6 RNU4D3*(BXP2(I,J)*BXP2(K,L)+BXP2(I,K)*BXP2(J,L)+
     7 BXP2(I,L)*BXP2(J,K)))
  100 CONTINUE
C
C     STORAGE OF STIFFNESS MATRICES
C
  110 CONTINUE
      WRITE(11) E2K
      IF (IN(12).EQ.0) GOTO 120
      WRITE(11) E3K,E4K
  120 IF (IN(25).EQ.1) STOP
      REWIND 11
      RETURN
      END
      SUBROUTINE NONEND(P,D1,D2)
C
C     COMPUTATION OF NONLINEAR BOUNDARY CONDITIONS
C     FOR RIGID CYLINDER ENDS
C
      IMPLICIT REAL*8(A-H,O-Z)
      COMMON / WHOLE /IBC(2),INR,IN(50),IS,IT,IXCH,LCH,NBAND,NEC,
     1 NEL,NINTP,NINTS,NINTX,NL,NMAX,NN,NNC,NN5,NPD,NX,NX1,NP,NP1,
     2 N2P,N2X,NX2
      COMMON / PART  /BETA,BETA2,CBETA,CED,DB,DEG,DELTA,DELTAT,E,ED,
     1 EN,E2,FLEX,PEL,PEL2,PI,R,RL,RM,RN,RNU,RNU1,PREC,TH,XEL,TIME,
     2 DUMMY(5),DONM
      DIMENSION P(NN5)
C
      DO 10 I=1,NN5
   10 P(I)=0.D0
      IF (IS.EQ.1 .AND. IT.EQ.-1) BETA2=0.D0
      BETA1=BETA2
      BETA2=BETA1+D2
      PHI=0.D0
      C21=DCOS(BETA1)-DCOS(BETA2)
      S21=DSIN(BETA2)-DSIN(BETA1)
      DON1=DONM*D2
      DON2=DONM*(DSIN(BETA2)*BETA2-DSIN(BETA1)*BETA1)
      K=NN5-NNC*5
      DO 20 I=1,NNC
      L=(I-1)*5
      DC=DCOS(PHI)
      DS=DSIN(PHI)
      P(L+1)=D1-R*DC*S21+DON2*DS*DS
      P(L+2)=R*C21*DS*DC+DON1*DS
      P(L+3)=-R*C21*DC*DC
      P(L+4)=S21*DC
      P(L+5)=C21*DS*DC-DON1*DS/R
      IF (IN(1).EQ.1) GOTO 20
      LK=L+K
      P(LK+1)=-P(L+1)
      P(LK+2)=P(L+2)
      P(LK+3)=P(L+3)
      P(LK+4)=-P(L+4)
      P(LK+5)=P(L+5)
   20 PHI=PHI+PEL2
      RETURN
      END
      SUBROUTINE NORMD(DNORM,IX)
```

```
C
C     CALCULATION OF THE NORMALIZED DETERMINANT OF A TRIANGULAR
C     STIFFNESS MATRIX WITH VALUES OF 1 FOR ALL NONZERO TERMS
C
      REAL*8 DNORM
      COMMON / WHOLE /IBC(2),INR,IN(50),IS,IT,IXCH,LCH,NBAND,NEC,
     1 NEL,NINTP,NINTS,NINTX,NL,NMAX,NN,NNC,NN5,NPD,NX,NX1,NP,NP1,
     2 N2P,N2X,NX2
      DIMENSION IX(NN5)
C
      IF (NX.EQ.1.AND.NP.EQ.1) X=ALOG10(2.)
      IF (NX.EQ.1.AND.NP.GE.2) X=ALOG10(16.)+(NP-2)*ALOG10(6.)
      IF (NX.GE.2.AND.NP.EQ.1) X=ALOG10(80.)+FLOAT(NX-2)*ALOG10(108.)
      IF (NX.GE.2.AND.NP.EQ.2) X=ALOG10(17472.)+FLOAT(NX-2)*ALOG10(3344.)
      IF(NX.GE.2.AND.NP.GE.3) X=ALOG10(2056320.)+FLOAT(NX-2)*
     1 ALOG10(85008.)+FLOAT(NP-3)*ALOG10(114.)+FLOAT((NX-2)*(NP-3))*
     2 ALOG10(25.)
      DNORM=X
      NMAX=0
      DO 10 I=1,NN5
   10 IF (IX(I).EQ.1) NMAX=NMAX+1
      RETURN
      END
      SUBROUTINE OVAL(H,OD)
C
C     ADDING DISPLACEMENTS TO CYLINDRICAL ENDS TO OBTAIN
C     DEFORMATIONS EQUIVALENT TO THE MID-LENGTH OF CYLINDER
C
      IMPLICIT REAL*8(A-H,O-Z)
      COMMON / WHOLE /IBC(2),INR,IN(50),IS,IT,IXCH,LCH,NBAND,NEC,
     1 NEL,NINTP,NINTS,NINTX,NL,NMAX,NN,NNC,NN5,NPD,NX,NX1,NP,NP1,
     2 ISTART,IHALF,NEXTIT,LCAUSE,NEXTIS,NEXTOV,ITOVAL
      COMMON / PART  /BETA,BETA2,CBETA,CED,DB,DEG,DELTA,DELTAT,E,ED,
     1 EN,E2,FLEX,PEL,PEL2,PI,R,RL,RM,RN,RNU,DNORM,PREC,TH,XEL,TIME,
     2 XD,REDUCE,FLOAD,FSTEP
      DIMENSION H(NN5),OD(NN5)
C
      ITOVAL=ITOVAL+1
      DELTA=0.D0
      WB=(OD(NN5-2)-OD(NN5-NP*5-2))/2.D0
      SB=DSIN(BETA2)
      CBM=1.D0-DCOS(BETA2)
      PHI=0.D0
      K=NN5-NNC*5
C
      DO 10 I=1,NNC
      L=(I-1)*5
      DS=DSIN(PHI)
      DC=DCOS(PHI)
      VM=OD(L+K+2)
      WM=OD(L+K+3)
      VS=VM-WB*DS
      WS=WM+WB*DC
      S2=-WS*DC+VS*DS
      S3=DC*R-S2
      S4=S3*CBM
      H(L+1)=-S3*SB+DELTA-DELTAT/2.D0-OD(L+1)
      H(L+2)=VS+S4*DS-OD(L+2)
      H(L+3)=WS-S4*DC-OD(L+3)
      H(L+4)=0.D0
      H(L+5)=(DC*CBM*(R*DS+WS*DS+VS*DC)-VM)/R-OD(L+5)
      PHI=PHI+PEL2
   10 CONTINUE
      IA=L+6
      DO 20 I=IA,NN5
      H(I)=0.D0
   20 CONTINUE
C
      NEXTOV=0
      RETURN
      END
      SUBROUTINE PRTMAT(A,I1,IS,JS,NR,NC,ANAME)
      REAL*8 A(I1,NC),ANAME
C
      JMAX=JS+NC-1
      IE=IS+NR-1
      JJS=JS
      JJE=JS+7
   10 IF (JJE.GT.JMAX) JJE=JMAX
      WRITE(8,20) ANAME
   20 FORMAT('1',20X,'MATRIX ',A8,//)
      WRITE(8,30)
   30 FORMAT(' * COLUMN',/,'  *',/,'   *',/,'    *',/,'     *')
      WRITE(8,40) (J,J=JJS,JJE)
   40 FORMAT('/ ROW *    ',8(6X,I3,6X))
      WRITE(8,50)
   50 FORMAT(7X,'*',/,8X,'*',/)
      DO 60 I=IS,IE
   60 WRITE(8,70) (I,(A(I,J),J=JJS,JJE))
   70 FORMAT(2X,I3,6X,8E15.7)
      IF (JJE.GE.JMAX) GOTO 80
      JJS=JJS+8
      JJE=JJE+8
      GOTO 10
   80 CONTINUE
      RETURN
      END
      SUBROUTINE RSTART(OKT,P,OD,NOEL,OF,IX,DV,IV,IH,VL,NPL,IXNEW)
C
C     STORING AND READING OF DATA FOR RESTART
C
      IMPLICIT REAL*8(A-H,O-Z)
      COMMON / EIK   /E2K(20,20),E3K(1540),E4K(8855)
      COMMON / WHOLE /IBC(2),INR,IN(50),IS,IT,IXCH,LCH,NBAND,NEC,
     1 NEL,NINTP,NINTS,NINTX,NL,NMAX,NN,NNC,NN5,NPD,NX,NX1,NP,NP1,
     2 ISTART,IHALF,NEXTIT,LCAUSE,NEXTIS,NEXTOV,ITOVAL,ITOVIT,NOVA,
     3 NCONV
      COMMON / PART  /BETA,BETA2,CBETA,CED,DB,DEG,DELTA,DELTAT,E,ED,
     1 EN,E2,FLEX,PEL,PEL2,PI,R,RL,RM,RN,RNU,DNORM,PREC,TH,XEL,TIME,
     2 XD,REDUCE,FLOAD,FSTEP,FDELTA,DONM,XDN
      COMMON / TMINUS/ T(20,20)
      DIMENSION OKT(NBAND,NN5),P(NN5),OD(NN5),NOEL(4,NEL),OF(NN5),
     1 IX(NN5),DV(53),IV(NN5),IH(NN5),VL(NL),NPL(NL),IXNEW(NL)
C
      CALL GTCPL(TMNEW)
      IF (ISTART.EQ.3) GOTO 20
      IF (ISTART.EQ.1) GOTO 40
      IF (IN(23).NE.1) RETURN
      TMMIN=(TIME-TMNEW)*1.1D0+10.D0
      WRITE(7,10) TMNEW,TMMIN
   10 FORMAT(//' REMAINING CPU-TIME =',F8.3/' REQUIRED  CPU-TIME =',
     1 F8.3)
      LCAUSE=1
      IF (TMNEW.LT.TMMIN) GOTO 30
      TIME=TMNEW
      RETURN
C
C     STORING OF RESTART VARIABLES
C
   20 IF (LCAUSE.EQ.3) GOTO 30
      LCAUSE=2
   30 REWIND 13
      READ(13) IV,IH
      REWIND 10
      WRITE(10) IBC,INR,IN,IS,IT,IXCH,LCH,NBAND,NEC,NEL,NEXTIT,
     1 LCAUSE,NINTP,NINTS,NINTX,NL,NMAX,NN,NNC,NN5,NPD,NX,NX1,NP,
     2 NP1,IHALF,NEXTIS,NEXTOV,ITOVAL,ITOVIT,NOVA
      WRITE(10) BETA,BETA2,CBETA,CED,DB,DEG,DELTA,DELTAT,E,ED,
     1 EN,E2,FLEX,PEL,PEL2,PI,R,RL,RM,RN,RNU,DNORM,PREC,TH,XEL,
     2 REDUCE,FLOAD,FSTEP,FDELTA,DONM,XDN,NCONV,
     3 T,OD,NOEL,IX,IV,IH,P,OF,DV,PREC,TIME,XD,VL,NPL,IXNEW
      IF (IN(14).NE.2) WRITE(10) OKT
      STOP
C
```

```
C     READING OF RESTART VARIABLES
C
   40 READ(10) BETA,BETA2,CBETA,CED,DB,DEG,DELTA,DELTAT,E,ED,
     1 EN,E2,FLEX,PEL,PEL2,PI,R,RL,RM,RN,RNU,DNORM,PREC,TH,XEL,
     2 REDUCE,FLOAD,FSTEP,FDELTA,DONM,XDN,NCONV,
     3 T,OD,NOEL,IX,IV,IH,P,OF,DV,PREC,TIME,XD,VL,NPL,IXNEW
      READ(11) E2K
      READ(11) E3K,E4K
      IF (IN(14).NE.2) READ(10) OKT
      REWIND 13
      WRITE(13) IV,(IH(I),I=1,NN5)
      REWIND 12
      WRITE(12) OD
      TIME=TMNEW
      CALL MAINR(OKT,P,OD,NOEL,OF,IX,DV,IV,VL,NPL,IXNEW)
C
      STOP
      END
      SUBROUTINE SALF(X,P)
C
C     COEFFICIENTS KAPPA FOR (LINEAR) OUT-OF-PLANE STRAINS
C
      IMPLICIT REAL*8(A-H,O-Z)
      COMMON / TMINUS/T(20,20)
      COMMON / PART  /BETA,BETA2,CBETA,CED,DB,DEG,DELTA,DELTAT,E,ED,
     1 EN,E2,FLEX,PEL,PEL2,PI,R,RL,RM,RN,RNU,RNU1,SIGMA,TH,XEL,TIME
      COMMON / AF    /AXF(20),APF(20),APXF(20)
C
      SDR=DSIN(P)/R
      XP=X*P
      XDR=X/R
      XX=XDR*X/2.D0
      RP=R*P
      R2P=RP*P/2.D0
      DO 10 I=1,20
      AXF(I)=T(8,I)*SDR+T(12,I)+T(13,I)*X+T(14,I)*P+T(15,I)*XP
      APF(I)=T(16,I)+T(17,I)*X+T(18,I)*P+T(19,I)*XP
   10 APXF(I)=T(14,I)*XDR+T(15,I)*XX+T(17,I)*RP+T(19,I)*R2P+T(20,I)
      RETURN
      END
      SUBROUTINE SHORT(DV,DELTA,DELTAT,IS)
C
C     ESTIMATE OF SHORTAGE OF CYLINDER FOR NEXT LOAD STEP
C
      IMPLICIT REAL*8(A-H,O-Z)
      DIMENSION DV(53)
C
      IF (IS.GT.2.) GOTO 30
      IF (IS.EQ.2) GOTO 10
      DV(2)=DELTAT
      DV(3)=0.D0
      DV(4)=DELTAT
      DV(5)=DELTAT*4.D0
      GOTO 40
   10 DV(1)=DELTAT
      DV(5)=DELTAT
   20 DV(6)=6.D0*DV(1)-15.D0*DV(2)
      GOTO 40
   30 DV(IS+3)=DELTAT
      DV(IS+4)=-DV(IS-2)+6.D0*DV(IS-1)-15.D0*DV(IS)+20.D0*DV(IS+1)-
     1 15.D0*DV(IS+2)+6.D0*DV(IS+3)
   40 DELTA=(DV(IS+3)-DV(IS+4))/2.D0
      RETURN
      END
      SUBROUTINE SOLVE(OKT,P,IV,OD,NOEL,IX,DV,OF,VL,NPL,IXNEW)
C
C     SOLVING OF "K * V = P" AND ITERATION CONTROL
C
      IMPLICIT REAL*8(A-H,O-Z)
      COMMON / EIK   /E2K(20,20),E3K(1540),E4K(8855)
      COMMON / WHOLE /IBC(2),INR,IN(50),IS,IT,IXCH,LCH,NBAND,NEC,
     1 NEL,NINTP,NINTS,NINTX,NL,NMAX,NN,NNC,NN5,NPD,NX,NX1,NP,NP1,
     2 ISTART,IHALF,NEXTIT,LCAUSE,NEXTIS,NEXTOV,ITOVAL,ITOVIT,NOVA,
     3 NCONV
      COMMON / PART  /BETA,BETA2,CBETA,CED,DB,DEG,DELTA,DELTAT,E,ED,
     1 EN,E2,FLEX,PEL,PEL2,PI,R,RL,RM,RN,RNU,DNORM,PREC,TH,XEL,TIME,
     2 XD,REDUCE,FLOAD,FSTEP,FDELTA,DONM,XDN
      DIMENSION OKT(NBAND,NN5),P(NN5),IV(NN5),ID(605),IF(4),DV(53),
     1 OD(NN5),NOEL(4,NEL),OF(NN5),IX(NN5),IH(605),VL(NL),NPL(NL),
     2 IXNEW(NL)
      LOGICAL SUCCES
C
      NEXTIS=1
      IF (IS.LE.0) NEXTIS=0
      IF (LCAUSE.EQ.2) GOTO 470
      IF (LCAUSE.EQ.3) GOTO 260
      IF (ISTART.EQ.1) GOTO 470
      IF (IN(9).EQ.1) WRITE (7,10) (I,P(I),I=1,NN5)
   10 FORMAT(' '///10X,'LOAD VECTOR'//5X,'NR.     (MM OR ANGLE)'/
     1 /(I7,E14.6))
      DO 20 I=1,NN5
   20 OF(I)=P(I)
      NEXTIT=1
      NOVA=0
      NEXTOV=0
      ITOVAL=0
      ITOVIT=0
      IF (IS.EQ.-1) NEXTIT=0
      PREC=0.1D-15
      DEG=BETA2*57.2957977509D0
      RMO=RM
      DELTA=0.D0
C
C     EQUILIBRIUM ITERATIONS
C
   30 IT=IT+1
      RNO=RN
      TLOAD=CBETA*FLOAD
      CSTEP=CBETA*FSTEP
      WRITE(7,40) IS,IT,TLOAD,CSTEP,IHALF,DEG
   40 FORMAT(//' ',60('**')/' LOAD STEP =',I3/,' ITERATION =',I3/,
     1 ' CURRANT LOAD FACTOR =',F9.6,' OF CLASSICAL BUCKLING LOAD',/
     2 ' CURRANT STEP SIZE    =',F9.6/,
     3 ' REFINEMENT=',I3/,' ROTATION  =',E14.6,' DEGREES')
      IF (NOVA.EQ:0) GOTO 60
      IF (NEXTOV.EQ.1) ITPLUS=ITOVAL+1
      IF (NEXTOV.EQ.1) ITOVIT=0
      IF (NEXTOV.EQ.0) ITOVIT=ITOVIT+1
      WRITE(7,50) ITPLUS,ITOVIT
   50 FORMAT(' OVALIZATION STEP',I3,', EQUILIBRIUM ITERATION',I3)
C
C     STIFFNESS MATRIX, LOAD VECTOR, AND DISPLACEMENT VECTOR
C
   60 D1=COST(0)
      WRITE(7,70) D1
   70 FORMAT(/' BEFORE ASOKT:',F7.2)
      IF (IT.EQ.0) GOTO 120
      IF (IN(14).EQ.0 .OR. (IN(14).EQ.1.AND.IT.GT.1)) GOTO 90
      CALL ASOKT(NOEL,OD,OKT,IX)
      PREC=0.1D-15
      DAS=COST(0)
      WRITE(7,80) DAS
   80 FORMAT(' AFTER  ASOKT:',F7.2)
      GOTO 100
   90 IF (IN(13).NE.2 .AND. NOVA.EQ.0) GOTO 120
  100 CALL LOADS(IX,IV,P,OKT,VL,NPL,IXNEW,OD)
      PREC=0.1D-15
      DO 110 I=1,NN5
  110 OF(I)=OF(I)+P(I)
  120 IF (LCH.GT.0) CALL LOADS2(VL,OF,NPL,IXNEW,1)
      CALL VBSOLV(NBAND-1,NN5,PREC,NN5,OF,OKT,ID,NBAND,DET,IEXDET,
     1 IV,.TRUE.,SUCCES)
      IF (IN(8).GE.2) CALL PRTMAT(OKT,NBAND,1,1,NBAND,NN5,'L=OKT/LT')
      IF (.NOT.SUCCES) CALL ERROR(9,IS,IT)
      DVB=COST(0)
      IF (PREC.LT.0.D0) GOTO 210
C
C     OUTPUT OF THE DETERMINANT AND ITS RELATIVE CONDITION
C
      KK=IDINT(DLOG10(DFLOAT(IABS(IEXDET))))+1
      WRITE(9,130) KK
  130 FORMAT(13H(    1H+,32X,I,I2,')')
      REWIND 9
      READ(9,140) IF(1),IF(2),IF(3),IF(4)
  140 FORMAT(4A4)
      WRITE(7,150) DVB,DET
  150 FORMAT(' AFTER VBSOLV:',F7.2//
     1 ' DETERMINANT =',F10.6,' * 10 **')
      WRITE(7,IF) IEXDET
      IF (IN(22).EQ.1) CALL TEST(OKT,DET,IEXDET,DNORM)
      INN5=NN5
      DO 160 I=1,NN5
  160 INN5=INN5-ID(I)
      IF (INN5.EQ.0) GOTO 200
      WRITE(7,170)
  170 FORMAT(' NEGATIVE DIAGONAL ELEMENTS IN FOLLOWING ROWS:'/)
      DO 190 I=1,NN5
      IF (ID(I).EQ.-1) WRITE(7,180) I
  180 FORMAT(' ',I4)
  190 CONTINUE
      GOTO 250
  200 PREC=-0.1D-15
C
C     CHECK OF CONVERGENCE OF DISPLACEMENTS
C
  210 DO 220 I=1,NN5
  220 OD(I)=OD(I)+OF(I)
      IF (IS.EQ.-1) GOTO 310
      XDN=0.D0
      DO 230 I=1,NN5
      A=OF(I)
  230 XDN=XDN+OF(I)*A
      XDN=DSQRT(XDN)
      WRITE(7,240) XDN
  240 FORMAT(/' DISPLACEMENT NORM: ',E11.4)
      IF (IT.EQ.0) XD=XDN
      IF (XDN.LE.XD*1.001D0) GOTO 280
      IF (IN(28).EQ.0) CALL ERROR(10,IS,IT)
  250 IF (IHALF.LT.IN(28)) GOTO 270
      LCAUSE=3
      ISTART=3
      CALL RSTART(OKT,P,OD,NOEL,OF,IX,DV,IV,IH,VL,NPL,IXNEW)
  260 CONTINUE
      LCAUSE=0
      ISTART=0
  270 CALL ITERA(3,DV,OD)
      RETURN
C
  280 NCONV=0
      IF (XDN.LT.XD*10.D0**IN(19)) NCONV=1
      WRITE(7,290,END=300) (OF(I),I=1,NN5)
  290 FORMAT(/' INCREMENTAL DISPLACEMENTS'/(10E12.4))
  300 CONTINUE
C
C     EQUILIBRIUM FORCES, AXIAL FORCE AND END MOMENT
C
  310 IF (IN(16).GT.1) CALL FORCE1(NOEL,OD)
      IF (NCONV.GT.NOVA .OR. IS.EQ.-1) GOTO 380
      IF (IN(13).EQ.1) CALL LONGER(OD,DELTA)
      CALL EQ(OD,OF,NOEL)
      DEQ=COST(0)
      IF (IN(16).EQ.1) CALL FORCE2(OF,OD)
      WRITE(7,320) DEQ
  320 FORMAT(/' AFTER EQ:',F11.2)
      I=IN(27)
      IF (I.GT.0) WRITE(7,330) I,OF(I)
  330 FORMAT(/' INTERNAL FORCE NR.',I4,' =',E14.6)
      IF (IN(21).EQ.1) WRITE(7,340) (OF(I),I=1,NN5)
  340 FORMAT(/' (NEGATIVE) INTERNAL FORCES'/(10E12.4))
      DO 350 I=1,NN5
  350 IF(IX(I).NE.1) OF(I)=0.D0
      XOF=0.D0
      DO 360 I=1,NN5
  360 XOF=XOF+OF(I)*OF(I)
      XOF=DSQRT(XOF)
      WRITE(7,370) XOF
  370 FORMAT(' ',/' NORM OF FREE EQUILIBRIUM FORCES =',E14.6)
      GOTO 400
  380 DO 390 I=1,NN5
  390 OF(I)=0.D0
  400 IF (IN(13).EQ.0 .OR. IT.EQ.0 .OR. ITOVIT.LT.NOVA) GOTO 430
      IF ((IT.GT.1 .AND. NOVA.EQ.0) .OR. ITOVIT.GT.1) GOTO 410
      GOTO 420
  410 FLEX=DMAX1(DMIN1(DELTA/(RN0-RN),FLEX*0.8D0),FLEX*1.25D0)
  420 DELTA=FLEX*RN
  430 DELTAT=-OD(1)-OD(NP*5+1)
      WRITE(7,440) RN,RM,DELTAT
  440 FORMAT(/' AXIAL FORCE =',E18.10,' N'/' MOMENT       =',E18.10,
     1 ' NMM'/' SHORTENING  =',E18.10,' MM')
C
C     CHECK FOR MORE EQUILIBRIUM OR OVALIZATION ITERATIONS,
C     RESTART, OR OUTPUT
C
      IF (IN(30).EQ.2 .AND. NCONV.EQ.1) NOVA=1
      IF ((ITOVAL.GE.IN(3) .AND. (ITOVIT.GE.IN(4) .OR. NCONV.EQ.1))
     1 .OR. IT.GE.IN(18)) NOVA=0
      IF (( (ITOVAL+ITOVIT).EQ.0.OR.ITOVIT.GE.IN(4) .OR. NCONV.EQ.1)
     1 .AND. NOVA.EQ.1) NEXTOV=1
      IF (IT.GE.IN(18) .OR. (NCONV.EQ.1. AND. NOVA.EQ.0)) NEXTIT=0
      IF (NEXTIT.GT.NCONV) GOTO 460
C
      WRITE (7,450) (I,OD(I),I=1,NN5)
  450 FORMAT(' '///10X,'RESULT-VECTOR'//5X,'NR. ',
     1 ' (MM OR ANGLE)'/,(1X,5(I6,E16.8)))
      IF (IN(32).GT.0) CALL STRESS(NOEL,OD)
  460 IF (NEXTIT.EQ.1) GOTO 30
      IF (IS.EQ.IN(17) .OR. (RM0.GT.RM.AND.IN(20).GT.IHALF)
     1 .OR. (IHALF.GT.0.AND.IHALF.GE.IN(28))) NEXTIS=0
      IF (IN(24).EQ.1 .AND. NEXTIS.EQ.0) ISTART=3
C
      CALL RSTART(OKT,P,OD,NOEL,OF,IX,DV,IV,IH,VL,NPL,IXNEW)
  470 IF (ISTART.EQ.0) GOTO 480
      ISTART=0
      LCAUSE=0
      NEXTIT=1
      NEXTIS=1
      IF (IN(30).EQ.2 .AND. NCONV.EQ.1) NOVA=1
      IF ((ITOVAL.GE.IN(3) .AND. (ITOVIT.GE.IN(4) .OR. NCONV.EQ.1))
     1 .OR. IT.GE.IN(18)) NOVA=0
      IF ( ((ITOVAL+ITOVIT).EQ.0.OR.ITOVIT.GE.IN(4) .OR. NCONV.EQ.1)
     1 .AND. NOVA.EQ.1) NEXTOV=1
      IF (IT.GE.IN(18) .OR. (NCONV.EQ.1. AND. NOVA.EQ.0)) NEXTIT=0
      IF (NEXTIT.EQ.1) GOTO 30
C
C     END OF EQUILIBRIUM ITERATION
C
  480 IF (IS.EQ.IN(17) .OR. (RM0.GT.RM.AND.IN(20).GT.IHALF)
     1 .OR. (IHALF.GT.0.AND.IHALF.GE.IN(28))) NEXTIS=0
      IF (IN(13).NE.0) CALL SHORT(DV,DELTA,DELTAT,IS)
      IF (IN(28).EQ.0) RETURN
      IF (INN5.EQ.0 .AND. XDN.LT.(XD*10.D0**(DFLOAT(IN(19))/2.D0)))
     1 GOTO 490
      CALL ITERA(2,DV,OD,VL)
      RETURN
  490 CALL ITERA(1,DV,OD,VL)
      RETURN
      END
      SUBROUTINE SPARSE(IV,IH)
```

```
C
C     COMPUTATION OF FIRST ROW AND LAST COLUMN UNEQUAL ZERO OF
C     GLOBAL STIFFNESS MATRIX
C
      IMPLICIT REAL*8(A-H,O-Z)
      COMMON / WHOLE /IBC(2),INR,IN(50),IS,IT,IXCH,LCH,NBAND,NEC,
     1 NEL,NINTP,NINTS,NINTX,NL,NMAX,NN,NNC,NN5,NPD,NX,NX1,NP,NP1,
     2 N2P,N2X,NX2
      DIMENSION IV(NN5),IH(NN5)
C
      DO 10 I=1,NBAND
   10 IV(I)=1
      IF (NP.EQ.1) GOTO 30
      DO 20 I=3,NP1
      I5=I*5-9
      K=I5+4
      DO 20 J=1,5
   20 IV(K+J)=I5
   30 IE=NN-1
      IA=NP1+2
      I5=1
      DO 40 I=IA,IE
      I5=I5+5
      K=I*5
      DO 40 J=1,5
   40 IV(K+J)=I5
      IF (NX.EQ.1) GOTO 60
      DO 50 I=2,NX
      I5=(I-1)*NP1*5+1
      K=I*NP1*5
      DO 50 J=1,5
   50 IV(K+J)=I5
   60 CONTINUE
      DO 70 I=1,NN5
   70 IH(I)=NN5+1-IV(NN5+1-I)
      WRITE(13) IV,IH
      REWIND 13
      RETURN
      END
      SUBROUTINE STH(X,P)
C
C     COEFFICIENTS OF IN-PLANE STRESS FUNCTIONS
C
      IMPLICIT REAL*8(A-H,O-Z)
      COMMON / PART  /BETA,BETA2,CBETA,CED,DB,DEG,DELTA,DELTAT,E,ED,
     1 EN,E2,FLEX,PEL,PEL2,PI,R,RL,RM,RN,RNU,RNU1,SIGMA,TH,XEL,TIME
      COMMON / TMINUS/T(20,20)
      COMMON / TF    /TXF(20),TPF(20),TPXF(20)
C
      S=DSIN(P)
      X2DR=X*X/2.D0/R
      X2PDR=X2DR*P
      X3DR=X2DR*X/3.D0
      X3PDR=X3DR*P
      DO 10 I=1,20
      TXF(I)=T(7,I)+T(8,I)*S
      TPF(I)=T(9,I)+T(10,I)*X-T(12,I)*X2DR-T(13,I)*X3DR-T(14,I)*
     1 X2PDR-T(15,I)*X3PDR
   10 TPXF(I)=T(11,I)
      RETURN
      END
      SUBROUTINE STRESS(NOEL,OD)
C
C     CALCULATION OF STRESS DISTRIBUTION ALONG THE CIRCUMFERENCE
C
      IMPLICIT REAL*8(A-H,O-Z)
      COMMON / WHOLE /IBC(2),INR,IN(50),IS,IT,IXCH,LCH,NBAND,NEC,
     1 NEL,NINTP,NINTS,NINTX,NL,NMAX,NN,NNC,NN5,NPD,NX,NX1,NP,NP1
      COMMON / PART  /BETA,BETA2,CBETA,CED,DB,DEG,DELTA,DELTAT,E,ED,
     1 EN,E2,FLEX,PEL,PEL2,PI,R,RL,RM,RN,RNU,RNU1,PREC,TH,XEL,TIME
      COMMON / TF    /BX1(20),BP2(20),TPXF(20)
      COMMON / BF    /BP3(20),BX3(20),BX2(20),BP1(20)
      DIMENSION V(24),V2(24),NOEL(4,NEL),OD(NN5)
C
      IF (IN(33).LE.0) RETURN
      DP=PI/NP/DFLOAT(IN(33))
      ENU=EN/TH/R
      X=XEL
C     IF (IN(32).EQ.1) GOTO 2
C     CALL GAUSS(V,V2,24,XEL,NINTS)
C     X=V(NINTS)
C
   10 I1=1
      I2=NP
      WRITE(7,20)
   20 FORMAT(' '//,' STRESSES AT THE CYLINDER END',/)
      GOTO 50
C
   30 X=-X
      I1=NEL-NP+1
      I2=NEL
      WRITE(7,40)
   40 FORMAT(' '//,' STRESSES AT THE CYLINDER MIDDLE',/)
C
   50 DO 150 I=I1,I2
      WRITE(7,60) I
   60 FORMAT(' '/' ELEMENT NR.',I3,
     1 '    SIGMA X       SIGMA PHI     SIGMA X-PHI  ',/)
      DO 70 J=1,4
      L1=(J-1)*5
      L2=(NOEL(J,I)-1)*5
      DO 70 L=1,5
   70 V(L1+L)=OD(L2+L)
      S=-PEL-DP
C
C     LINEAR STRESSES
C
      IIE=IN(33)+1
      DO 140 II=1,IIE
      S=S+DP
      CALL STH(X,S)
      T1=0.D0
      T2=0.D0
      T3=0.D0
      DO 80 K=1,20
      W=V(K)
      T1=T1+BX1(K)*W
      T2=T2+BP2(K)*W
   80 T3=T3+TPXF(K)*W
      BETAX1=0.D0
      BETAX2=0.D0
      BETAX3=0.D0
      BETAP1=0.D0
      BETAP2=0.D0
      BETAP3=0.D0
      IF (IN(15).EQ.0) GOTO 120
C
C     NONLINEAR STRESS CONTRIBUTIONS
C
      CALL BXP(X,S)
      DO 90 K=1,20
      BETAX3=BETAX3+BX3(K)*V(K)
   90 BETAP3=BETAP3+BP3(K)*V(K)
      IF (IN(31).LT.1) GOTO 120
C
      DO 100 K=1,20
      BETAX2=BETAX2+BX2(K)*V(K)
  100 BETAP1=BETAP1+BP1(K)*V(K)
      IF (IN(31).NE.2) GOTO 120
C
      BETAX1=T1
  110 BETAP2=T2
C
  120 EPSX=T1+(BETAX1*BETAX1+BETAX2*BETAX2+BETAX3*BETAX3)/2.D0
```

```
      EPSP=T2+(BETAP1*BETAP1+BETAP2*BETAP2+BETAP3*BETAP3)/2.DO
      EPSXP=T3+(BETAP1*BETAX1+BETAP2*BETAX2+BETAP3*BETAX3)/2.DO
      SX=ENU*(EPSX+RNU*EPSP)
      SP=ENU*(EPSP+RNU*EPSX)
      SXP=E*EPSXP/(1.DO+RNU)
      WRITE(7,130) S,SX,SP,SXP
  130 FORMAT(F10.6,'    ',3E14.6)
  140 CONTINUE
  150 CONTINUE
      IF (I1.EQ.1) GOTO 30
      RETURN
      END
      SUBROUTINE STUFF(OKT,NBAND,J1,INS,EK,ICO,J3,NTNODE,IEL,IX)
C
C***********************************************************************
C
C   THIS SUBROUTINE INSERTS AN ELEMENT STIFFNESS MATRIX AND CONSISTENT
C   LOAD. ROWS AND COLUMNS ARE DELETED FOR THE ZERO BOUNDARY CONDITIONS.
C
C   OKT   = AN I1XJ1 MATRIX CONTAINING THE TRANSPOSE OF THE LOWER HALF
C           BAND OF THE STRUCTURE STIFFNESS MATRIX.
C   EK    = AN I2XI2 MATRIX CONTAINING THE UPPER HALF OF THE ELEMENT
C           STIFFNESS MATRIX
C   ICO   = AN I3XJ3 MATRIX OF INTEGERS. THE (I,J)TH TERM CONTAINS
C           THE ITH NODE NUMBER OF THE JTH ELEMENT.
C   IEL   = THE NUMBER OF THE ELEMENT BEING INSERTED
C   NTNODE= THE TOTAL NUMBER OF NODES IN THE ASSEMBLED STRUCTURE
C   NBAND = ( THE BANDWIDTH OF THE STRUCTURE STIFFNESS MATRIX )
C   IX    = A VECTOR CONTAINING THE BOUNDARY CONDITION INFORMATION
C           IX(I) = 0 DEGREE OF FREEDOM I SET EQUAL TO ZERO
C           IX(I) = 1 DEGREE OF FREEDOM I FREE
C
C***********************************************************************
C
      IMPLICIT REAL*8(A-H,O-Z)
      DIMENSION OKT(NBAND,J1),EK(20,20)
      DIMENSION ICO(4,J3),IX(J1),INS(NTNODE),IES(20)
C
      IF (IEL.NE.1) GOTO 20
      DO 10 I=1,NTNODE
   10 INS(I)=(I-1)*5
   20 DO 30 I=1,4
   30 IES(I)=(I-1)*5
      DO 70 JN=1,4
      JJN=ICO(JN,IEL)
      KJ=INS(JJN)
      MJ=IES(JN)
      DO 70 IN=JN,4
      IIN=ICO(IN,IEL)
      KI=INS(IIN)
      MI=IES(IN)
      DO 70 J=1,5
      JJ=J+MJ
      JJJ=J+KJ
      IF ((IX(JJJ).EQ.0) .AND. (IN.NE.JN)) GOTO 70
      DO 60 I=1,5
      II=I+MI
      III=I+KI
      JO=III
      IO=NBAND-III+JJJ
      IF ((III.GE.JJJ) .OR. (IN.EQ.JN)) GOTO 40
      JO=JJJ
      IO=NBAND-JJJ+III
   40 IF (IX(III).EQ.0 .OR. IX(JJJ).EQ.0) GOTO 50
      IF (IO.GT.NBAND) GOTO 60
      OKT(IO,JO)=OKT(IO,JO)+EK(JJ,II)
      GOTO 60
   50 IF (III.EQ.JJJ) OKT(IO,JO)=1.DO
   60 CONTINUE
   70 CONTINUE
      RETURN
      END
      SUBROUTINE TEST(OKT,DET,IEXDET,DNORM)
C
C     THIS SUBROUTINE NORMALIZES THE DETERMINANT
C     OF A LOWER TRIANGULAR MATRIX BY DIVIDING EACH J-TH ROW BY
C     SQUARE ROOT ( SUM ( A ,IJ ) ) ; I=1,N
C     AND MULTIPLICATION WITH THE NORMALIZED DETERMINANT OF A
C     TRIANGULAR MATRIX WITH ONLY '1' VALUES
C
C     RELATIVE CONDITION = NMAX / NORMALIZED DETERMINANT
C
      IMPLICIT REAL*8(A-H,O-Z)
      COMMON / WHOLE /IBC(2),INR,IN(50),IS,IT,IXCH,LCH,NBAND,NEC,
     1 NEL,NINTP,NINTS,NINTX,NL,NMAX,NN,NNC,NN5,NPD,NX,NX1,NP,NP1,
     2 N2P,N2X,NX2
      DIMENSION OKT(NBAND,NN5)
C
      DO 20 I=1,NN5
      S=0.D0
      DO 10 J=1,NBAND
      SS=OKT(J,I)
   10 S=S+SS*SS
      DET=DET/S
      K=IDINT(DLOG10(DABS(DET)))
      DET=DET/10.D0**K
   20 IEXDET=IEXDET+K
      DEXDET=(DFLOAT(IEXDET)+DLOG10(DABS(DET))+DNORM)/2.D0
      RCOND=0.1D0**(DEXDET/DFLOAT(NMAX))
      WRITE(7,30) RCOND
   30 FORMAT(' RELATIVE CONDITION =',E14.6)
      RETURN
      END
      SUBROUTINE TMAT
C
C     EXPLICIT INVERSION OF MATRIX T (UNKNOWN DISPLACEMENT PARAMETERS)
C
      IMPLICIT REAL*8(A-H,L,O-Z)
      COMMON / PART  /BETA,BETA2,CBETA,CED,DB,DEG,DELTA,DELTAT,E,ED,
     1 EN,E2,FLEX,PEL,PEL2,PI,R,RL,RM,RN,RNU,RNU1,SIGMA,TH,XEL,TIME
      COMMON / TMINUS/T(20,20)
C
      P=PEL
      L=XEL
      S=DSIN(P)
      C=DCOS(P)
      A=C*P-S
      DO 10 J=1,20
      DO 10 I=1,20
   10 T(I,J)=0.D0
C
      H=.25D0/S
      T(1,2)=H
      T(1,7)=H
      T(1,12)=-H
      T(1,17)=-H
      H=H*R
      T(1,5)=H
      T(1,10)=H
      T(1,15)=-H
      T(1,20)=-H
      H=.25D0/L/S
      T(2,2)=H
      T(2,7)=-H
      T(2,12)=H
      T(2,17)=-H
      H=H*R
      T(2,5)=H
      T(2,10)=-H
      T(2,15)=H
      T(2,20)=-H
      H=-L/8.D0/R/S
      T(3,1)=H
      T(3,6)=-H
      T(3,11)=H
      T(3,16)=-H
      H=-P/4.DO/A
      T(3,2)=H
      T(3,7)=H
      T(3,12)=H
      T(3,17)=H
      H=.25DO/A
      T(3,3)=H
      T(3,8)=H
      T(3,13)=-H
      T(3,18)=-H
      H=-P*R/4.DO/A
      T(3,5)=H
      T(3,10)=H
      T(3,15)=H
      T(3,20)=H
      H=-P/4.DO/L/A
      T(4,2)=H
      T(4,7)=-H
      T(4,12)=-H
      T(4,17)=H
      H=.25DO/L/A
      T(4,3)=H
      T(4,8)=-H
      T(4,13)=H
      T(4,18)=-H
      H=-H*R*P
      T(4,5)=H
      T(4,10)=-H
      T(4,15)=-H
      T(4,20)=H
      H=.25DO
      T(5,1)=H
      T(5,6)=H
      T(5,11)=H
      T(5,16)=H
      H=-R*C/4.DO/L/S
      T(5,2)=H
      T(5,7)=-H
      T(5,12)=H
      T(5,17)=-H
      H=-R*R*(2.DO*C+S*P)/8.DO/S/L
      T(5,5)=H
      T(5,10)=-H
      T(5,15)=H
      T(5,20)=-H
      H=-P*L/16.DO/R
      T(6,1)=H
      T(6,6)=-H
      T(6,11)=H
      T(6,16)=-H
      H=-S*(2.DO+P*P)/8.DO/A
      T(6,2)=H
      T(6,7)=H
      T(6,12)=H
      T(6,17)=H
      H=-H*C/S
      T(6,3)=H
      T(6,8)=H
      T(6,13)=-H
      T(6,18)=-H
      H=-P*L/16.DO
      T(6,4)=H
      T(6,9)=-H
      T(6,14)=H
      T(6,19)=-H
      H=-P*R*(2.DO*C+S*P)/8.DO/A
      T(6,5)=H
      T(6,10)=H
      T(6,15)=H
      T(6,20)=H
      H=.25D0/L
      T(7,1)=H
      T(7,6)=-H
      T(7,11)=-H
      T(7,16)=H
      H=H/S
      T(8,1)=H
      T(8,6)=-H
      T(8,11)=H
      T(8,16)=-H
      H=C/4.D0/R/S
      T(9,2)=H
      T(9,7)=H
      T(9,12)=-H
      T(9,17)=-H
      H=.25D0/R
      T(9,3)=H
      T(9,8)=H
      T(9,13)=H
      T(9,18)=H
      H=-L/8.D0/R
      T(9,4)=H
      T(9,9)=-H
      T(9,14)=-H
      T(9,19)=H
      H=A/4.D0/S/P
      T(9,5)=H
      T(9,10)=H
      T(9,15)=-H
      T(9,20)=-H
      H=C/4.D0/L/R/S
      T(10,2)=H
      T(10,7)=-H
      T(10,12)=H
      T(10,17)=-H
      H=0.375D0/R/L
      T(10,3)=H
      T(10,8)=-H
      T(10,13)=-H
      T(10,18)=H
      H=-0.125D0/R
      T(10,4)=H
      T(10,9)=H
      T(10,14)=H
      T(10,19)=H
      H=A/4.D0/S/L/P
      T(10,5)=H
      T(10,10)=-H
      T(10,15)=H
      T(10,20)=-H
      H=0.25D0/P/R
      T(11,1)=H
      T(11,6)=H
      T(11,11)=-H
      T(11,16)=-H
      H=-S*P*P/12.D0/L/A
      T(11,2)=H
      T(11,7)=-H
      T(11,12)=-H
      T(11,17)=H
      H=0.25D0/P/L+P*(3.D0*C*P-S)/24.D0/L/A
      T(11,3)=H
      T(11,8)=-H
      T(11,13)=H
      T(11,18)=-H
      H=-P/24.D0
      T(11,4)=H
      T(11,9)=H
      T(11,14)=-H
      T(11,19)=-H
      H=(-S*P*P-3.D0*A)*R/12.D0/L/A
      T(11,5)=H
```

```
2593          T(11,10)=-H
2594          T(11,15)=-H
2595          T(11,20)=H
2596          H=-0.25DO/L
2597          T(12,4)=H
2598          T(12,9)=-H
2599          T(12,14)=-H
2600          T(12,19)=H
2601          H=.75DO/L/L/L
2602          T(13,3)=H
2603          T(13,8)=-H
2604          T(13,13)=-H
2605          T(13,18)=H
2606          H=-0.75DO/L/L
2607          T(13,4)=H
2608          T(13,9)=H
2609          T(13,14)=H
2610          T(13,19)=H
2611          H=-0.25DO/L/R/P
2612          T(14,1)=H
2613          T(14,6)=-H
2614          T(14,11)=H
2615          T(14,16)=-H
2616          H=-0.25DO/P/L
2617          T(14,4)=H
2618          T(14,9)=-H
2619          T(14,14)=H
2620          T(14,19)=-H
2621          H=.75DO/P/L/L/L
2622          T(15,3)=H
2623          T(15,8)=-H
2624          T(15,13)=H
2625          T(15,18)=-H
2626          H=-H*L
2627          T(15,4)=H
2628          T(15,9)=H
2629          T(15,14)=-H
2630          T(15,19)=-H
2631          H=-0.25DO/R/P
2632          T(16,5)=H
2633          T(16,10)=H
2634          T(16,15)=-H
2635          T(16,20)=-H
2636          H=H/L
2637          T(17,5)=H
2638          T(17,10)=-H
2639          T(17,15)=H
2640          T(17,20)=-H
2641          H=L/8.DO/P/R/R/R
2642          T(18,1)=H
2643          T(18,6)=-H
2644          T(18,11)=H
2645          T(18,16)=-H
2646          H=S/4.DO/R/R/A
2647          T(18,2)=H
2648          T(18,7)=H
2649          T(18,12)=H
2650          T(18,17)=H
2651          H=-C/4.DO/R/R/A
2652          T(18,3)=H
2653          T(18,8)=H
2654          T(18,13)=-H
2655          T(18,18)=-H
2656          H=L/8.DO/P/R/R
2657          T(18,4)=H
2658          T(18,9)=-H
2659          T(18,14)=H
2660          T(18,19)=-H
2661          H=S/4.DO/R/A
2662          T(18,5)=H
2663          T(18,10)=H
2664          T(18,15)=H
```

```
      T(18,20)=H
      H=S/4.D0/L/R/R/A
      T(19,2)=H
      T(19,7)=-H
      T(19,12)=-H
      T(19,17)=H
      H=(S-3.D0*C*P)/8.D0/P/L/R/R/A
      T(19,3)=H
      T(19,8)=-H
      T(19,13)=H
      T(19,18)=-H
      H=0.125D0/P/R/R
      T(19,4)=H
      T(19,9)=H
      T(19,14)=-H
      T(19,19)=-H
      H=S/4.D0/R/L/A
      T(19,5)=H
      T(19,10)=-H
      T(19,15)=-H
      T(19,20)=H
      H=-0.0625D0/P/R/R
      T(20,1)=H
      T(20,6)=H
      T(20,11)=-H
      T(20,16)=-H
      H=-S*P*P/9.6D0/R/L/A
      T(20,2)=H
      T(20,7)=-H
      T(20,12)=-H
      T(20,17)=H
      H=(5.D0*P*P*(3.D0*C*P-S)-18.D0*A)/96.D0/R/P/L/A
      T(20,3)=H
      T(20,8)=-H
      T(20,13)=H
      T(20,18)=-H
      H=(12.D0-5.D0*P*P)/96.D0/P/R
      T(20,4)=H
      T(20,9)=H
      T(20,14)=-H
      T(20,19)=-H
      H=-(5.D0*P*P*S+9.D0*A)/48.D0/L/A
      T(20,5)=H
      T(20,10)=-H
      T(20,15)=-H
      T(20,20)=H
      RETURN
      END
      SUBROUTINE UVW(X,P)
C
C     COMPUTATION OF ELEMENT DISPLACEMENTS
C
      IMPLICIT REAL*8(A-H,O-Z)
      COMMON / PART  /BETA,BETA2,CBETA,CED,DB,DEG,DELTA,DELTAT,E,ED,
     1 EN,E2,FLEX,PEL,PEL2,PI,R,RL,RM,RN,RNU,RNU1,SIGMA,TH,XEL,TIME
      COMMON / TMINUS/T(20,20)
      COMMON / DELVW /RV(20),RW(20)
C
      DS=DSIN(P)
      DC=DCOS(P)
      X2=X*X/2.D0
      RX=X*R
      XP=X*P
      P2=P*P/2.D0
      XD4=X/4.D0
      R2=R*R
      X2CR=X2*DC/R
      X2SR=X2*DS/R
      S=X*(P2-1.D0)
      DO 10 I=1,20
      RV(I)=(T(1,I)+T(2,I)*X)*DS-(T(3,I)+T(4,I)*X)*DC+T(6,I)-
     1 T(8,I)*X2CR+T(11,I)*XD4+
     2 R2*(T(16,I)*P+T(17,I)*XP+T(18,I)*P2+T(19,I)*S)+T(20,I)*RX
      RW(I)=-(T(1,I)+T(2,I)*X)*DC-(T(3,I)+T(4,I)*X)*DS-T(8,I)*X2SR+
     1 R*(T(9,I)+T(10,I)*X)-
     2 X2*(T(12,I)+T(13,I)*X/3.D0+T(14,I)*P+T(15,I)*XP/3.D0)-
     3 R2*(T(16,I)+T(17,I)*X+T(18,I)*P+T(19,I)*XP)
   10 CONTINUE
      RETURN
      END
END OF FILE
```

Appendix B.2

Input Description

The input format for the program is given below with an example of the input for the pinched cylinder problem.

```
M,
TITLE
RL,R,TH,E,RNU,
NX,NP,
IBC(1),IBC(2),
NINTX,NINTP,NINTS,
CBETA,CED,
INL,INL1,INN,
IN(1), ..., IN(INL),         (INL values)
IN(INL1), ..., IN(INN),      (INN-INL1+1 values)
IXCH,LCH,
K,L,                         (IXCH lines)
K,L,F,                       (LCH lines)
```

Input data for the pinched cylinder problem

```
1,
TEST WITH THIN PINCHED CYLINDER
10.35,4.953,0.01548,10500000,0.3125,
1,1,
2,2,
16,16,16,
0,0,
12,16,33,
1,0,0,0,1,  1,0,0,0,1,          0,0,0,0,0,
0,1,0,0,0,  1,0,0,0,0,  785398164,0,0,0,0, 0,0,0,
10,1,
1,1,
3,1,
4,1,
6,1,
7,1,
8,1,
9,1,
11,1,
13,1,
14,1,
33,3,0.025,
```

Explanation of Input Variables

M	computational indicator 1: initial program run 2: restart run
TITLE	heading for output
RL	length of cylinder
R	radius of cylinder
TH	thickness of cylinder
E	Young's modulus
RNU	Poisson's ratio
NX	number of elements in the longitudinal direction
NP	number of elements in the circumferential direction
IBC	symmetry conditions about longitudinal axes, IBC(1): 1=asymmetry 2=symmetry about axes at mid half, IBC(2): 1=asymmetry 2=symmetry (as yet, the program is only tested for double symmetry)
NINTX	gaussian integration order for the x-direction
NINTP	gaussian integration order for the ϕ-direction
NINTS	gaussian integration order for stress computation
CBETA	ratio of (applied end rotation per load step) / (angle which causes classical cylinder-buckling stress)
CED	ratio of (applied shortening of cylinder) / (shortening which causes the lesser of cylinder or column buckling stress)
INL,INL1,INN	first and last indices to read array IN(I)
IN(I)	parameter vector. if no values are given, the description is in effect for a value of '1' and not in effect for a value of '0' 1 one quarter of the cylinder is analyzed 2 print matrix 'E2K' 3 number of ovalization iterations 4 number of equilibrium iterations per ovalization 5 output of material properties and geometry 6 output of boundary condition etc. 7 print matrix 'OK,FIRST' 8 print matrix 'OK,+LOAD' 0 no output of matrix 1 before VBSOLV 2 after VBSOLV 3 both, 1 and 2 9 print load vector 10 print deformation vector 11 element stiffness matrices are read from file 11 12 nonlinear analysis is performed 13 maintain a specified axial force

- 0 axial force is not maintained
- 1 adjustments of all u - displacements
- 2 load vector and boundary condition are changed

14 tangent stiffness matrix is recalculated
- 0 before each load step
- 1 as 0 and before each first iteration
- 2 as 0 and before each equilibrium iteration

15 calculation of forces includes nonlinear terms (always included, if IN(16) = 1)

16 cylinder forces are calculated from
- 0 (no calculation)
- 1 equilibrium forces
- 2 stress integration along boundary
- 3 stress integration at integration points

17 maximum number of successful load steps

18 maximum number of equilibrium iterations

19 pivot number to control iteration (if XD < XDN * 10 ** IN(19), stop iteration), XD is the vector norm of the first deflection increment, XDN is the vector norm of an increment during an equilibrium iteration

20 no load steps after decreasing end moment

21 output of out-of-balance forces

22 output of determinants
- 0: output of determinant of altered stiffnes matrix only
- 1: compute normalized determinant
- 2: compute determinant of unchanged stiffness matrix

23 restart: (local and global time limit is set)

24 restart: storage of variables without time limits being reached

25 only stiffness calculation

26 if IN(26) > 0, PEL=IN(26)/10**9 PEL=half of angle subtended by element (for non-cylinder problems)

27 if IN(27) > 0, output of equilibrium force: IN(27)

28 number of refinements for buckling load (IN(20) is ignored)

29 if IN(29) > 0, REDUCE=IN(29)/10**4

30 boundary condition flag
- 0: rigid cylinder ends
- 1: include donnell-stretch in nonlinear boundary conditions
- 2: iterate to cross-section of mid-length of cylinder

31 inclusion of nonlinear strain parts for the computation of nonlinear stiffness matrices
- 0: simplest expression for nonlinear strains
- 1: extended expression for nonlinear strains
- 2: full expression for nonlinear strains

	32 calculation of stresses at the circumference 0: no calculation 1: stresses at the boundaries of cylinder 2: stresses at the nearest integration points for the longitudinal direction
	33 number of points for stress calculation
	34 to 50: not used
IXCH	Number of changes of boundary conditions
LCH	Number of changes of loads
K,L	K: degree of freedom to be changed, L: new degree of freedom 0: displacement restricted to a value of 0 1: displacement is free, load may be prescribed 2: displacement with value other than 0 is prescribed
K,L,F	K: degree of freedom to be changed, L: description whether load or displacement is to be discribed, and whether it is held constant or increased with each load step 3: constant load is prescribed 4: additional load per load step 5: constant displacement is specified 6: additional displacement per load step F: value of prescribed load or displcament

The necessary data to restart the program is given below.

```
2,
NCHIN,NED,NDB,NREDUC,0,0,
I,J                                    (NCHIN lines)
EDNEW                                  (if NED≠0),
DBNEW                                  (if NDB≠0),
REDUCE                                 (if NREDUC≠0)
```

Hereby are

NCHIN	number of changes for parameter vector "IN"
NED	factor for input variable "CED"
NDB	factor for input varialbe "CBETA"
I,J	parameter IN("I") is given the value "J"
REDUCE	factor with which the load step size is reduced if a negativ determinant is detected

The following files are needed during the computation:

5	input data
6	error diagnosis
7	input echo, results
8	temporary storage for global stiffness matrix
9	temporary storage for format construction
10	storage for restart
11	storage of stiffness matrices
12	temporary storage during step size iteration
13	temporary storage of reference vectors